PAUL SCHERRER INSTITUT

Powder Technology course
Autumn semester 2017

Cold compaction

Peter M Derlet
Condensed Matter Theory
Paul Scherrer Institut

peter.derlet@psi.ch

Semestre d'hiver 2017

Week-DATE	File. no.	Powder Technology – Wednesday 10.15-12.00 – MXG 110
1- sept 20	1	Introduction - PB
2 – sept 27	2	Powder packing and compaction - 1- PB -
3 – oct 4	3	Powder packing and compaction - 2-PB- and guest lecturer - MS
4 – oct 11	4	Powder packing and compaction -3- PD
5 – oct 18	4	Powder packing and compaction - 4 – PD
6 – oct 25	5	Particle – Particle Interactions 1 - PB
7 – nov1	6	Particle – Particle Interactions 2- PB
8 – nov 8	7	Particle – Particle Interactions - 3-PB
9 – nov -15	8	Introduction to atomistic scale simulations PD
10 – nov 22	9	Compaction, Sintering & Defects in metals at atomistic scale - PD
11 -nov-29	10	Sintering Mechanisms& New Technologies - 1 – PB
12 - dec 6	11	Sintering Mechanisms & New Technologies - 2 - PD
13 – dec 13	11	Sintering Mechanisms &New Technologies -3 PD
14 – dec 20	11	Sintering Mechanisms & New Technologies- and exam 4 – PB
		PB – Prof. Paul Bowen (EPFL), PD – Dr. Peter Derlet (PSI)
		MS- Dr. Mark Sawley (EPFL)

References

- German, R.M. (1994) Powder metallurgy science, in Metal Powder Industries Federation, 2nd edn, Princeton, New York.
- Modelling of Powder Die Compaction, Herausgeber: Brewin, P.R., Coube, O., Doremus, P., Tweed, J.H. (Eds.), Engineering Materials and Processes, 2008 Springer-Verlag London Limited.
- Poquillon et al., Powder Technology 126 (2002) 65-74.
- Arzt, E., Acta Metall. Mater. 30 (1982) 1883-1890.
- C.L. Martin et al., J. Mech. Phys. Solids 51 (2003) 667-693.

Lecture outline

- Recap
- Cold compaction of powders – overview
- Phenomenology
- Elasto-plastic Constitutive Modelling Primer
  - Stress invariants
  - Porous elasticity
  - Yield surfaces and “associated” models
- Macroscopic constitutive models
  - Cam Clay model
  - The Drucker-Prager-Cap (DPC) model
- Microscopic constitutive models
  - Densification of random packings
  - Discrete element methods

Recap

PM production process involves:

1) Powder production
2) Adding of lubricants
3) Blending
4) Hot or Cold compaction → green compact
5) Scintering of green compact
6) Secondary or finishing operation

Recap

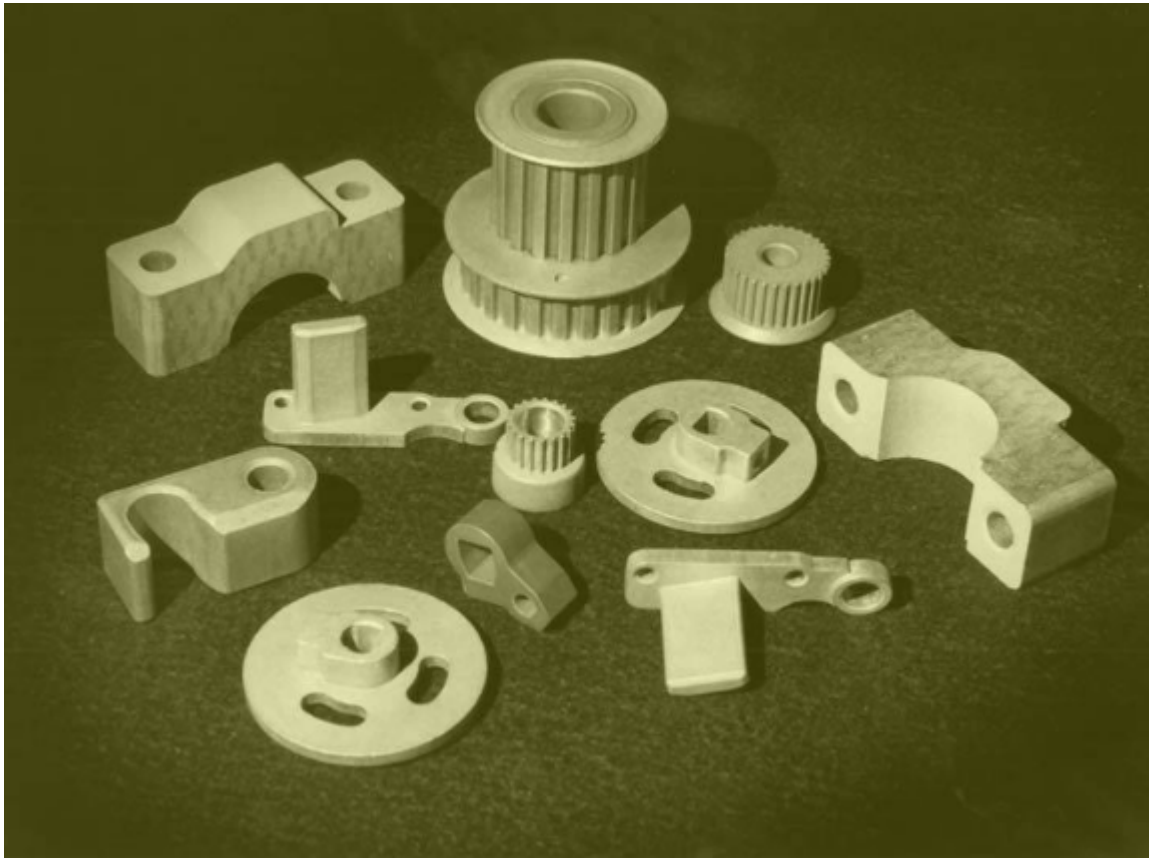

Chapter 24. Powder Metallurgy
Joseph W. Newkirkn
Handbook of Aluminum
Vol. 1: Physical Metallurgy and Processes

Cold compaction of powders

Cold compaction can involve:

- Pressing
- Iso-static pressing
- Rolling
- Extrusion
- Injection molding

End product is the green compact

Cold compaction of powders

- Results in the required shape of the part
- Increases the density
- Properties of the green compact depends on the applied stresses levels and precise protocol
- Porosities typically start high, and can be reduced to values such that the density of the green compact comes close to that of the bulk materials.

$$\text{fractional porosity} = p = \frac{V - V_{\text{bulk}}}{V}$$

$$\text{relative density} = \rho_{\text{r}} = \frac{\rho}{\rho_{\text{bulk}}} = \frac{1/V}{1/V_{\text{bulk}}} = \frac{V_{\text{bulk}}}{V}$$

$$p = 1 - \rho_{\text{r}}$$

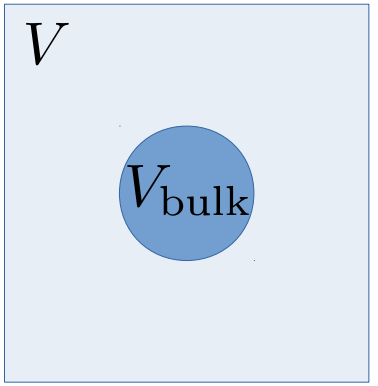

Cold compaction of powders

TABLE 18-1 Typical Compacting Pressures for Various Applications

Application	Compaction Pressures tons/in.^{2}	Mpa
Porous metals and filters	3–5	40–70
Refractory metals and carbides	5–15	70–200
Porous bearings	10–25	146–350
Machine parts (medium-density iron & steel)	20–50	275–690
High-density copper and aluminum parts	18–20	250–275
High-density iron and steel parts	50–120	690–1650

http://academic.uprm.edu/pcaceres/Courses/ManufProc/MP-PM.pdf

Cold compaction of powders

TABLE 17.1

Compacting Pressures for Various Powders

Metal	Pressure (MPa)
Aluminum	70-275
Brass	400-700
Bronze	200-275
Iron	350-800
Tantalum	70-140
Tungsten	70-140
Other materials	
Aluminum oxide	110-140
Carbon	140-165
Cemented carbides	140-400
Ferrites	110-165

http://academic.uprm.edu/pcaceres/Courses/ManufProc/MP-PM.pdf

Cold compaction of powders

Green density is the density of the green compact

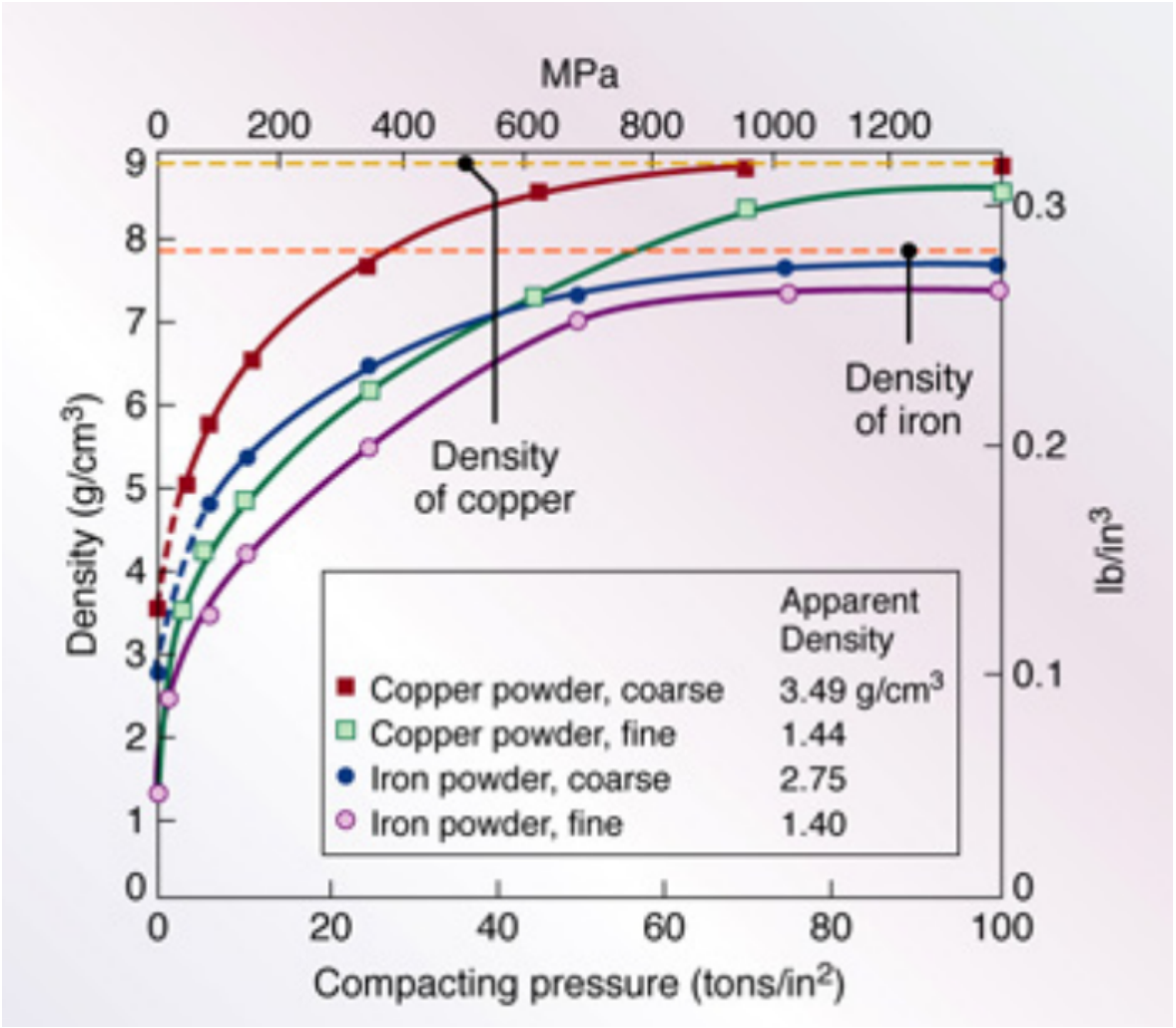

F.V. Lenel Powder Metallurgy: Principles and Applications. Princeton, NJ; Metal Powder Industries Federation, 1980

Cold compaction of powders

- The higher the density, generally, the higher the strength and elastic moduli

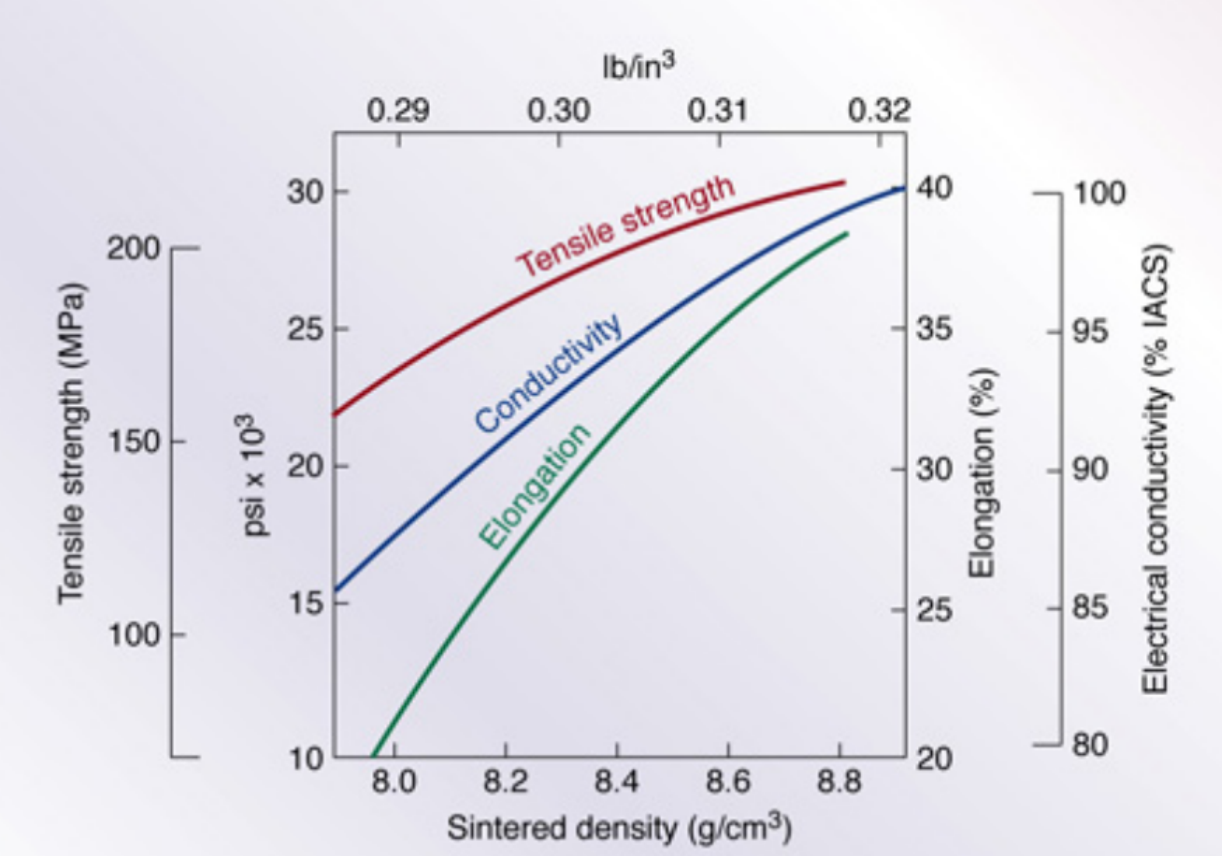

http://academic.uprm.edu/pcaceres/Courses/ManufProc/MP-PM.pdf

Phenomenology of compaction

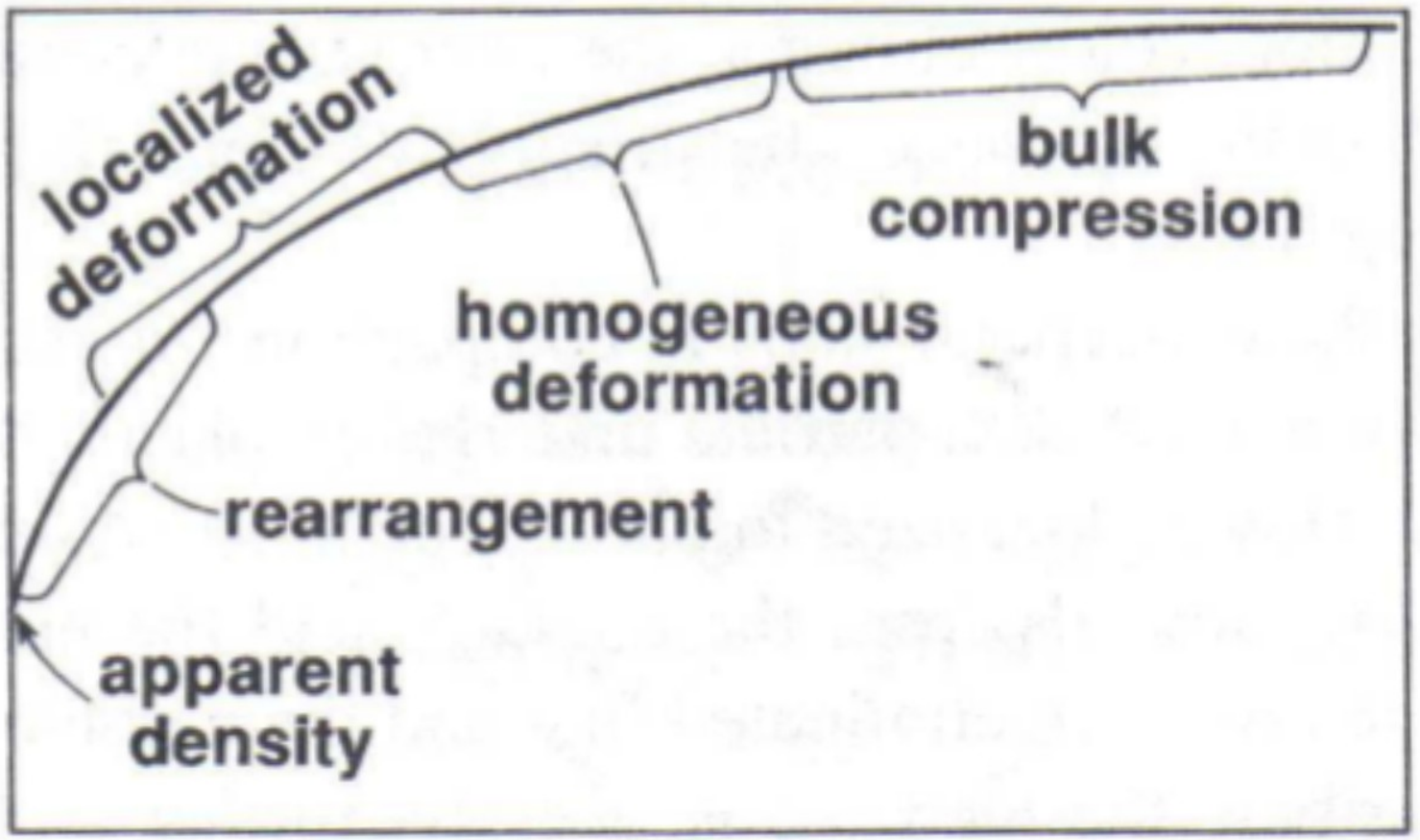

Phenomenology of compaction

Stages of compaction:

- Stage 0 – packing
- Stage 1 – the surrounding of particles with connected pores (relative density 60%-80%)
- Stage 2 – the sealing off of the pores between particles (relative density 80%-90%) → porous solid

Phenomenology of compaction

Stages of compaction:

- High pressures increase density by contact enlargement through plastic deformation.
- Pressure causes localized deformation at the contacts – new contacts form as the gaps between particles collapse.
- The inter-particle contact zones take on a flattened appearance with a circular profile.
- The four major mechanisms controlling densification are rearrangement, plastic deformation, power-law creep and diffusional flow

Phenomenology of compaction

- Relationship between relative density and contact area

$$\text{relative density} = \rho_\text{r} = \frac{\rho}{\rho_\text{bulk}} = \frac{1/V}{1/V_\text{bulk}} = \frac{V_\text{bulk}}{V}$$

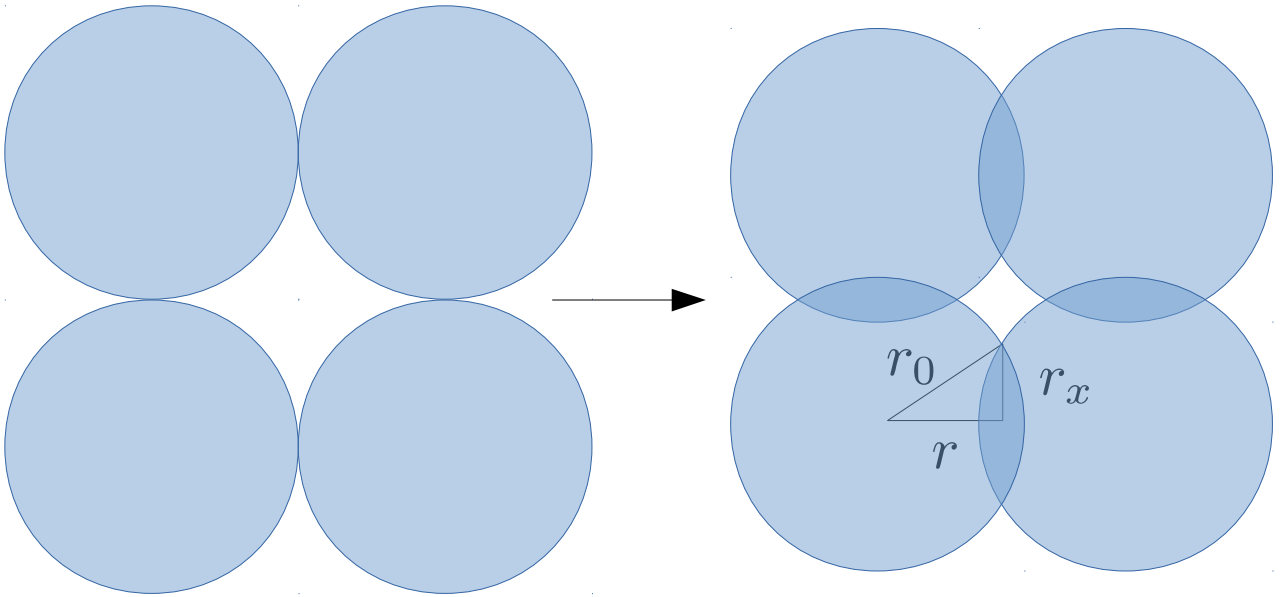

$$r_x = r_0 \left(1 - \left(\frac{\rho_\text{r}^0}{\rho_\text{r}}\right)^{\frac{2}{3}}\right)^{\frac{1}{2}}$$

$$\rho_\text{r}^0 = \frac{\frac{4}{3}\pi r_0^3}{8 r_0^3}$$

$$\rho_\text{r} = \frac{\frac{4}{3}\pi r_0^3}{8 r^3} \longrightarrow \frac{\rho_\text{r}}{\rho_\text{r}^0} = \left(\frac{r_0}{r}\right)^3$$

Phenomenology of compaction

- During deformation, cold welding at the inter-particle contacts contributes to the development of strength in the compact → the green strength
- The large pores are eliminated first and the particle coordination number increases to further distribute the load

Phenomenology of compaction

Coordination number varies with relative (fractional) density

$$N_{\mathrm{c}} = 14 - 10.4\varepsilon^{0.32}$$

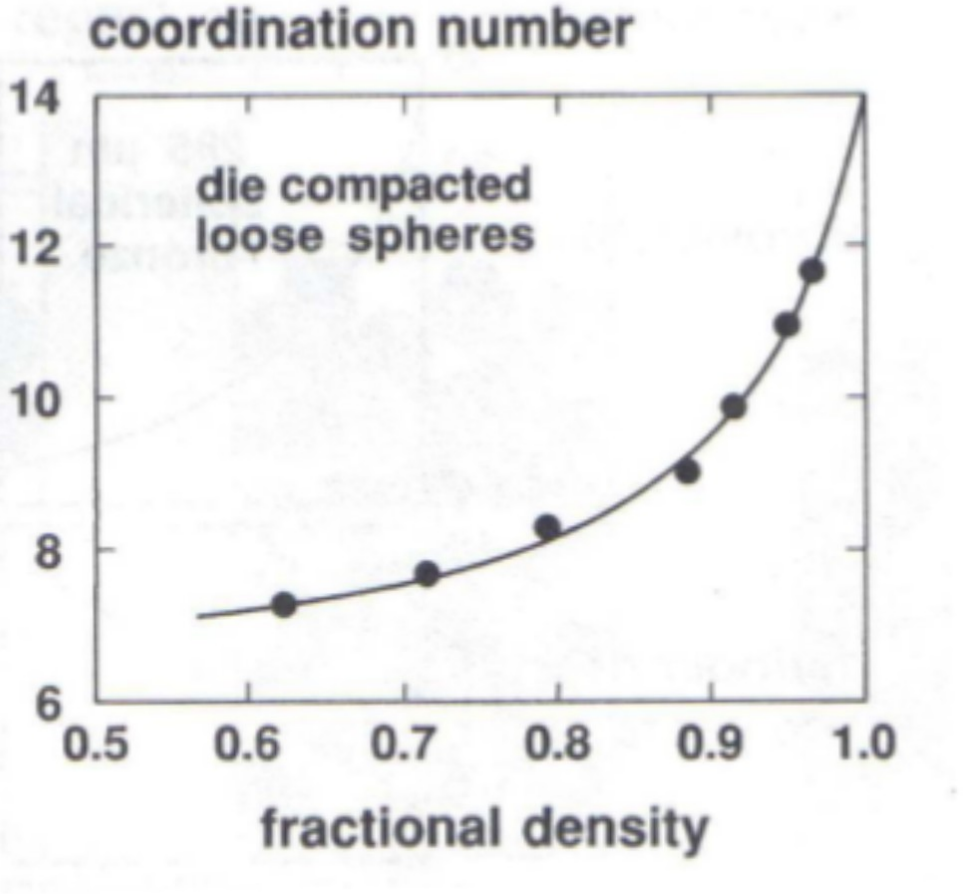

Phenomenology of compaction

Interface between particles after cold pressing

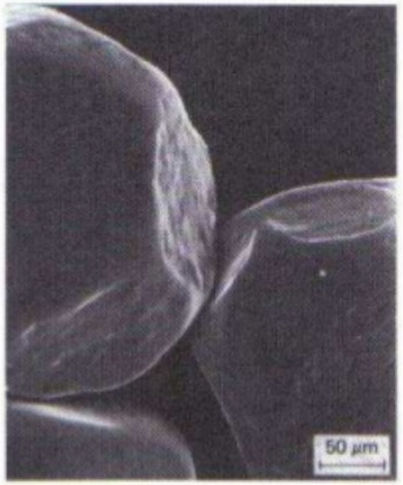

a)

b)

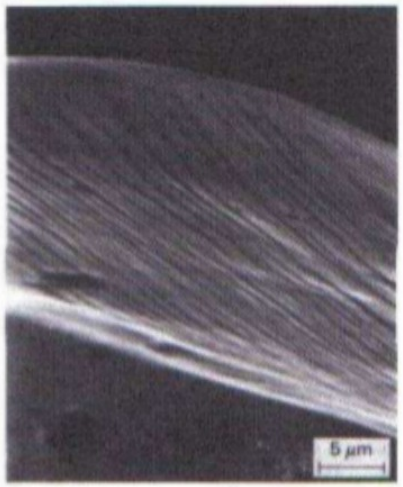

c)

Bild 38. Mit 400 MPa gepreßte Kugelpackung, $a = 125$ µm;
a) Kontaktflächen im Preßling aus polykristallinen Pulvern ($\overline{L}_{G_0} = 8$ µm),
b) Ausschnitt von a),
c) Ausschnitt von der Kontaktfläche eines monokristallinen Teilchens (nach [68]).

- Strong plastic deformation
- High amount of energy is stored in the deformed area
- High concentration of dislocations (fast diffusion)

Phenomenology of compaction

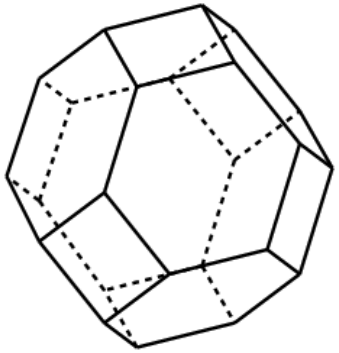

$$V = \sqrt{128}L^3$$

$$S = \left(\sqrt{432} + 6\right)L^2$$

$$G = \sqrt{8}L$$

A tetradecahedron is a 14-sided polyhedron, sometimes called a tetrakaidecahedron.

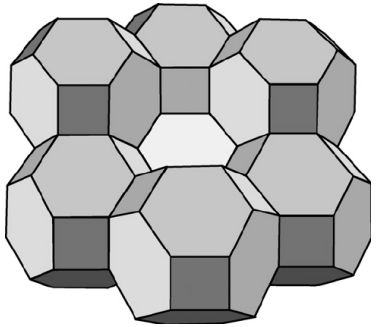

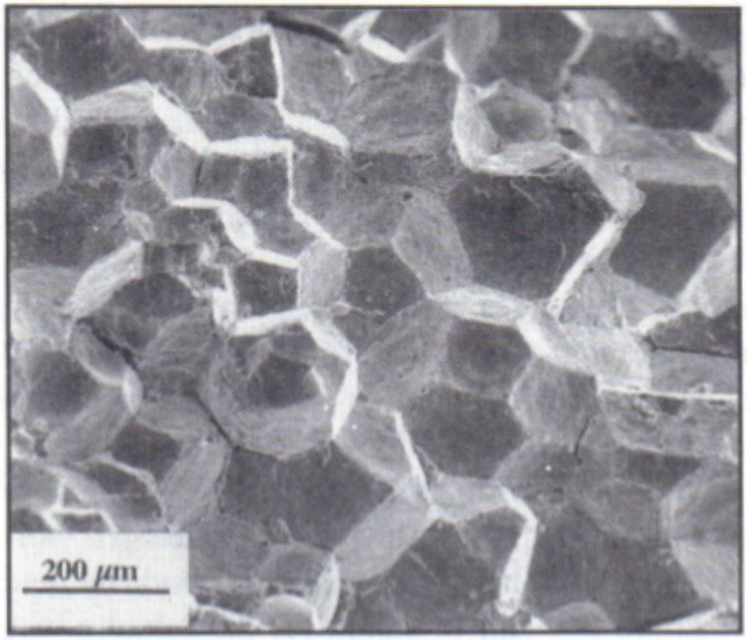

Fragmentation can also occur

Phenomenology of compaction

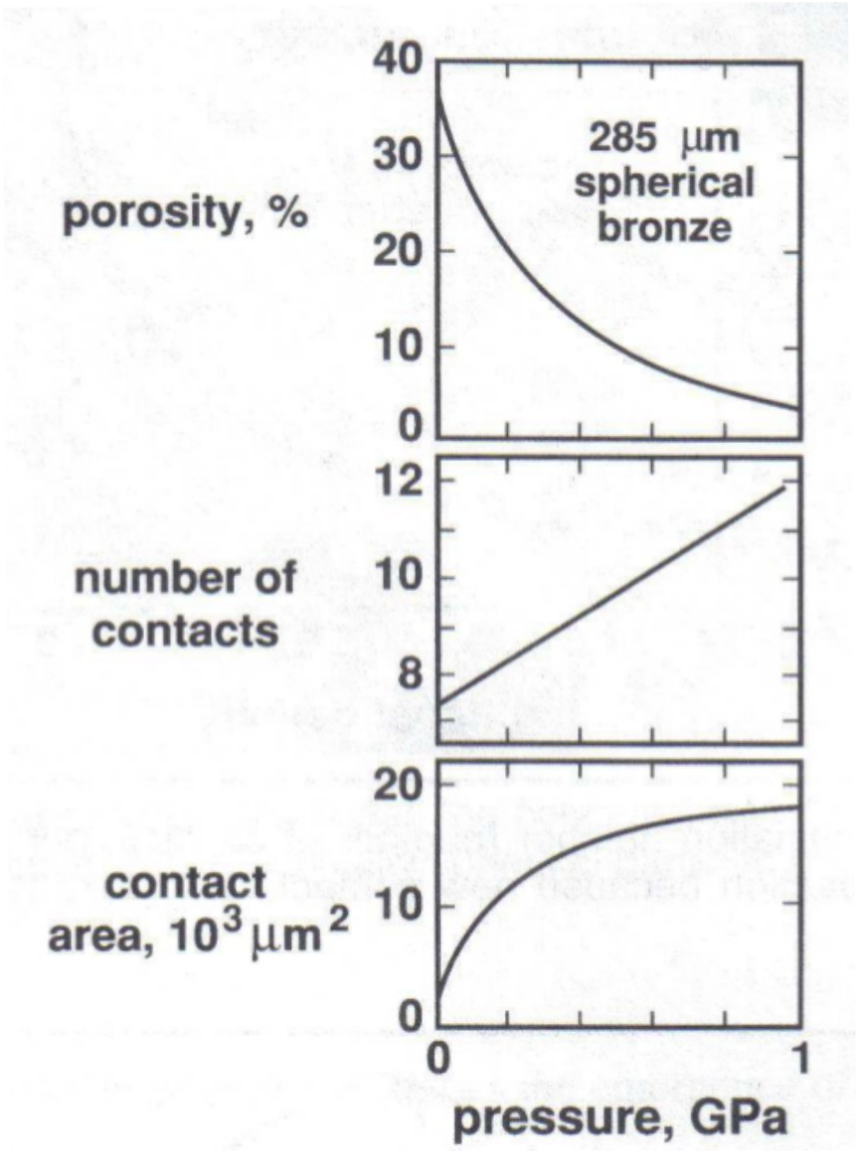

Data for the die compaction of a spherical bronze powder. Compaction involves both particle replacing and deformation mechanisms (German)

The fundamentals of compaction

- There are fundamental obstacles to obtaining a uniform internal stress.
- To maximize uniform internal stress (and therefore maximize uniform internal properties) quite complex pressure protocols (multiple punches) are used

The balance of forces during die compaction

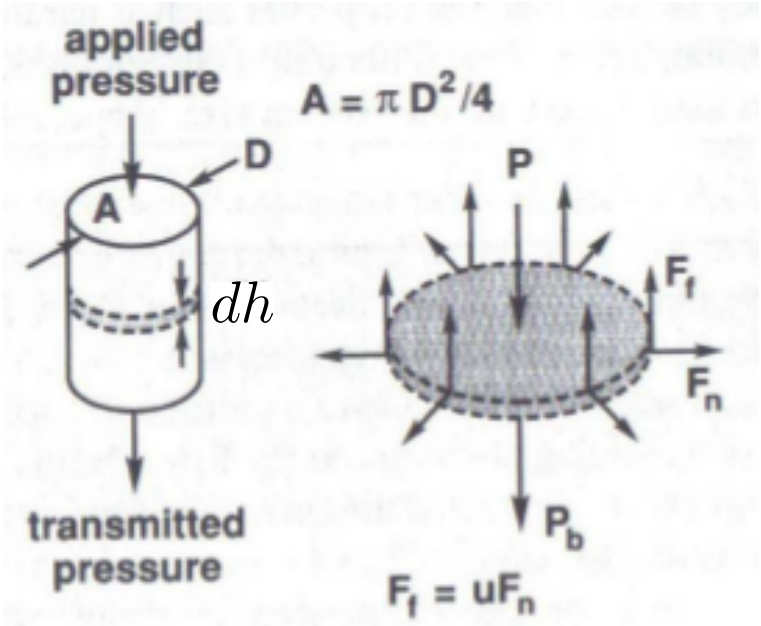

$$A(P - P_{\mathrm{b}}) - F_{\mathrm{f}} = 0$$

$$F_{\mathrm{f}} = \mu F_{\mathrm{n}}$$

$$F_{\mathrm{n}} = \pi D \sigma_{\mathrm{r}} \Delta h = \pi D z P \Delta h$$

$$\Delta P = P_{\mathrm{b}} - P = -\mu \frac{F_{\mathrm{n}}}{A} = -\frac{4\mu z P}{D} \Delta h$$

$$\frac{dP}{dh} = -\frac{4\mu z P}{D}$$

$$P(h) = P \exp\left(-\frac{4\mu z h}{D}\right)$$

Internal pressure profile

- The wall friction contributes to a decreased pressure with depth

$$P(h) = P \exp\left(-\frac{4\mu z h}{D}\right)$$

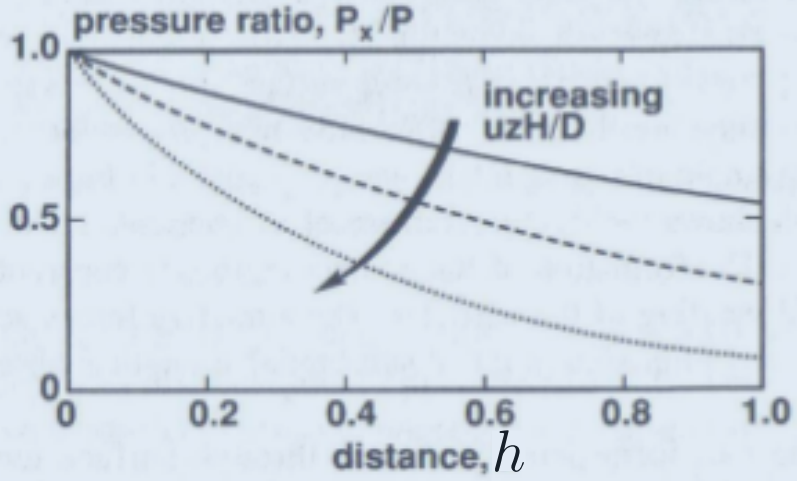

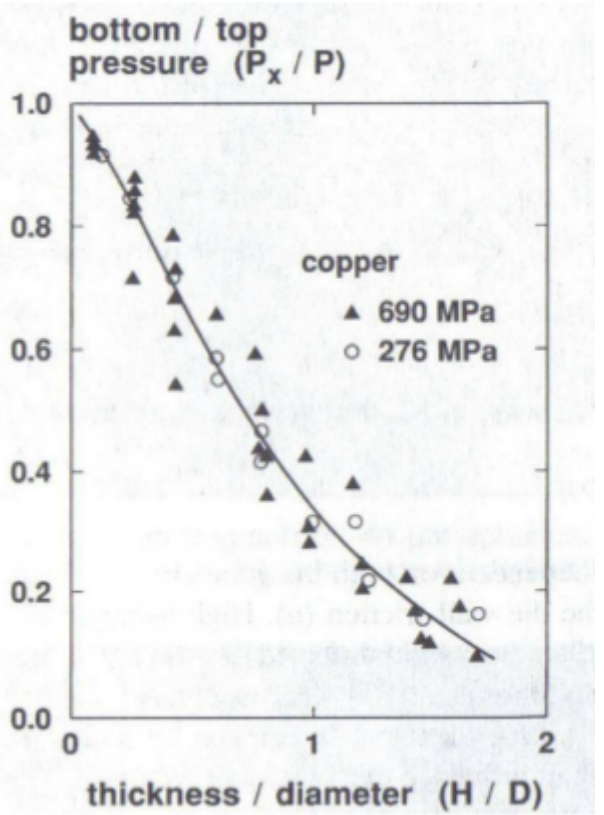

The transmitted pressure in a copper powder compact as a ratio of the compact thickness, with both parameter normalized for the applied pressure and compact geometry (German).

Internal stress profiles

- The average stress within the compact is thus

$$\frac{1}{H}\int_0^H dh\, P(h) = \frac{PD}{4H\mu z}\left(1-\exp\left(-\frac{4\mu z H}{D}\right)\right)$$

$$\approx P\left(1-\frac{2\mu z H}{D}\right)$$

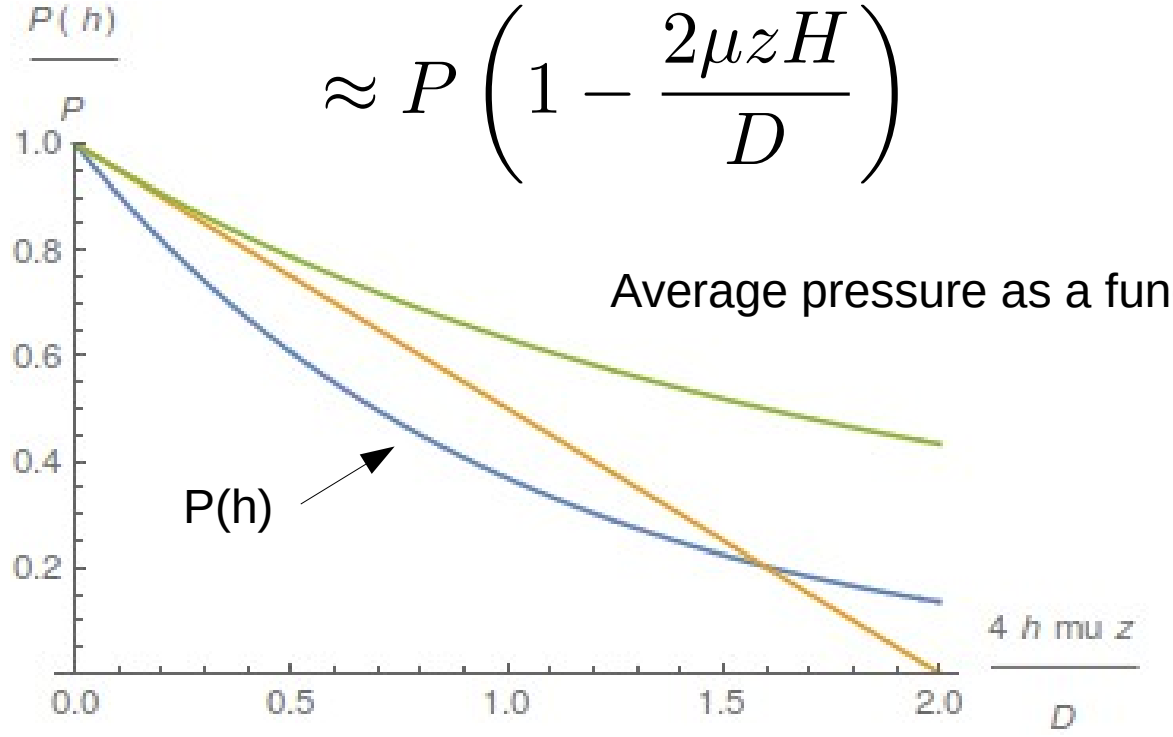

Average pressure as a function of H

Single-action vs double-action pressing

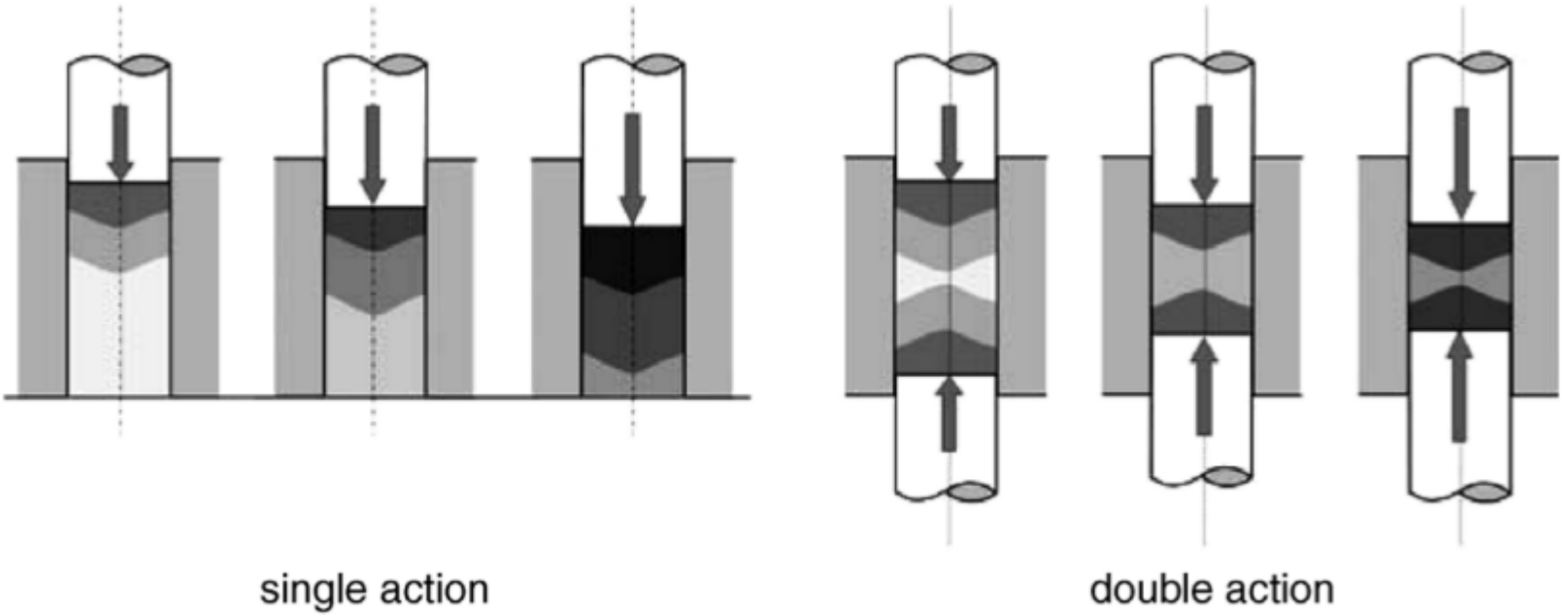

Ceramics Science and Technology: Volume3: Synthesis and Processing, First Edition.
Edited by Ralf Riedel and I-Wei Chen

Internal stress profiles

- Double acting compaction will have a simultaneous pressure profile from both the top and bottom punches.

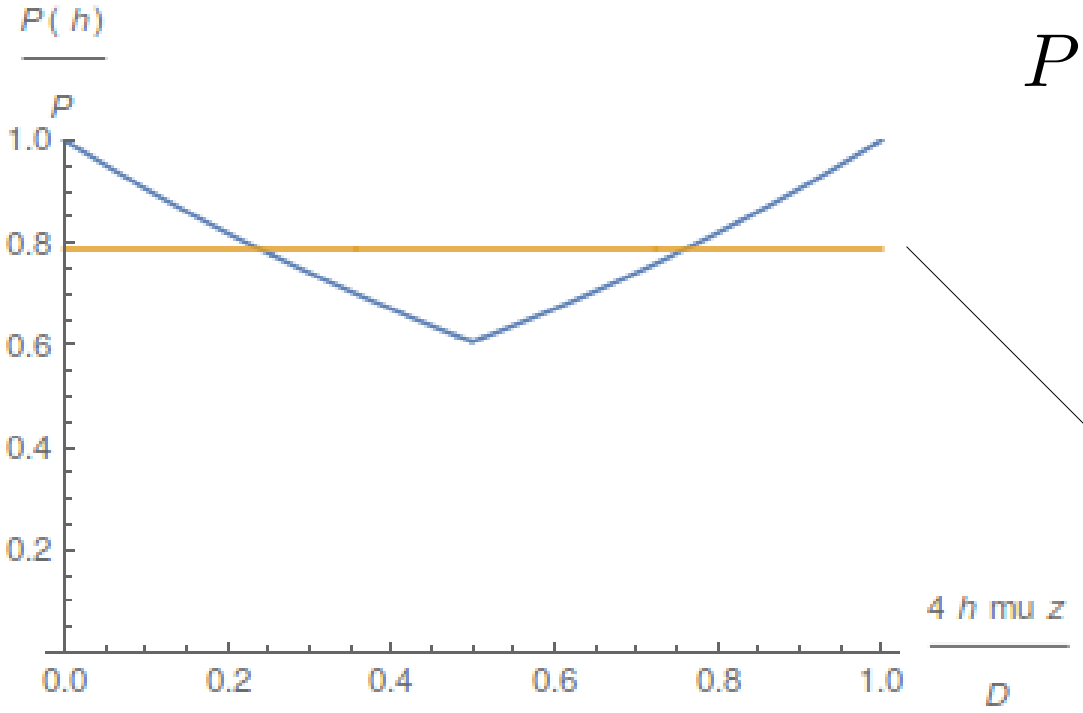

$$P(h) = P \exp\left(-\frac{4\mu z h}{D}\right)$$

The above equation is still valid, but h is taken as the distance to the nearest punch

$$\approx P\left(1 - \frac{\mu z H}{D}\right)$$

Average stress is higher than that for single action compaction.

Internal pressure profiles

- An important factor is the height to diameter ratio.
- As the ratio increases, density gradients in a compact increase and the overall compact density increases

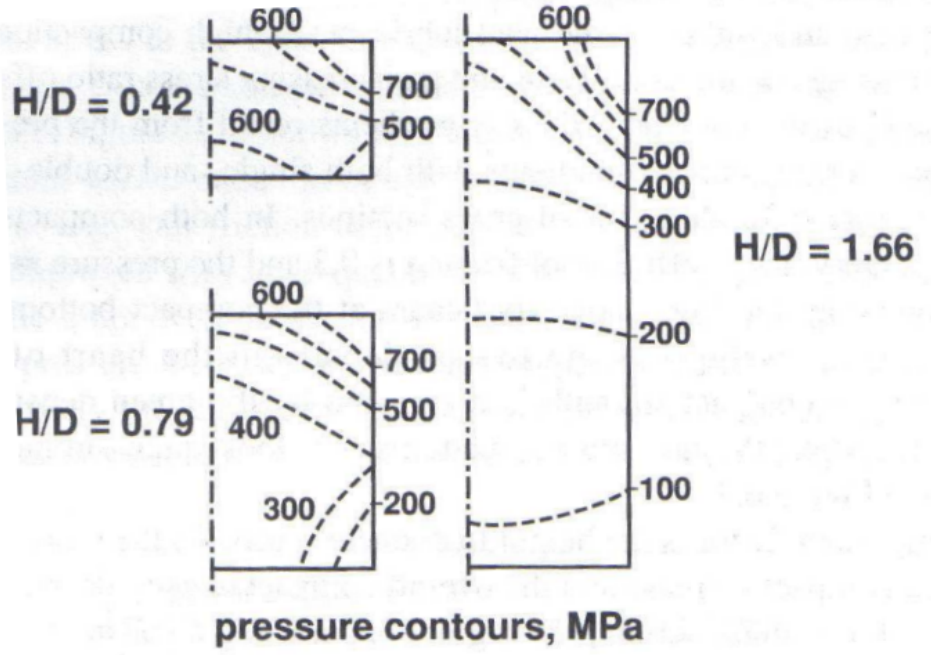

Pressure distributions in compacted copper powder cylinders (single-action pressing). Only the right half of the each cylinder is shown. The applied pressure is 700 Mpa (German)

Density gradients

- Density gradients result from pressure gradients

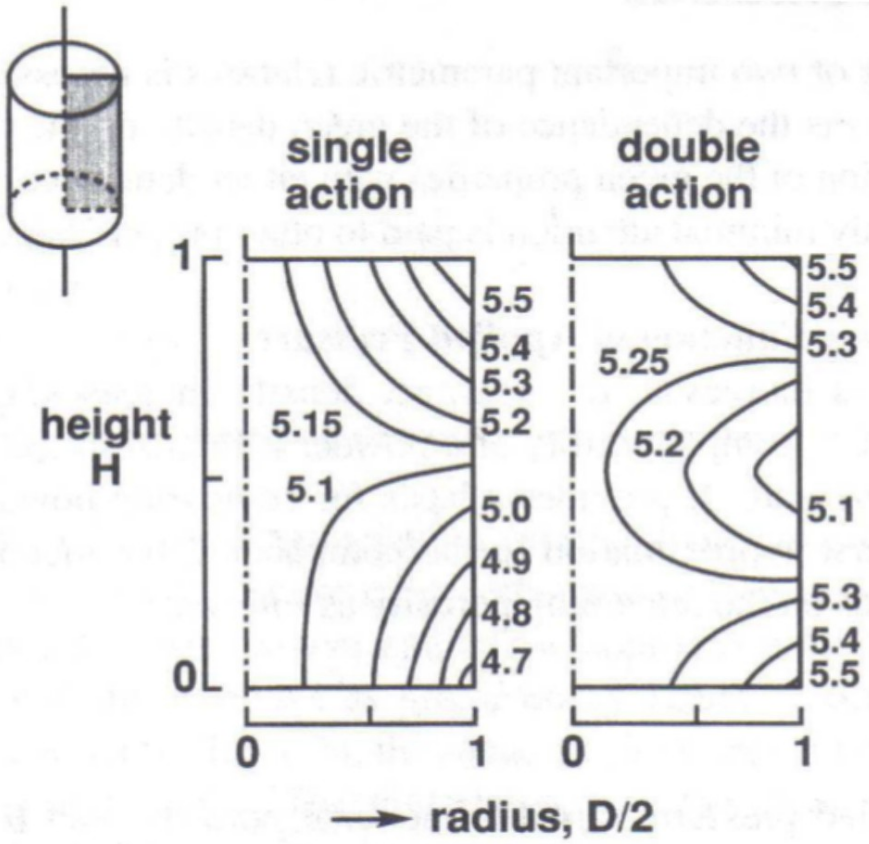

In single action pressing, lowest density occurs at the compact bottom

For the double action pressing the lowest density is at the center of the material

Constant density lines in cylinders of compacted copper powder. Contours are in g/cm^3 [German]

Density profiles from simulation

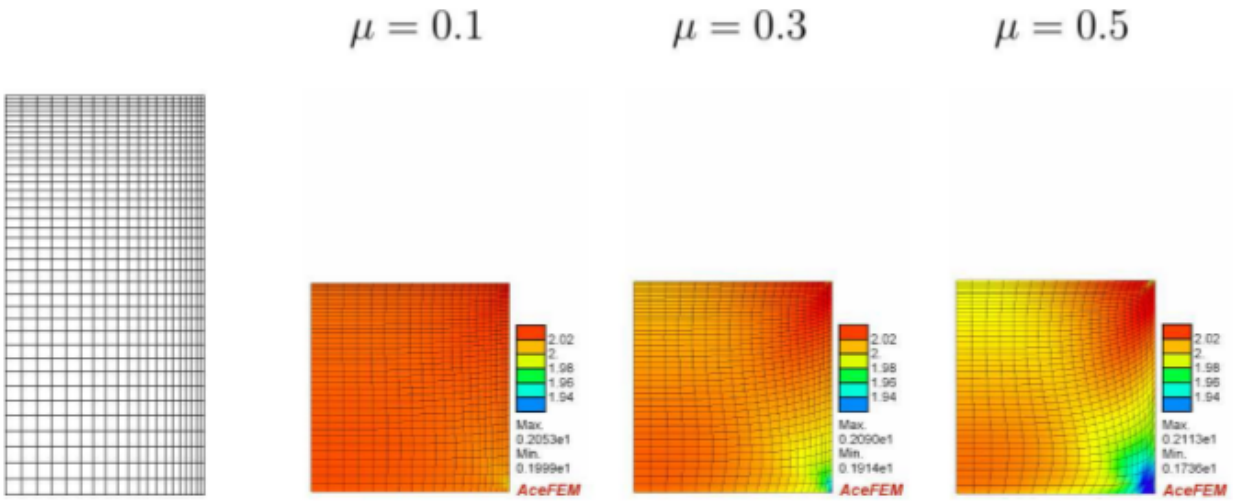

S. Stupkiewicz, A. Piccolroaz, D. Bigoni arXiv:1405.0213v1

Density profiles from simulation

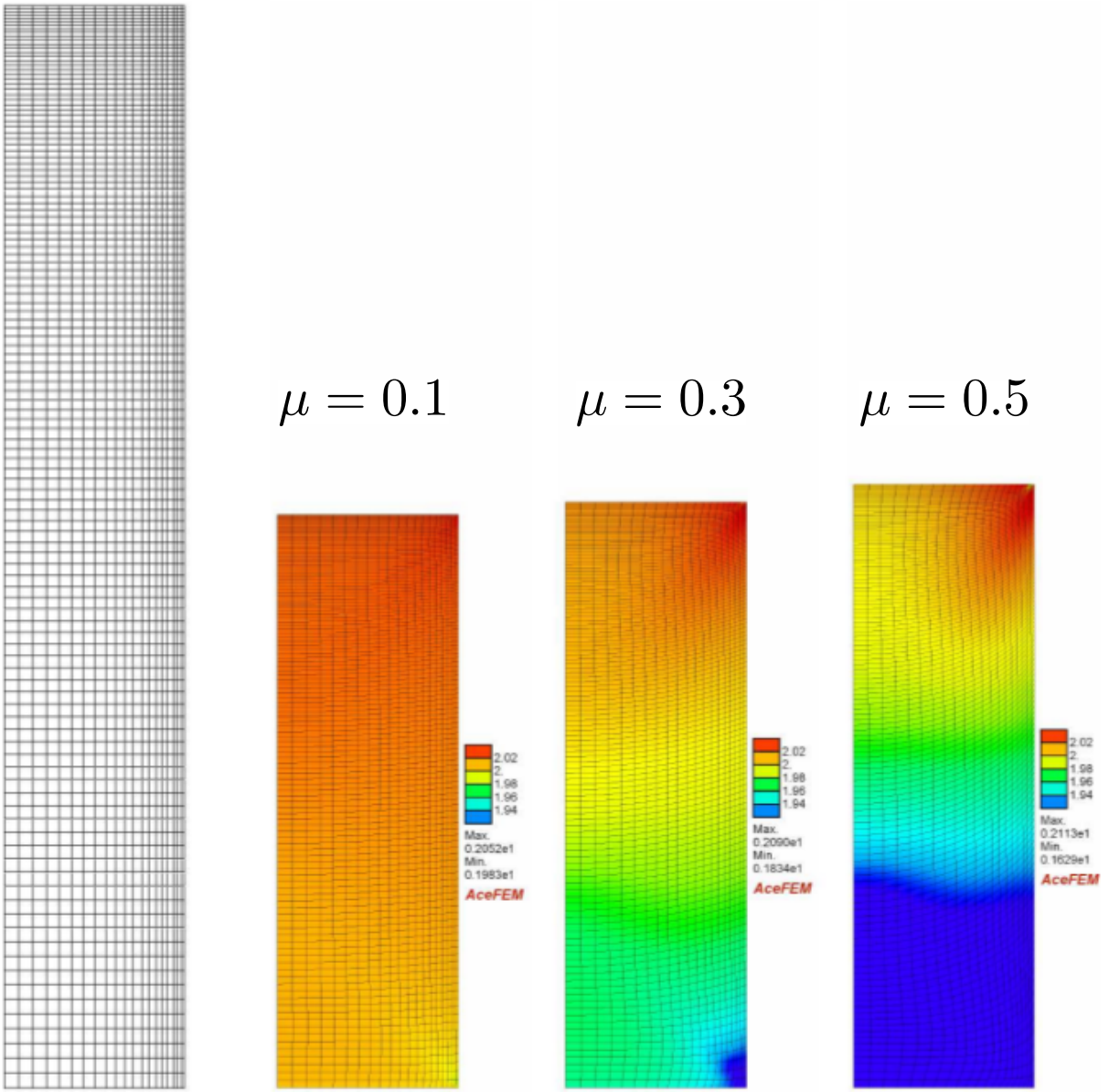

S. Stupkiewicz, A. Piccolroaz, D. Bigoni arXiv:1405.0213v1

Friction can be reduced when powder/wall is lubricated

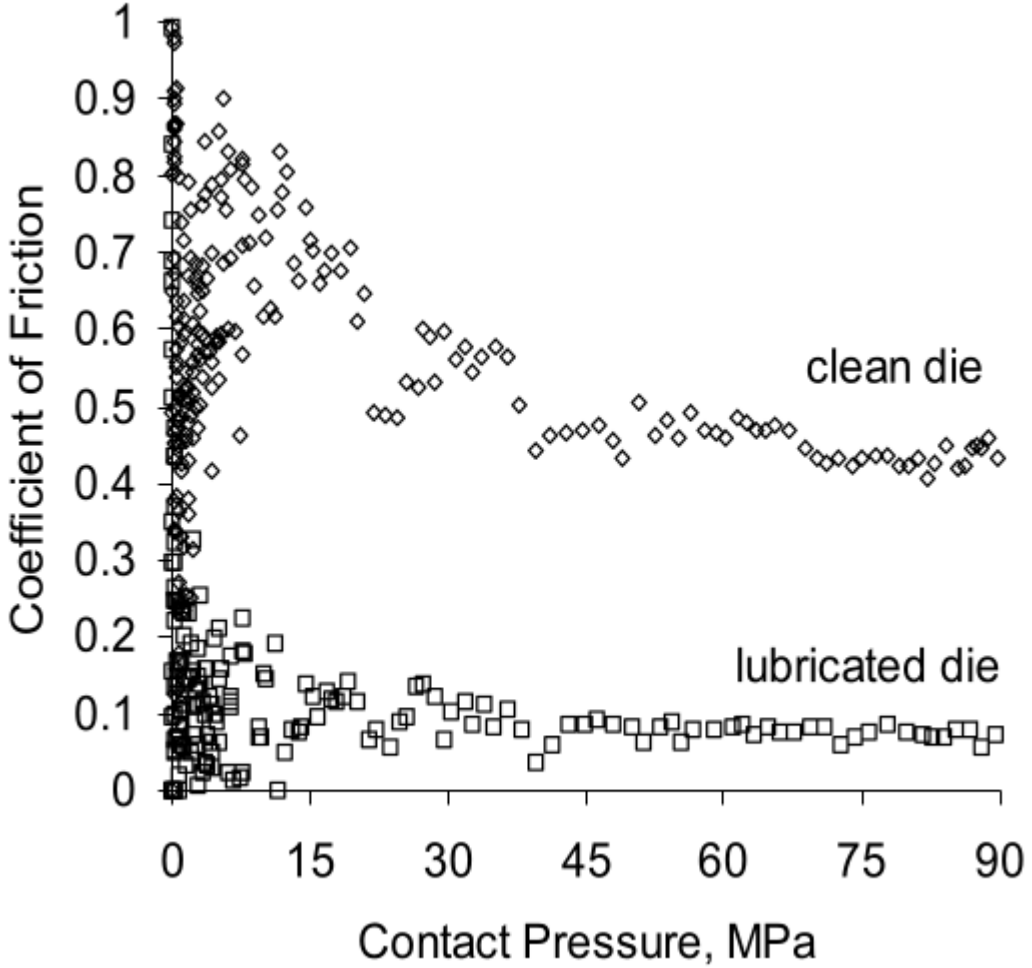

Powder Technology, Vol. 133, Sinka I.C., Cun-ningham J.C. and Zavaliangos A., The effect of wall friction in the compaction of pharmaceutical tablets with curved faces: A vali-
dation study of the Drucker-Prager Cap model,33 (2003)

Friction can be reduced when powder/wall is lubricated

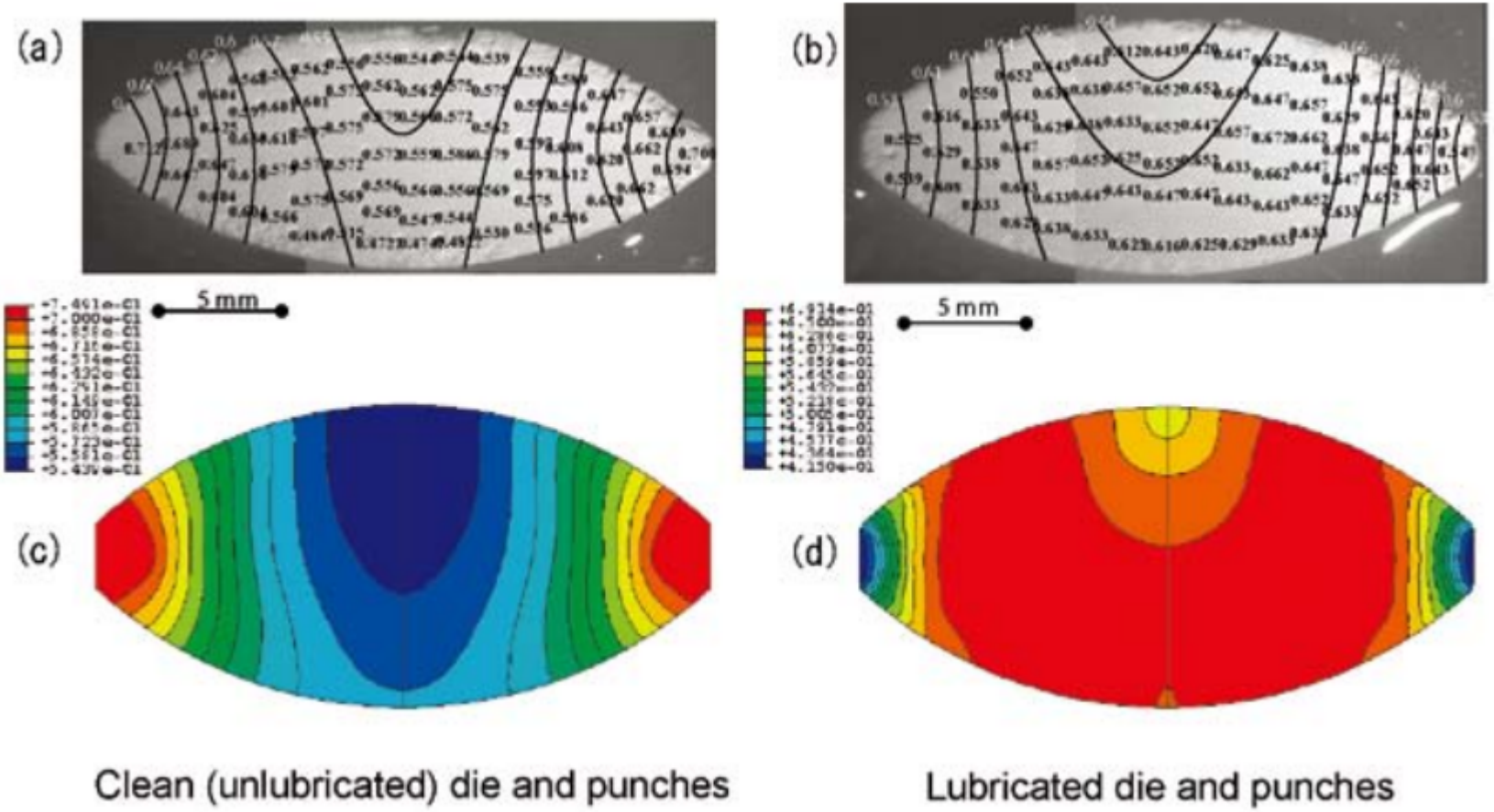

Powder Technology, Vol. 133, Sinka I.C., Cun-ningham J.C. and Zavaliangos A., The effect of wall friction in the compaction of pharmaceutical tablets with curved faces: A validation study of the Drucker-Prager Cap model,33 (2003)

Friction can be reduced when powder/wall is lubricated

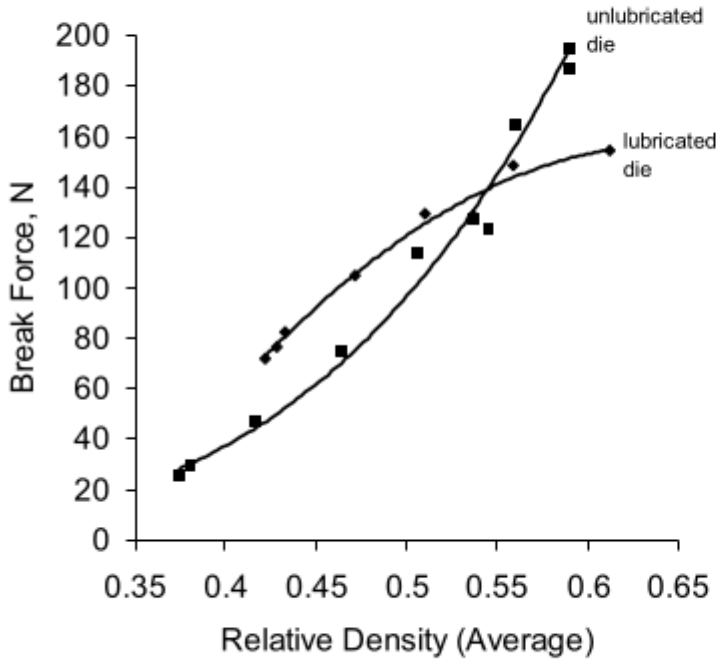

(a)

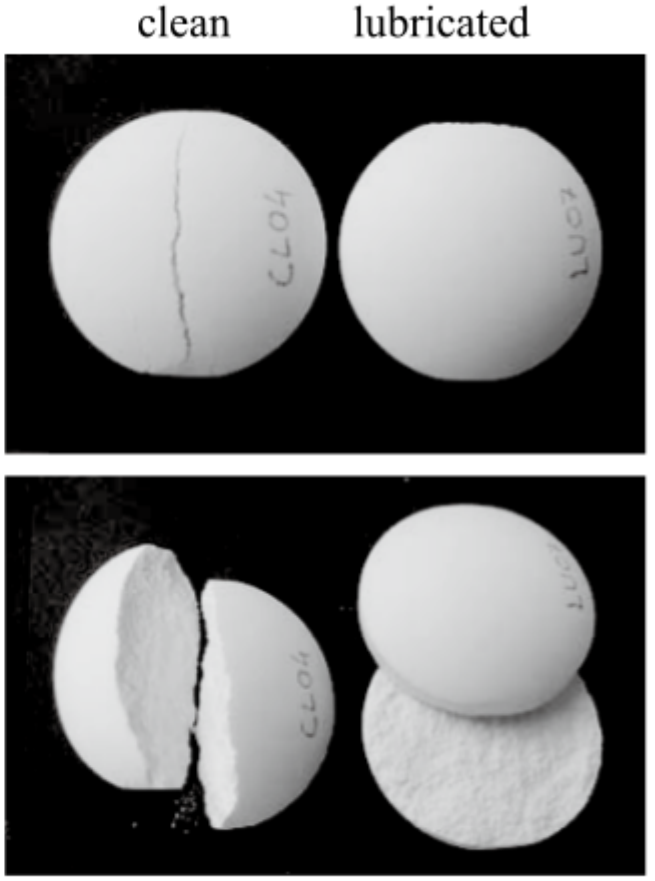

(b)

Powder Technology, Vol. 133, Sinka I.C., Cun-ningham J.C. and Zavaliangos A., The effect of wall friction in the compaction of pharmaceutical tablets with curved faces: A validation study of the Drucker-Prager Cap model,33 (2003)

Green density as a function of applied pressure

The compressibility of a powder is related to the density attained at a present compaction pressure.

$$dp = -\theta p \mathrm{d}P$$

$$\log\left(\frac{p}{p_0}\right) = -\theta P$$

To take into account rearrangement

$$\log\left(\frac{p}{p_0}\right) = B - \theta P$$

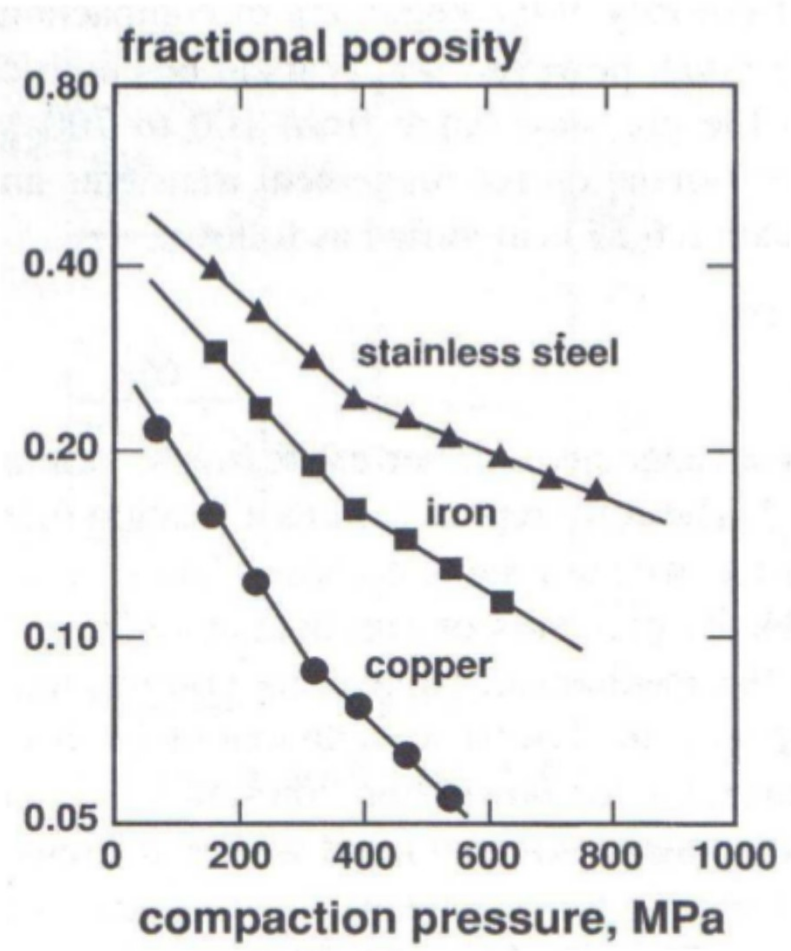

Green density as a function of applied pressure

The compressibility of a powder is related to the density attained at a present compaction pressure.

$$dp = -\theta p \mathrm{d}P$$

$$\log\left(\frac{p}{p_0}\right) = -\theta P$$

To take into account rearrangement

$$\log\left(\frac{p}{p_0}\right) = B - \theta P$$

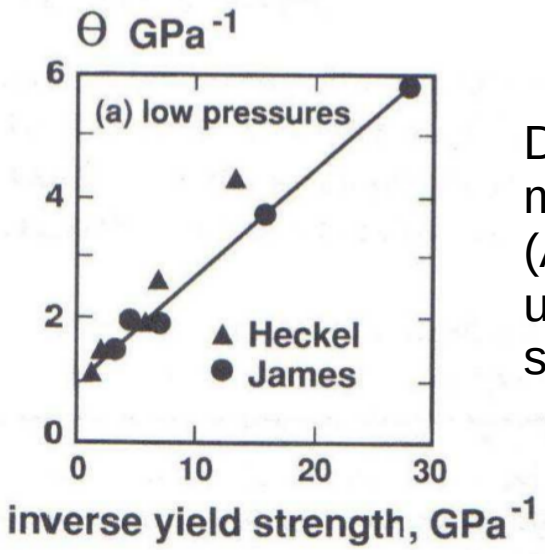

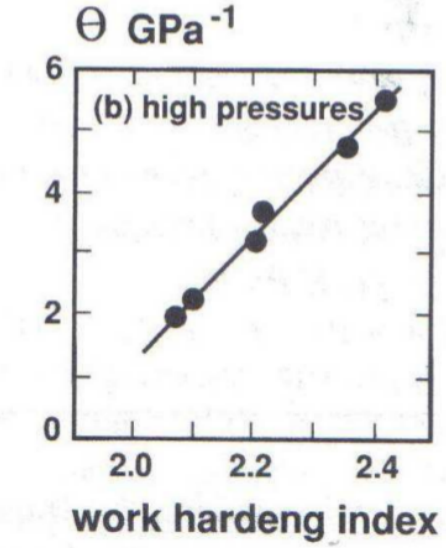

Data for various metal powders (Al,Zn,Ni,Fe,W,Cu and stainless steel) [German]

Green strength variation with density

- Pores reduce the effective load bearing area in a compact, reducing the bulk strength.
- Pores act as stress concentrators and are effective crack initiation sites.

→ Green strength will vary with density

$$\sigma = \sigma_0 C f(\rho)$$

For mono-sized spheres, the strength is directly linked to the contact zone size which depends on the pressed density

$$\sigma = \sigma_0 C \rho^m$$

Often, a power-law is seen (typically m~6)

Constitutive Modelling

- The basic components:
  - Equilibrium equations (balance of forces transmitted through the material)
  - Continuity equation (conservation of mass)
  - Geometry of the problem
  - Constitutive behavior of the powder (stress– strain behavior)
  - Boundary conditions including loading (e.g.,displacement and velocity) and friction between the tooling and the powder
  - Initial conditions (e.g., initial relative density of powder)

Elastoplastic Constitutive Models

3 components of the constitutive model that need to be defined:

- the yield criterion, which defines the transition of elastic to plastic deformation
- the plastic flow potential, which dictates the relative amounts of each component of the plastic flow
- the evolution of the microstructure, which in turn defines the resistance to further deformation.

Elastoplastic Constitutive Models

Some basic ingredients

Strain $$d\epsilon_{ij} = d\epsilon_{ij}^{\mathrm{el}} + d\epsilon_{ij}^{\mathrm{pl}}$$

Stress $$d\sigma_{ij} = \sum_{kl} C_{ijkl} d\epsilon_{kl}^{\mathrm{el}}$$

Yield function $$F(\sigma_{ij}; k_1, k_2, \dots) \begin{cases} \leq 0 & \text{Elastic deformation} \\ > 0 & \text{Plastic deformation} \end{cases}$$

The k_n are internal state variables characterizing all aspects of the material that affect yielding.

Elasticity

$$d\sigma_{ij} = \sum_{kl} C_{ijkl} d\varepsilon_{kl}^{\mathrm{el}}$$

By taking advantage of the symmetry of the stress and strain tensors, the stress and strain tensors can be represented as six-dimensional vectors

$$[\boldsymbol{\sigma}] = \begin{bmatrix} \sigma_{11} \\ \sigma_{22} \\ \sigma_{33} \\ \sigma_{23} \\ \sigma_{13} \\ \sigma_{12} \end{bmatrix} \equiv \begin{bmatrix} \sigma_1 \\ \sigma_2 \\ \sigma_3 \\ \sigma_4 \\ \sigma_5 \\ \sigma_6 \end{bmatrix} \quad ; \quad [\boldsymbol{\varepsilon}] = \begin{bmatrix} \varepsilon_{11} \\ \varepsilon_{22} \\ \varepsilon_{33} \\ 2\varepsilon_{23} \\ 2\varepsilon_{13} \\ 2\varepsilon_{12} \end{bmatrix} \equiv \begin{bmatrix} \varepsilon_1 \\ \varepsilon_2 \\ \varepsilon_3 \\ \varepsilon_4 \\ \varepsilon_5 \\ \varepsilon_6 \end{bmatrix}$$

And the 4th rank elasticity tensor as a matrix

$$[\mathsf{C}] = \begin{bmatrix} c_{1111} & c_{1122} & c_{1133} & c_{1123} & c_{1131} & c_{1112} \\ c_{2211} & c_{2222} & c_{2233} & c_{2223} & c_{2231} & c_{2212} \\ c_{3311} & c_{3322} & c_{3333} & c_{3323} & c_{3331} & c_{3312} \\ c_{2311} & c_{2322} & c_{2333} & c_{2323} & c_{2331} & c_{2312} \\ c_{3111} & c_{3122} & c_{3133} & c_{3123} & c_{3131} & c_{3112} \\ c_{1211} & c_{1222} & c_{1233} & c_{1223} & c_{1231} & c_{1212} \end{bmatrix} \equiv \begin{bmatrix} C_{11} & C_{12} & C_{13} & C_{14} & C_{15} & C_{16} \\ C_{12} & C_{22} & C_{23} & C_{24} & C_{25} & C_{26} \\ C_{13} & C_{23} & C_{33} & C_{34} & C_{35} & C_{36} \\ C_{14} & C_{24} & C_{34} & C_{44} & C_{45} & C_{46} \\ C_{15} & C_{25} & C_{35} & C_{45} & C_{55} & C_{56} \\ C_{16} & C_{26} & C_{36} & C_{46} & C_{56} & C_{66} \end{bmatrix}$$

The is referred to as the Voigt notation

Elasticity

$$[\mathsf{C}] = \begin{bmatrix} C_{11} & C_{12} & C_{13} & C_{14} & C_{15} & C_{16} \\ C_{12} & C_{22} & C_{23} & C_{24} & C_{25} & C_{26} \\ C_{13} & C_{23} & C_{33} & C_{34} & C_{35} & C_{36} \\ C_{14} & C_{24} & C_{34} & C_{44} & C_{45} & C_{46} \\ C_{15} & C_{25} & C_{35} & C_{45} & C_{55} & C_{56} \\ C_{16} & C_{26} & C_{36} & C_{46} & C_{56} & C_{66} \end{bmatrix}$$

$$\sigma_{\text{tensile}} = E\epsilon_{\text{tensile}}$$

For an elastically isotropic materials defined by a Youngs modulus (E) and Poisson ratio (ν), elastic stiffness matrix simplifies further

$$[\mathsf{C}] = \frac{E}{(1+\nu)(1-2\nu)} \begin{bmatrix} 1-\nu & \nu & \nu & 0 & 0 & 0 \\ \nu & 1-\nu & \nu & 0 & 0 & 0 \\ \nu & \nu & 1-\nu & 0 & 0 & 0 \\ 0 & 0 & 0 & (1-2\nu)/2 & 0 & 0 \\ 0 & 0 & 0 & 0 & (1-2\nu)/2 & 0 \\ 0 & 0 & 0 & 0 & 0 & (1-2\nu)/2 \end{bmatrix}$$

Bulk modulus → $K = \frac{E}{3(1-2\nu)}$ $\quad P = K(\epsilon_{11} + \epsilon_{22} + \epsilon_{33})$

Shear modulus → $G = \frac{E}{2(1+\nu)}$ $\quad \sigma_{xy} = G\gamma_{xy}$

Yield function

Yield function $F(\sigma_{ij}; k_1, k_2, \dots)$ $\begin{cases} \leq 0 & \text{Elastic deformation} \\ > 0 & \text{Plastic deformation} \end{cases}$

On what parts of the stress tensor should the yield function depend?

For isotropic materials, the representation of the stress state can be simplified by use of stress invariants.

These invariants should characterize pressure and shear

The Stress Invariants

$$I_1 = \sigma_{11} + \sigma_{22} + \sigma_{33}$$

$$I_2 = \begin{vmatrix} \sigma_{22} & \sigma_{23} \\ \sigma_{32} & \sigma_{33} \end{vmatrix} + \begin{vmatrix} \sigma_{11} & \sigma_{13} \\ \sigma_{31} & \sigma_{33} \end{vmatrix} + \begin{vmatrix} \sigma_{11} & \sigma_{12} \\ \sigma_{21} & \sigma_{22} \end{vmatrix}$$
$$= \sigma_{11}\sigma_{22} + \sigma_{22}\sigma_{33} + \sigma_{11}\sigma_{33} - \sigma_{12}^2 - \sigma_{23}^2 - \sigma_{13}^2$$

$$I_3 = \begin{vmatrix} \sigma_{11} & \sigma_{12} & \sigma_{13} \\ \sigma_{21} & \sigma_{22} & \sigma_{23} \\ \sigma_{31} & \sigma_{32} & \sigma_{33} \end{vmatrix}$$
$$= \sigma_{11}\sigma_{22}\sigma_{33} + 2\sigma_{12}\sigma_{23}\sigma_{31} - \sigma_{12}^2\sigma_{33} - \sigma_{23}^2\sigma_{11} - \sigma_{13}^2\sigma_{22}$$

$$P = \frac{1}{3}\left(\sigma_{11} + \sigma_{22} + \sigma_{33}\right) = \frac{1}{3}I_1$$

Hydrostatic pressure

The Stress Invariants

$$
\begin{aligned}
s_{ij} = &\quad \sigma_{ij} - p\delta_{ij} \\
&= \begin{bmatrix} \sigma_{11} - p & \sigma_{12} & \sigma_{13} \\ \sigma_{21} & \sigma_{22} - p & \sigma_{23} \\ \sigma_{31} & \sigma_{32} & \sigma_{33} - p \end{bmatrix}
\end{aligned}
$$

$$
\begin{aligned}
J_2 = &\quad \frac{1}{6}\left[(\sigma_{11} - \sigma_{22})^2 + (\sigma_{22} - \sigma_{33})^2 + (\sigma_{33} - \sigma_{11})^2\right] \\
&+\sigma_{12}^2 + \sigma_{23}^2 + \sigma_{31}^2 \\
= &\quad \frac{1}{3} I_1^2 - I_2
\end{aligned}
$$

$$\sigma_{\mathrm{v}} = \sqrt{3J_2}$$

von Mises stress

von Mises yield criterion

This criterion for the onset of yield in ductile materials was first formulated by Maxwell in 1865 but is generally attributed to von Mises in 1913 . Von Mises yield criterion can be interpreted physically in terms of the maximum distortion strain energy. This states that yielding in 3-D occurs when the distortion strain
energy reaches that required for yielding in uniaxial loading.

$$\sigma_{\mathrm{v}}^2 \leq \sigma_{\mathrm{y}}^2$$

Load scenario	Restrictions	Simplified von Mises equation
General	No restrictions	$\sigma_v = \sqrt{\frac{1}{2}[(\sigma_{11}-\sigma_{22})^2 + (\sigma_{22}-\sigma_{33})^2 + (\sigma_{33}-\sigma_{11})^2 + 6(\sigma_{12}^2+\sigma_{23}^2+\sigma_{31}^2)]}$
Principal stresses	No restrictions	$\sigma_v = \sqrt{\frac{1}{2}[(\sigma_1-\sigma_2)^2 + (\sigma_2-\sigma_3)^2 + (\sigma_3-\sigma_1)^2]}$
General plane stress	$\sigma_3 = 0$ $\sigma_{31} = \sigma_{23} = 0$	$\sigma_v = \sqrt{\sigma_{11}^2 - \sigma_{11}\sigma_{22} + \sigma_{22}^2 + 3\sigma_{12}^2}$
Principal plane stress	$\sigma_3 = 0$ $\sigma_{12} = \sigma_{31} = \sigma_{23} = 0$	$\sigma_v = \sqrt{\sigma_1^2 - \sigma_1\sigma_2 + \sigma_2^2}$
Pure shear	$\sigma_1 = \sigma_2 = \sigma_3 = 0$ $\sigma_{31} = \sigma_{23} = 0$	$\sigma_v = \sqrt{3}\lvert\sigma_{12}\rvert$
Uniaxial	$\sigma_2 = \sigma_3 = 0$ $\sigma_{12} = \sigma_{31} = \sigma_{23} = 0$	$\sigma_v = \sigma_1$

https://en.wikipedia.org/wiki/Von_Mises_yield_criterion

von Mises yield criterion

Coordinate transformation

$$\begin{bmatrix} \sigma_{xx} & \sigma_{xy} & \sigma_{xz} \\ \sigma_{xy} & \sigma_{yy} & \sigma_{yz} \\ \sigma_{xz} & \sigma_{yz} & \sigma_{zz} \end{bmatrix} \longrightarrow \begin{bmatrix} \sigma_1 & 0 & 0 \\ 0 & \sigma_2 & 0 \\ 0 & 0 & \sigma_3 \end{bmatrix}$$

Von Mises stress

$$\frac{1}{2}\left((\sigma_1-\sigma_2)^2+(\sigma_1-\sigma_3)^2+(\sigma_2-\sigma_3)^2\right)\leq\sigma_{\mathrm{y}}^2$$

von Mises yield criterion

$$\frac{1}{2}\left((\sigma_1-\sigma_2)^2+(\sigma_1-\sigma_3)^2+(\sigma_2-\sigma_3)^2\right)\leq\sigma_{\mathrm{y}}^2$$

$$F(\sigma_{ij};k_1,k_2,\dots)=\frac{1}{2}\left((\sigma_1-\sigma_2)^2+(\sigma_1-\sigma_3)^2+(\sigma_2-\sigma_3)^2\right)-\sigma_{\mathrm{y}}(\sigma_{ij};k_1,k_2,\dots)^2$$

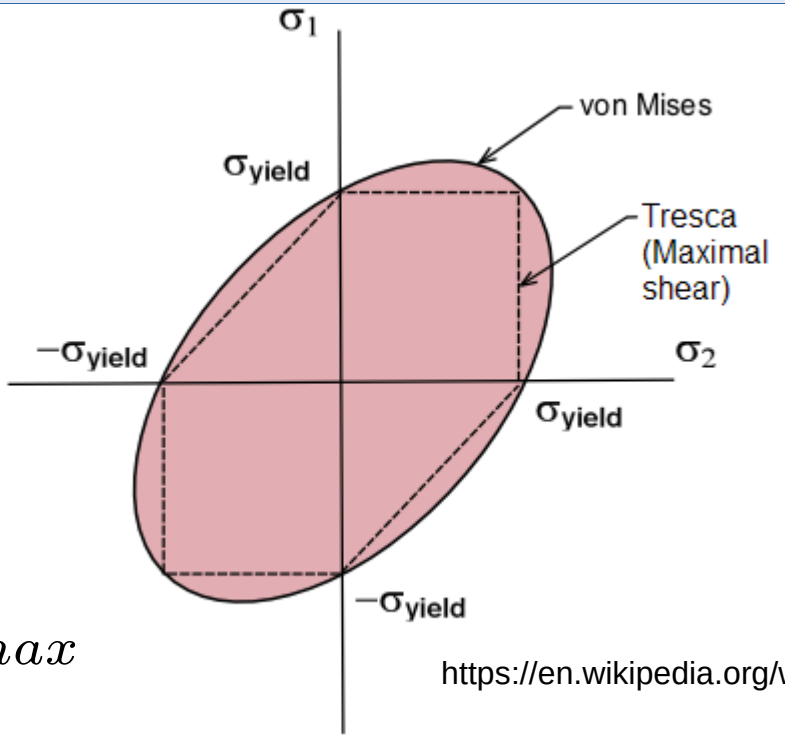

$$\sigma_{tresca}=\sigma_1-\sigma_2>\sigma_{max}$$

https://en.wikipedia.org/wiki/Von_Mises_yield_criterion

Elastoplastic Constitutive Models

Some basic ingredients

When the yield condition is satisfied, a flow potential is postulated to exist and determines the three dimensional character of plastic deformation:

Flow potential $$d\varepsilon_{ij}^{\mathrm{p}} = d\lambda \frac{\partial G(\sigma_{ij}; k_1, k_2, \dots)}{\partial \sigma_{ij}}$$

strain hardening parameter

The final constitutive model

Material properties

$$C_{ijkl}(\rho_{\mathrm{r}})$$

$$F(p, q; \rho_{\mathrm{r}})$$

$$G(p, q; \rho_{\mathrm{r}})$$

In the above there is one k_i, and it is taken as the relative density.

$$d\varepsilon_{ij} = d\varepsilon_{ij}^{\mathrm{e}} + d\varepsilon_{ij}^{\mathrm{p}}$$

$$d\sigma_{ij} = \sum_{kl} C_{ijkl} d\varepsilon_{kl}^{\mathrm{e}}$$

$$d\varepsilon_{ij}^{\mathrm{p}} = d\lambda \frac{\partial G(\sigma_{ij}; \rho_{\mathrm{r}})}{\partial \sigma_{ij}}$$

$$d\rho_{\mathrm{r}} = \rho_{\mathrm{r}} \sum_{i=1,3} d\varepsilon_{ii}^{\mathrm{p}}$$

$$= \rho_{\mathrm{r}} d\varepsilon_{\mathrm{v}}^{\mathrm{p}}$$

The FEM approach to constitutive modelling

The finite element method (FEM) is a numerical technique for finding approximate solutions to boundary value problems for partial differential equations. It is also referred to as finite element analysis (FEA). It subdivides a large problem into smaller, simpler parts. The simple equations that model these finite elements are then assembled into a larger system of equations that models the entire problem.

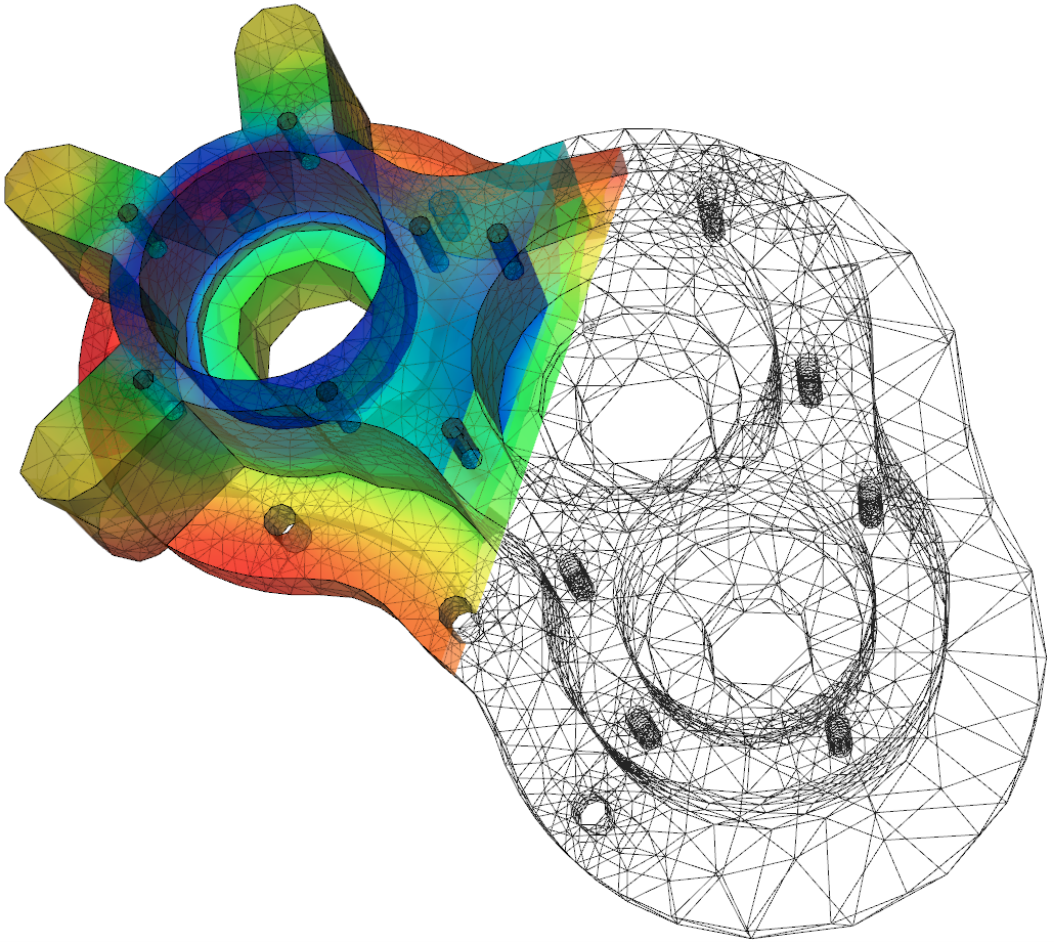

https://en.wikipedia.org/wiki/Finite_element_method

The p and q variables

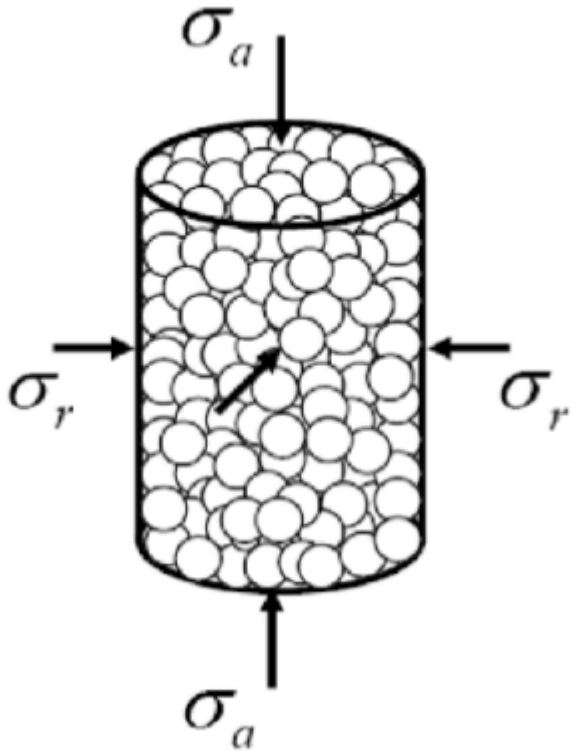

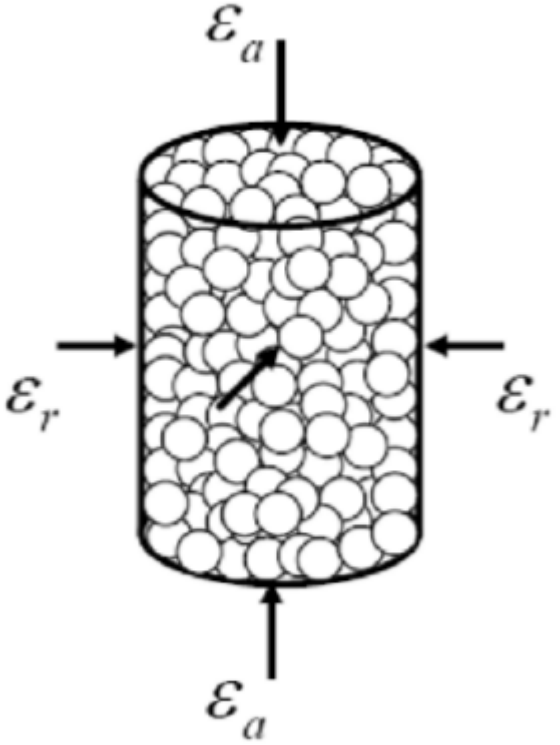

$$p = \frac{1}{3}\left(\sigma_{\mathrm{a}} + 2\sigma_{\mathrm{r}}\right) \qquad \varepsilon_{\mathrm{v}} = \varepsilon_{\mathrm{a}} + 2\varepsilon_{\mathrm{r}}$$

$$q = \left|\sigma_{\mathrm{a}} - \sigma_{\mathrm{r}}\right| \qquad \varepsilon_{\mathrm{e}} = \frac{2}{3}\left(\varepsilon_{\mathrm{a}} - \varepsilon_{\mathrm{r}}\right)$$

$$\varepsilon_{\mathrm{v}} = \frac{p}{K}$$

$$\varepsilon_{\mathrm{e}} = \frac{q}{3G}$$

Porous elasticity model

$$\Delta\varepsilon_{\mathrm{vol}}^{\mathrm{el}} = \log\left(\frac{\rho_{\mathrm{r}}^{0}}{\rho_{\mathrm{r}}}\right) = \log\left(\frac{1+e}{1+e_0}\right)$$

$$e = \frac{V - V_{\mathrm{bulk}}}{V_{\mathrm{bulk}}}$$

→ Volume occupied by the voids

→ Volume occupied by the solid

$$e = \frac{1-\rho_{\mathrm{r}}}{\rho_{\mathrm{r}}}$$

Relative density

The porous elasticity model is based on the experimental observation that in porous materials during elastic straining, the change in void ratio and the change in the logarithm of the equivalent pressure stress are linear related

$$de^{\mathrm{el}} = -\kappa d\left(\ln P\right)$$

$$P = P_0 \exp\left(\frac{e_0 - e}{\kappa}\right) = P_0 \exp\left(\frac{1}{\kappa}\left(\frac{1}{\rho_{\mathrm{r}}^{0}} - \frac{1}{\rho_{\mathrm{r}}}\right)\right)$$

$$= P_0 \exp\left(\frac{1}{\kappa\rho_{\mathrm{r}}^{0}}\left(1 - \exp\Delta\varepsilon_{\mathrm{vol}}^{\mathrm{el}}\right)\right)$$

Porous elasticity model

$$P = P_0 \exp\left(\frac{e_0 - e}{\kappa}\right) = P_0 \exp\left(\frac{1}{\kappa \rho_{\mathrm{r}}^0}\left(1 - \exp \Delta\varepsilon_{\mathrm{vol}}^{\mathrm{el}}\right)\right)$$

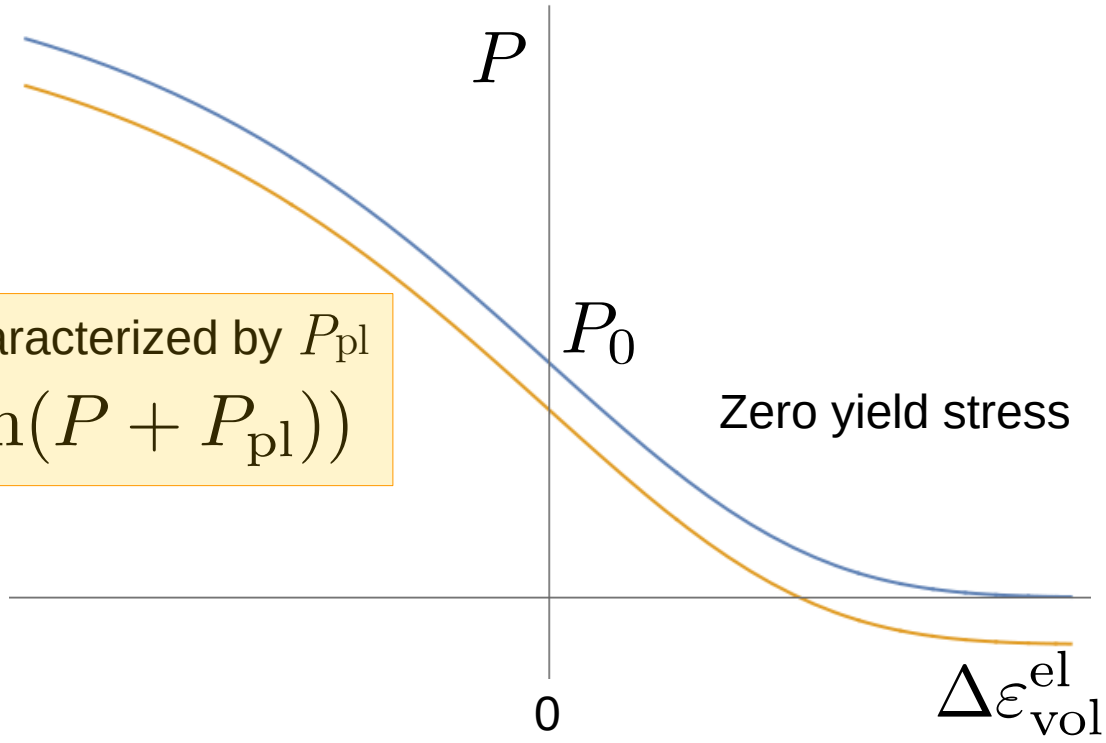

Finite yield stress characterized by P_{pl}

$$de^{\mathrm{el}} = -\kappa d\left(\ln(P + P_{\mathrm{pl}})\right)$$

Or assume linear elasticity but with elastic constant dependence on relative density

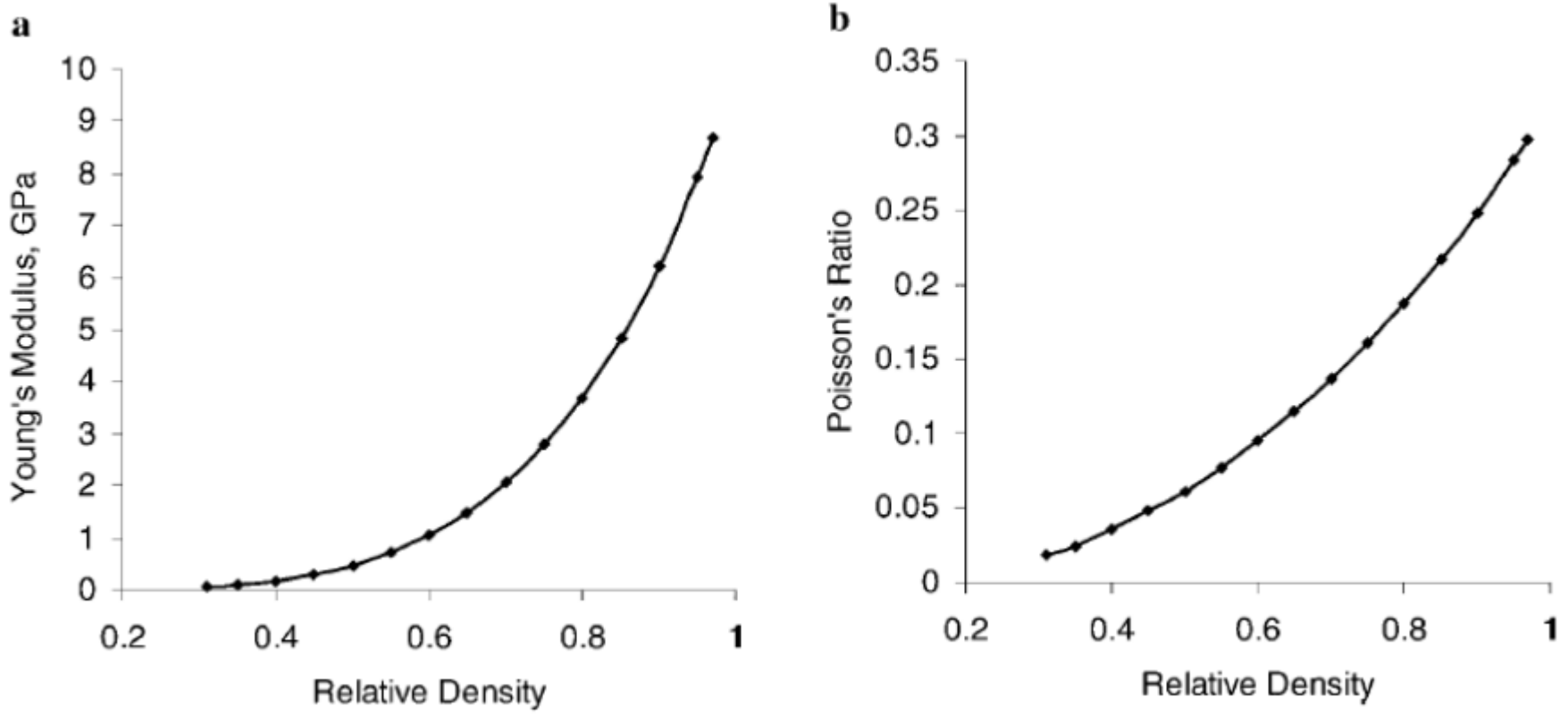

During a deformation, the relative density will change, and so will the elastic properties

Caution: Porous elastic and Plastic conventions

$$\Delta\varepsilon_{\mathrm{vol}}^{\mathrm{el}} = \log\left(\frac{\rho_{\mathrm{r}}^{0}}{\rho_{\mathrm{r}}}\right)$$

$$\rho = \rho_{\mathrm{r}}^{0}\exp\left(-\Delta\varepsilon_{\mathrm{vol}}^{\mathrm{el}}\right)$$

$$\rho \approx \rho_{\mathrm{r}}^{0}\left(1-\Delta\varepsilon_{\mathrm{vol}}^{\mathrm{el}}\right) \rightarrow d\rho_{\mathrm{r}} = -\rho_{\mathrm{r}} d\varepsilon_{\mathrm{vol}}^{\mathrm{el}}$$

Porous elastic model

$$d\rho_{\mathrm{r}} = \rho_{\mathrm{r}} d\varepsilon_{\mathrm{v}}^{\mathrm{p}}$$

Plastic regime

Yield surfaces & associated models

- If the model is “associated” then the yield and flow functions are the same → the yield surface and the plastic potential surface are coincident and, as a consequence, the plastic strain increment is normal to the yield surface.

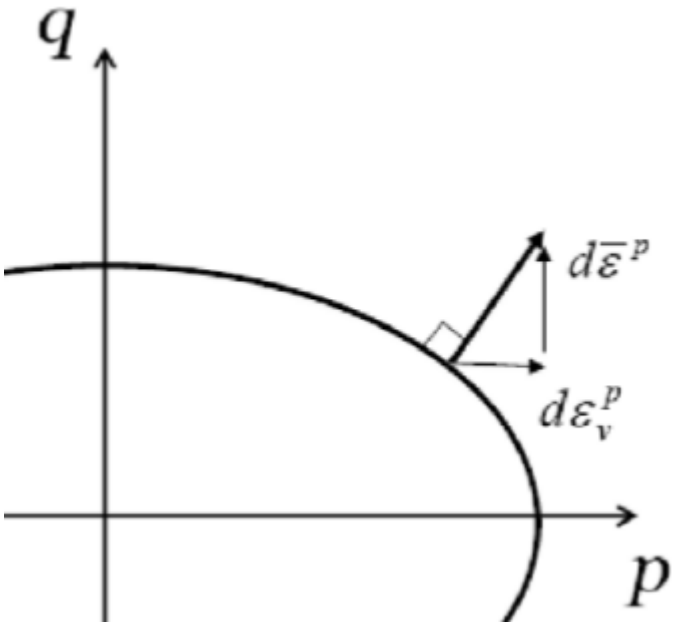

$$G(p, q; \rho_{\mathrm{r}}) = F(p, q; \rho_{\mathrm{r}})$$

$$d\varepsilon_{\mathrm{v}}^{\mathrm{p}} = d\lambda \frac{\partial F(p, q, \rho_{\mathrm{r}})}{\partial p}$$

$$d\varepsilon^{\mathrm{q}} = d\lambda \frac{\partial F(p, q, \rho_{\mathrm{r}})}{\partial q}$$

Compaction → densification

Yield surfaces & associated models

- If the model is “associated” then the yield and flow functions are the same → the yield surface and the plastic potential surface are coincident and, as a consequence, the plastic strain increment is normal to the yield surface.

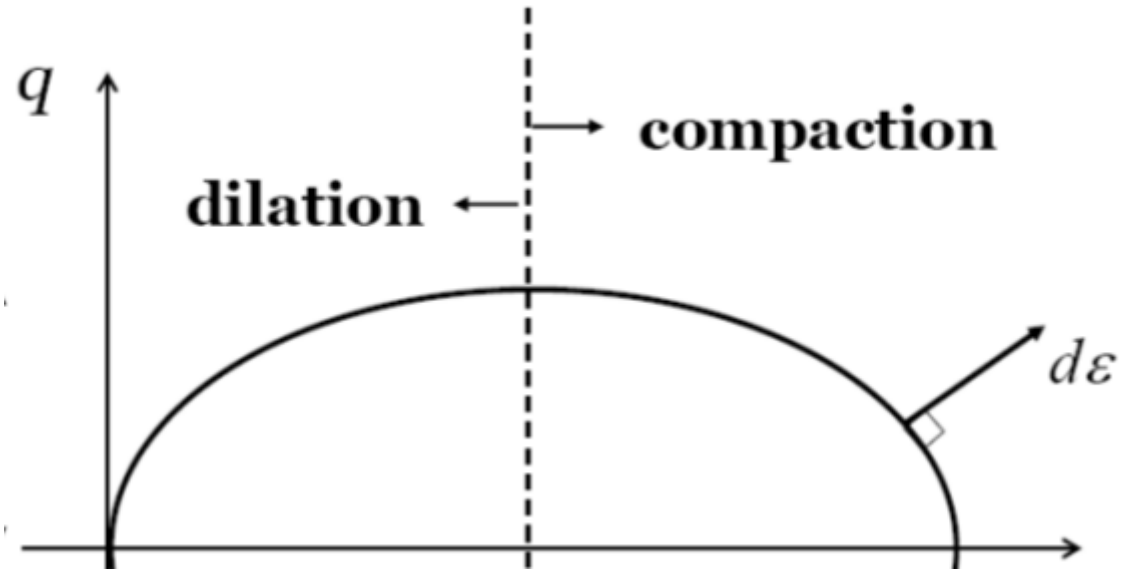

$$G(p, q; \rho_{\mathrm{r}}) = F(p, q; \rho_{\mathrm{r}})$$

$$d\varepsilon_{\mathrm{v}}^{\mathrm{p}} = d\lambda \frac{\partial F(p, q, \rho_{\mathrm{r}})}{\partial p}$$

$$d\varepsilon^{\mathrm{q}} = d\lambda \frac{\partial F(p, q, \rho_{\mathrm{r}})}{\partial q}$$

Yield surfaces & associated models

- The yield surface consists of the Drucker-Prager failure surface, and the elliptic cap surface.

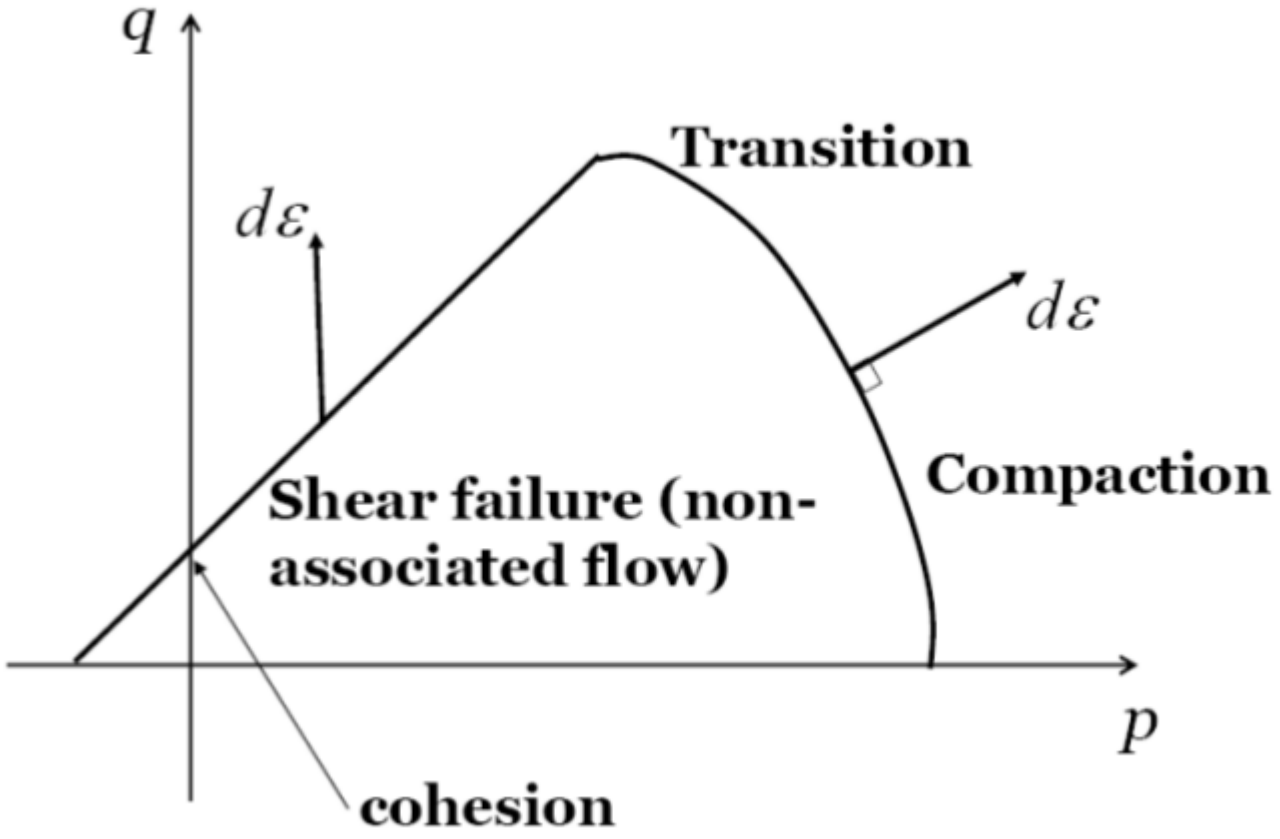

Cam-clay model

- The Cam-clay model is a classical plasticity model and is the basis for the inelastic constitutive theory for modelling cohesion less material.
- It is a basic soil model upon which other constitutive models are based
- The Cam-clay theory uses a strain rate decomposition in which the rate of mechanical deformation of the powder is decomposed into an elastic and a plastic part.
- The main features of the Cam-clay model are the use of either a linear elasticity or a porous elasticity model, which exhibits an increasing bulk elastic stiffness as the material undergoes compression.
- The clay plasticity model describes the inelastic behaviour of the material by a yield function that depends on either two or three stress invariants.

(Modified) Cam-clay model

$$F(\sigma_{ij};\rho_{\mathrm{r}}) = \frac{\left(p(\sigma_{ij}) - p_0\right)^2}{p_0^2} - \frac{q(\sigma_{ij})^2}{q_0^2} - 1$$

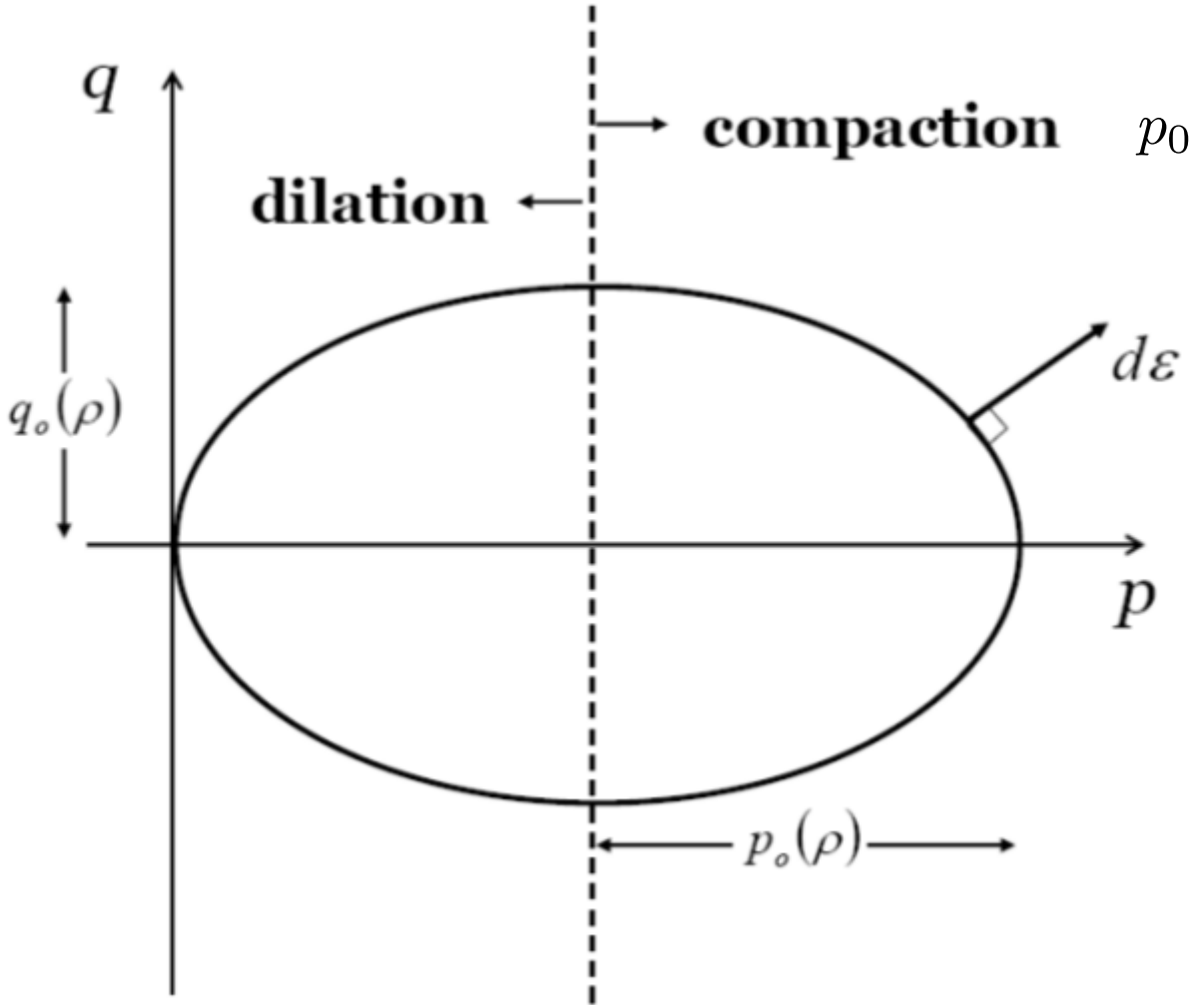

$$p_0 = K_1 \left(\log \left(1 - \frac{\rho_{\mathrm{r}} - \rho_{\mathrm{r}}^0}{\rho_{\mathrm{r}} - \rho_{\mathrm{r}}^{\max}} \right) \right)^{K_2}$$

$$q_0 = q_{\max} \tanh \left(\frac{K_3 p_0}{q_{\max}} \right)$$

(Modified) Cam-clay model

$$F(p, q; \rho_{\mathrm{r}}) = \frac{(p - p_0)^2}{p_0^2} - \frac{q^2}{q_0^2} - 1$$

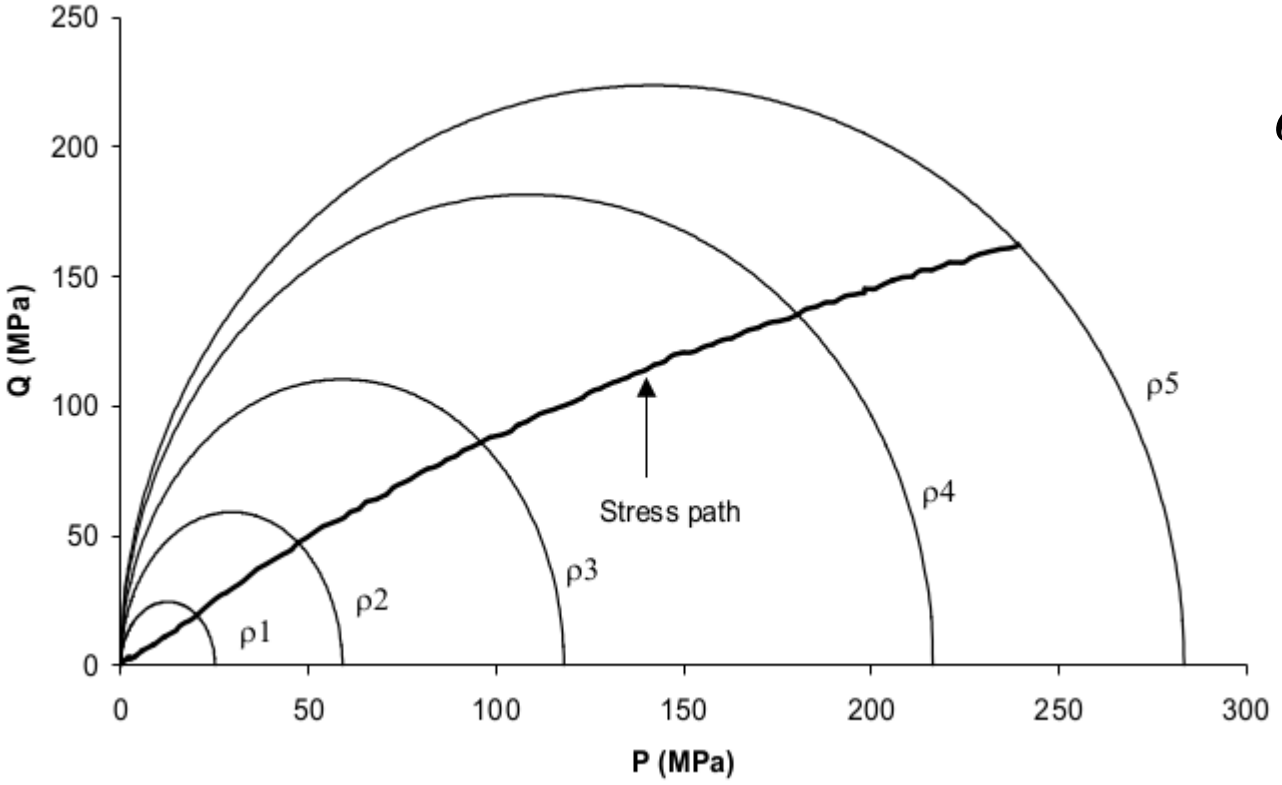

$$d\varepsilon_{\mathrm{v}}^{\mathrm{p}} = d\lambda \frac{\partial F(p, q, \rho_{\mathrm{r}})}{\partial p}$$

$$d\varepsilon^{\mathrm{q}} = d\lambda \frac{\partial F(p, q, \rho_{\mathrm{r}})}{\partial q}$$

$$\rightarrow \quad d\rho_{\mathrm{r}} = \rho_{\mathrm{r}} d\varepsilon_{\mathrm{v}}^{\mathrm{p}}$$

$\rightarrow$ Changes in

$$p_0^2 \ \& \ q_0^2$$

Another example...

$$f(p,q) = \frac{1}{\beta^2}\left(\frac{p}{q} - 1\right)^2 + \left(\frac{t}{Ma}\right)^2 - 1 = 0$$

M defines slope of critical state line

a is a hardening parameter that defines the size of the yield surface

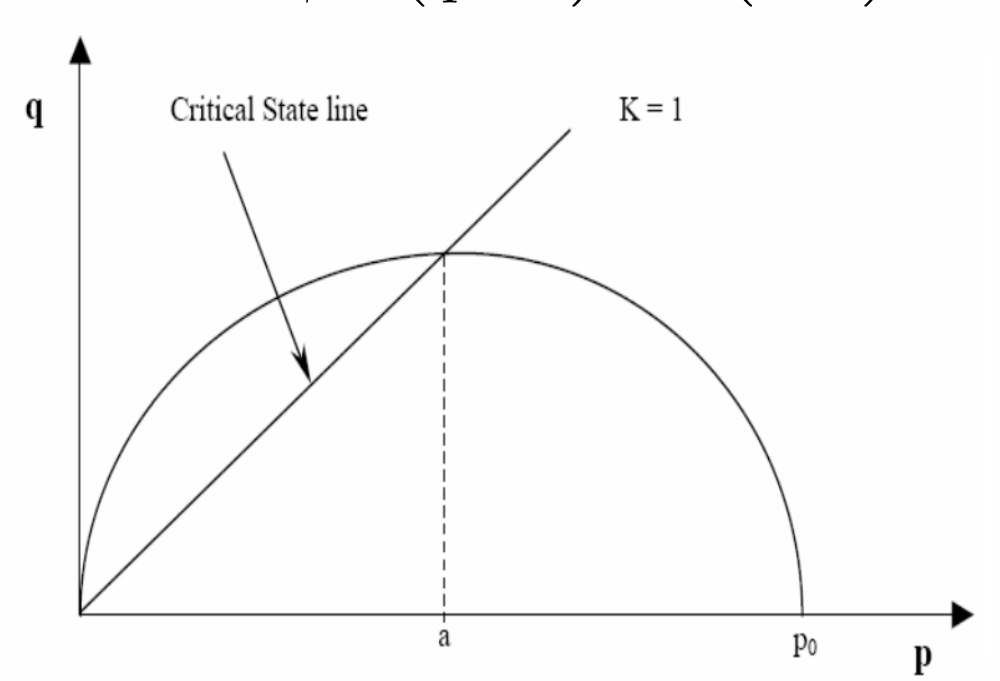

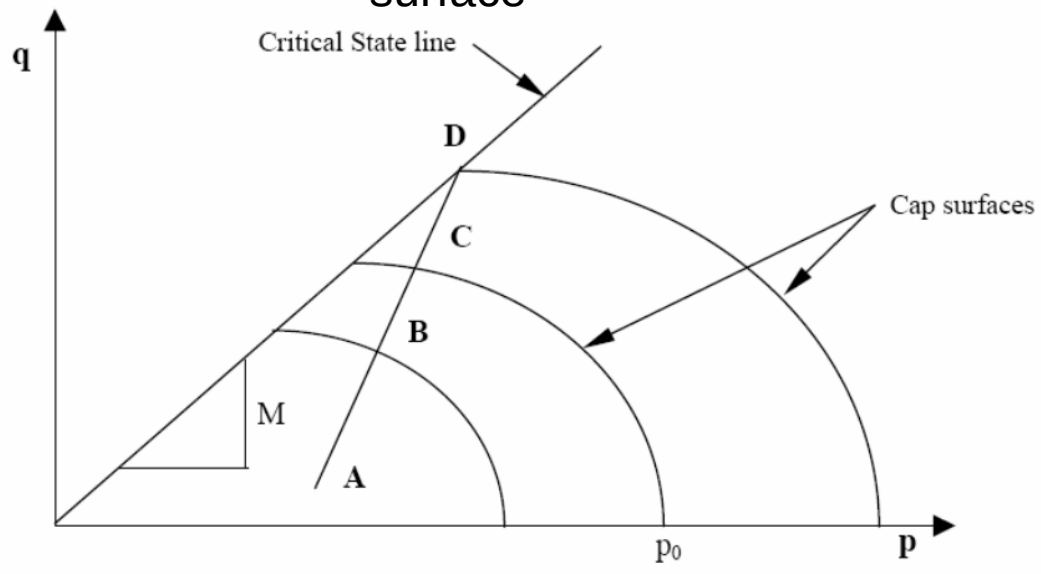

$$t = \frac{q}{2}\left(1 + \frac{1}{K} - \left(1 - \frac{1}{K}\right)\left(\frac{r}{q}\right)^3\right)$$

$$a = a_0 \exp\left((1+e_0)\frac{1 - J^{\mathrm{pl}}}{\lambda - \kappa J^{\mathrm{pl}}}\right)$$

$$\ln J^{\mathrm{pl}} = d\varepsilon_{\mathrm{vol}}^{\mathrm{pl}}$$

K is the ratio of flow stress in triaxial tension to the flow stress in triaxial compression

r is the third stress invariant

Another example...

$$f(p,q) = \frac{1}{\beta^2}\left(\frac{p}{q} - 1\right)^2 + \left(\frac{t}{Ma}\right)^2 - 1 = 0$$

M defines slope of critical state line

a is a hardening parameter that defines the size of the yield surface

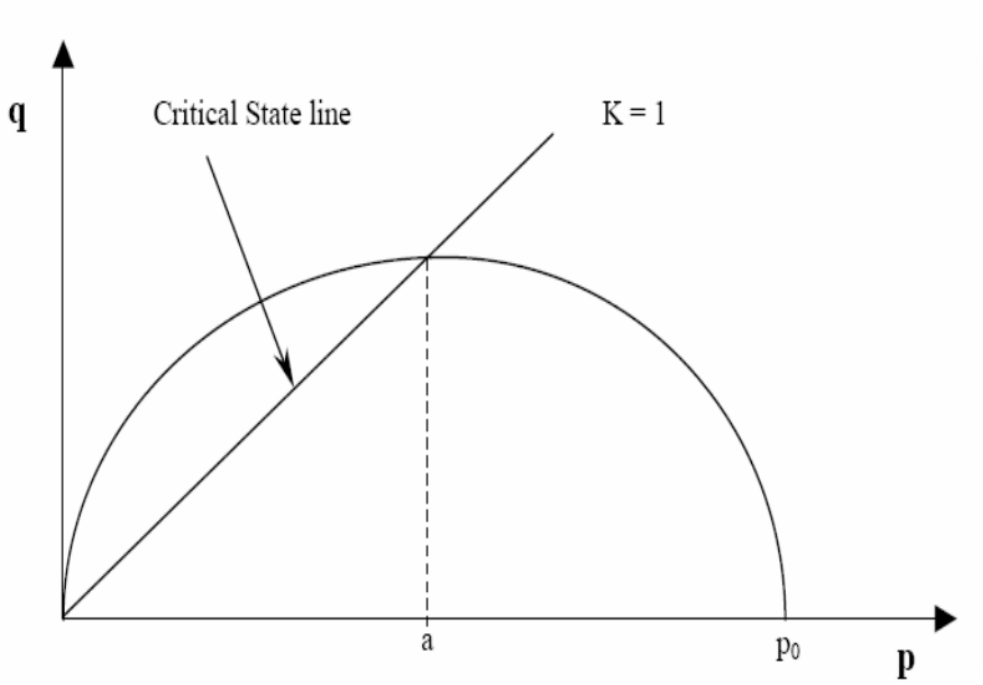

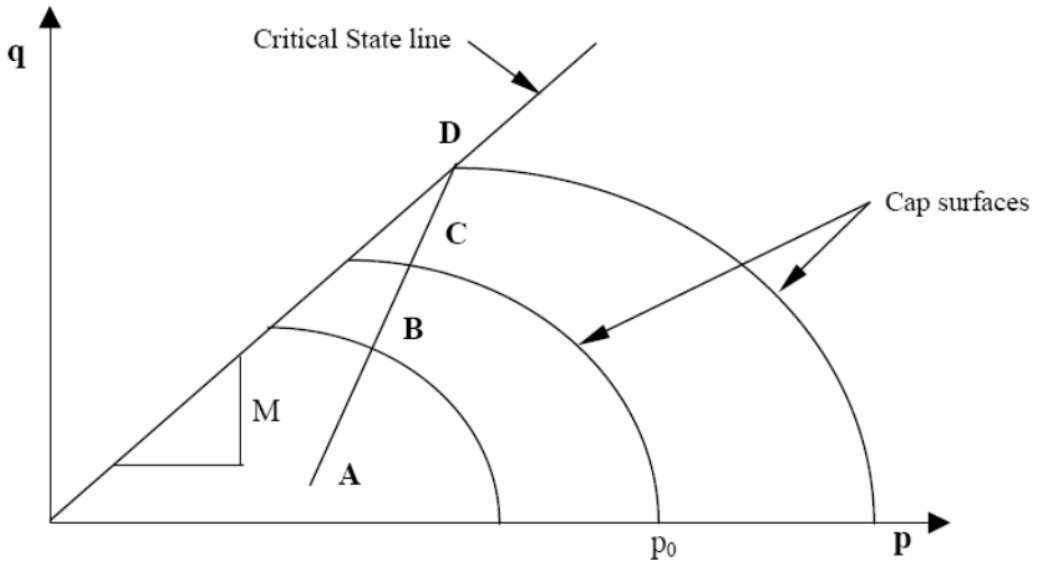

Consider the stress path of a sample at A subjected to compression. As the load is applied, the load path progresses from A to B with only elastic changes to the void ratio. Further loading produces an elastic-plastic response and subsequent yield surfaces are reached (C). Eventually the load path arrives at the critical state line (D) where failure occurs.

The Drucker-Prager-Cap (DPC) model

- The yield surface consists of the Drucker-Prager failure surface, and the elliptic cap surface.

$$F_{\mathrm{s}} = q - p\tan\beta - d = 0$$

$$F_{\mathrm{c}} = \sqrt{(p - p_{\mathrm{a}})^2 + (Rq)^2} - R(d + p_{\mathrm{a}}\tan\beta) = 0$$

R Cap eccentricity

d Cohesion strength

β Cohesion angle

p_{a} Hardening function depending on density

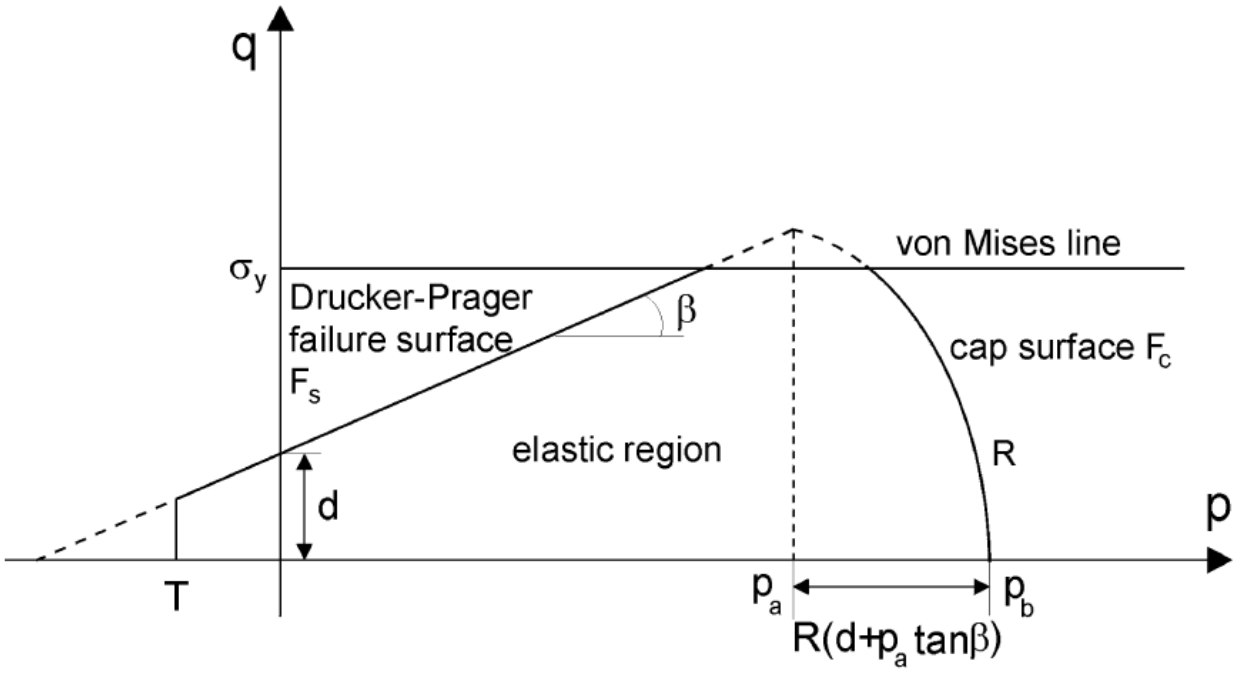

The parameters depend on relative desity/volumetric plastic strain

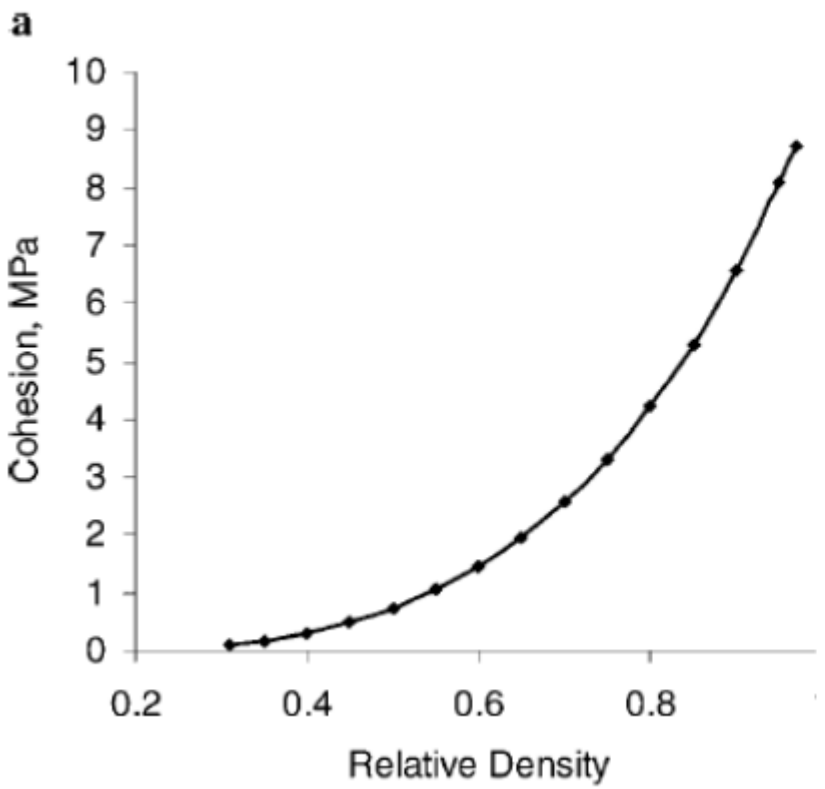

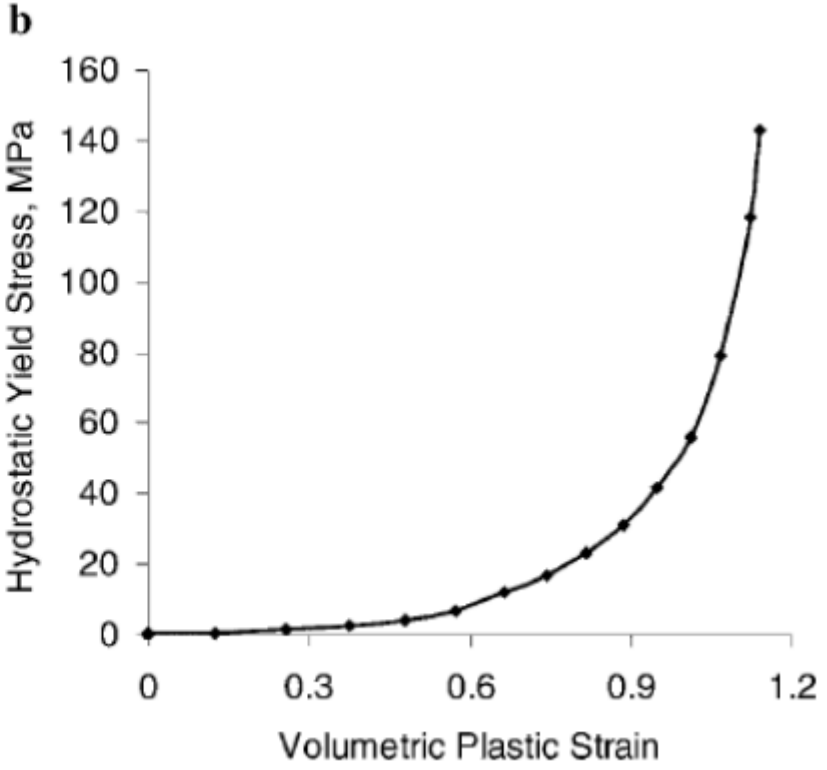

$$d \sim \exp(d_1 \rho_\mathrm{r})$$

$$R \sim \exp(R_1 \rho_\mathrm{r})$$

$$d\rho_\mathrm{r} = \rho_\mathrm{r} d\varepsilon_\mathrm{v}^\mathrm{p}$$

$$\varepsilon_{\mathrm{v},2}^\mathrm{p} - \varepsilon_{\mathrm{v},1}^\mathrm{p} = \log\left(\frac{\rho_{\mathrm{r},2}}{\rho_{\mathrm{r},1}}\right)$$

Yield stress dependence on relative density and load

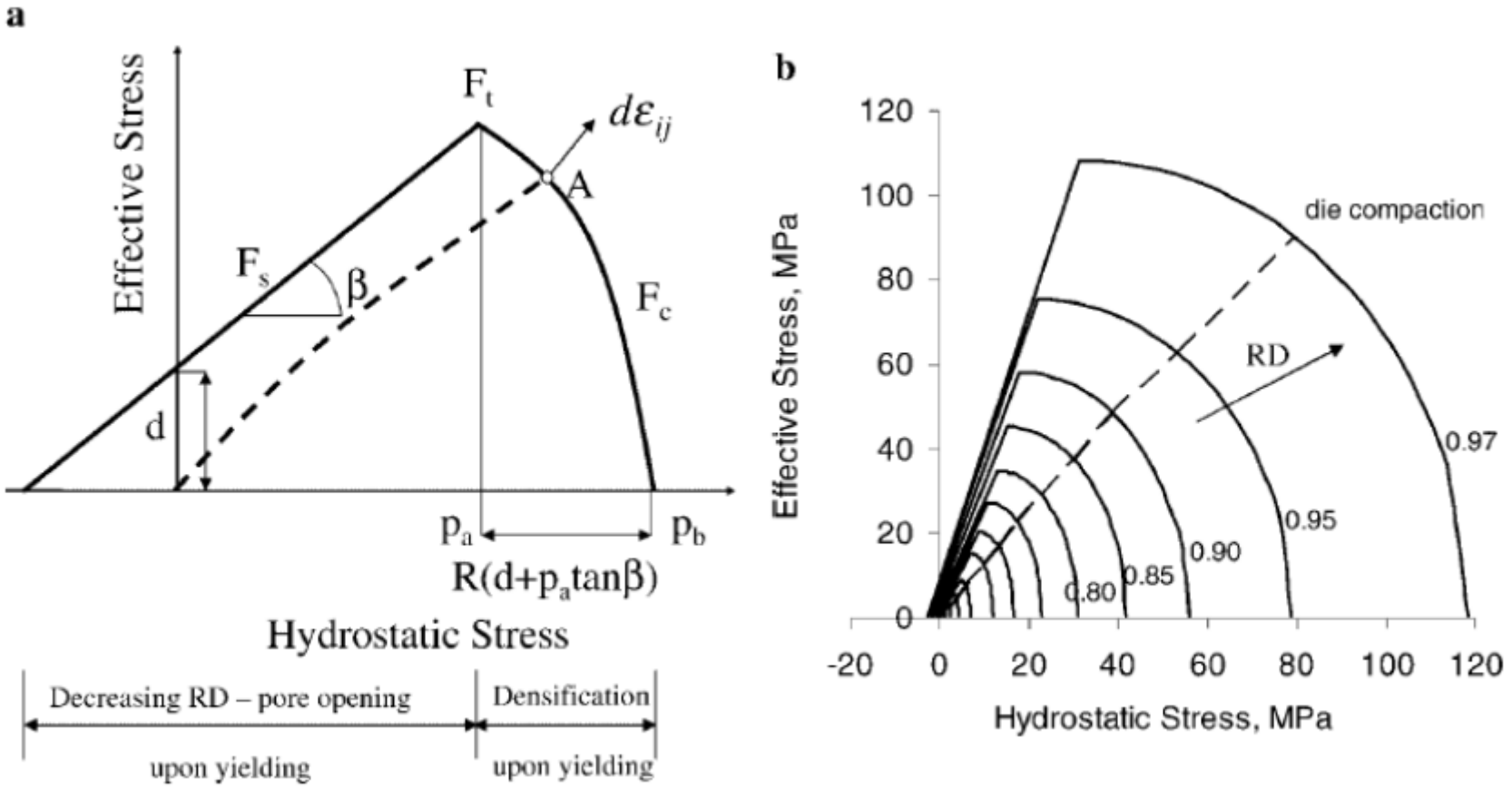

The Constitutive Model (a) model parameters, (b) family of DPC yield limits for different levels of relative density over the whole range of compaction

DPC model is then applied to complex geometries using FEM

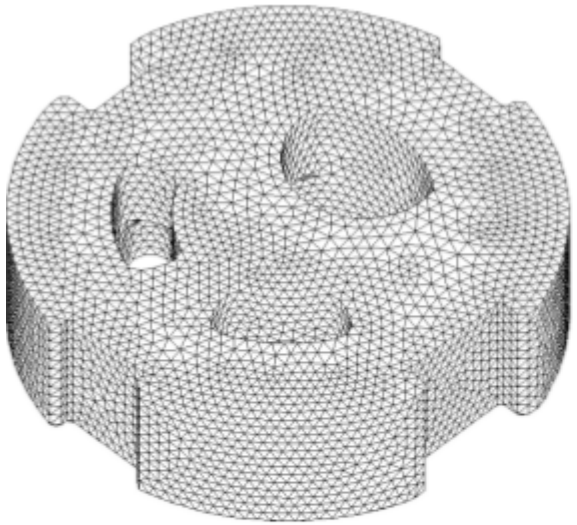

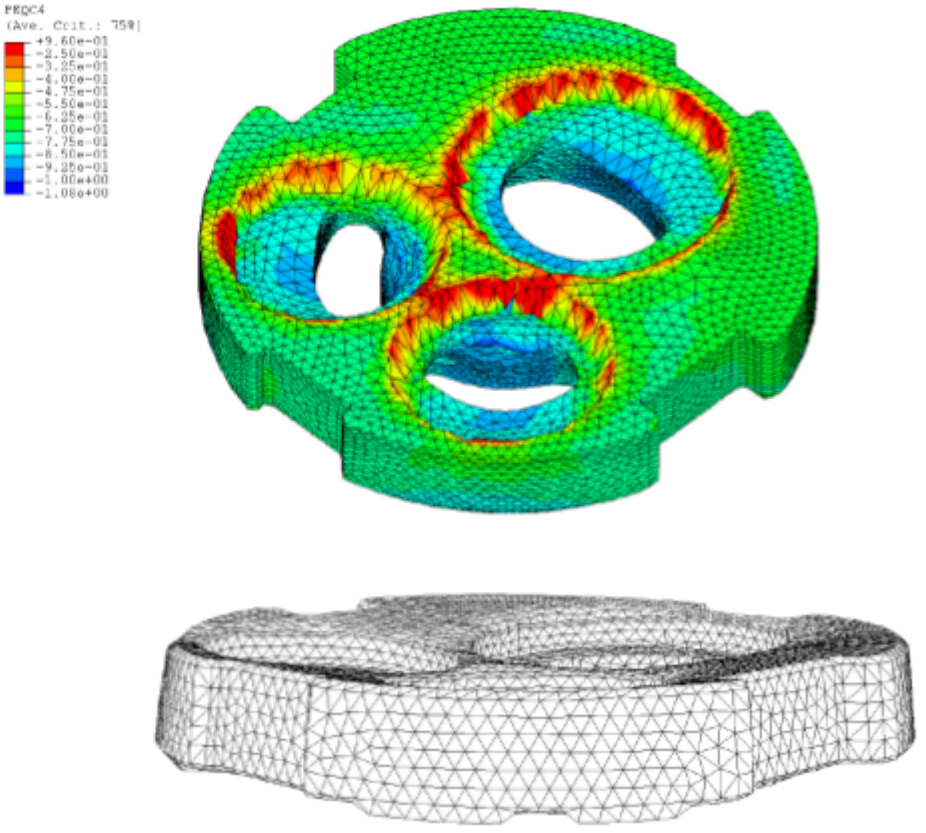

Example of Fe powders

ELSEVIER

Powder Technology 126 (2002) 65–74

POWDER TECHNOLOGY

www.elsevier.com/locate/powtec

Cold compaction of iron powders—relations between powder morphology and mechanical properties Part I: Powder preparation and compaction

D. Poquillon*, J. Lemaitre, V. Baco-Carles, Ph. Tailhades, J. Lacaze

CIRIMAT, UMR CNRS/UPS/INPT 5085, ENSIACET, 31077 Toulouse, France

Received 1 May 2001; received in revised form 1 January 2002; accepted 30 January 2002

Abstract

The effect of morphology of iron powders on their compaction behaviour has been studied in the case of compacts with a final relative density below 0.8. Two powders, one with spherical grains and the other with spongy grains, have been synthetized in order to prepare green compacts under pressures ranging from 100 to 350 MPa. The compaction behaviour of both powders has been experimentally described by the relation between the applied compaction pressure and the relative density of the material. Different stages have been identified at increasing compaction pressure: (i) fully elastic behaviour (Stage I), (ii) particle sliding (Stage II), (iii) particle irreversible deformation (Stage III). Spongy powder-based compacts achieved greater density at the same compaction pressure than spherical powder-based compacts. Models are proposed to describe the compaction behaviour of both powders.

Keywords: Iron powder; Compaction; Particles morphology; Oxalate precursor; Compaction model

Example of Fe powders

a

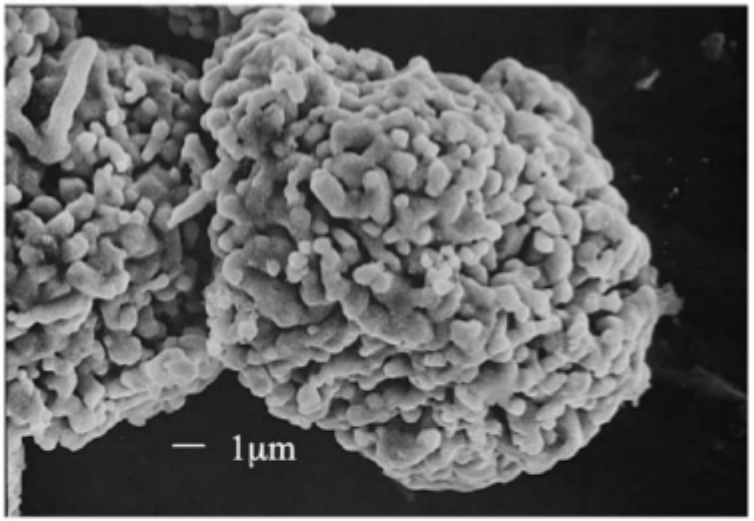

b

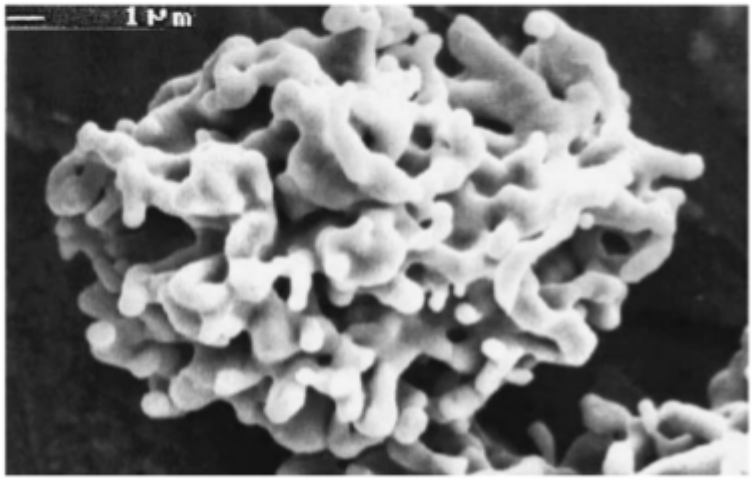

Spherical morphology (S,PS samples)

Spongy morphology (E,PE samples)

Example of Fe powders

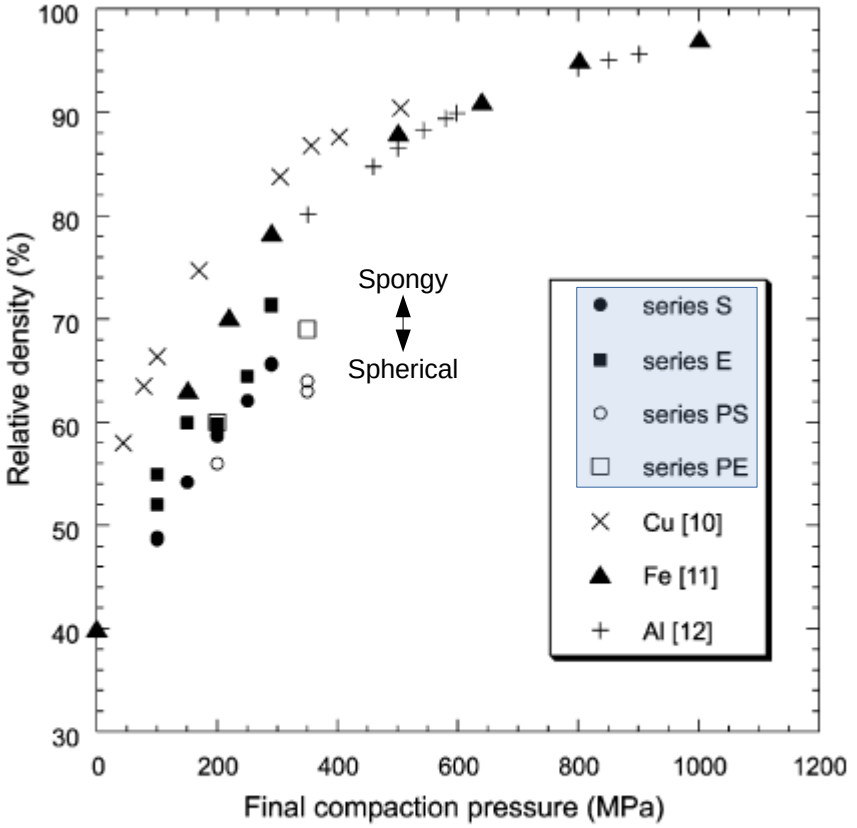

Fig. 3. Relative density of compacts vs. the final pressure applied. Comparison of the results obtained during this study with results obtained for copper [10], iron [11] and aluminium [12] powders.

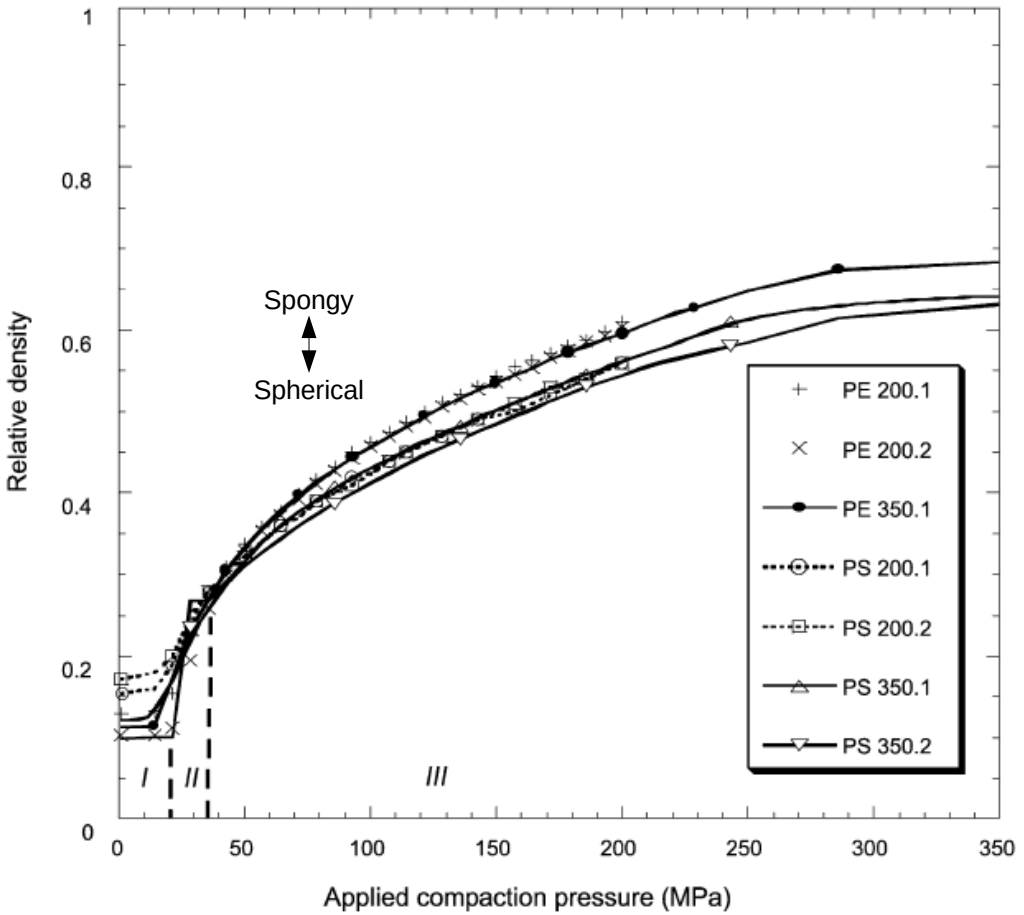

Fig. 4. Relative density of the compacts vs. the applied compaction pressure.

Powder E had better compressibility than powder S

Example of Fe powders

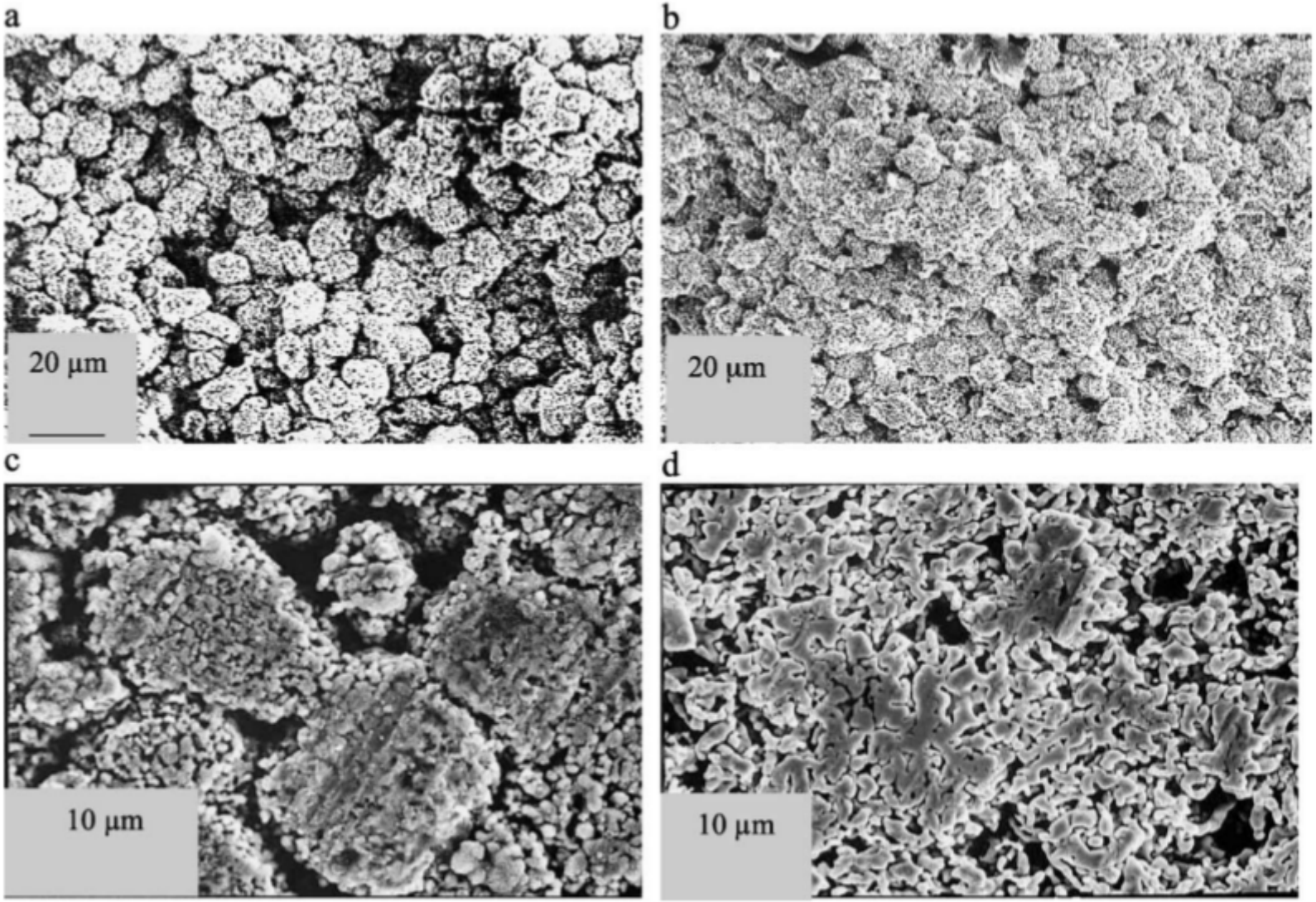

Fig. 5. Observation of the lateral surface of compacts: (a) Powder S, final pressure 100 MPa; (b) Powder S, final pressure 290 MPa; (c) Powder S, final pressure 290 MPa; (d) Powder E, final pressure 290 MPa.

Example of Fe powders

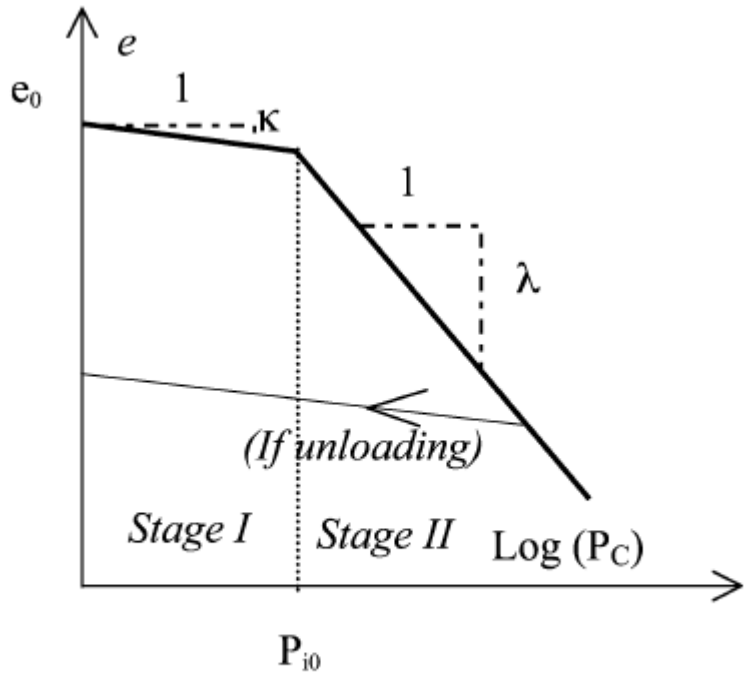

Fig. 6. Schematic representation of the evolution of the void ratio with the compaction pressure according to the CAM-CLAY model. Definition of the slopes κ and λ.

Compaction proceeds along three successive stages involving:
Stage I – elastic deformation of the grains.
Stage II – interparticle sliding with elastic deformation.
Stage III – plastic deformation of the grains.

Example of Fe powders

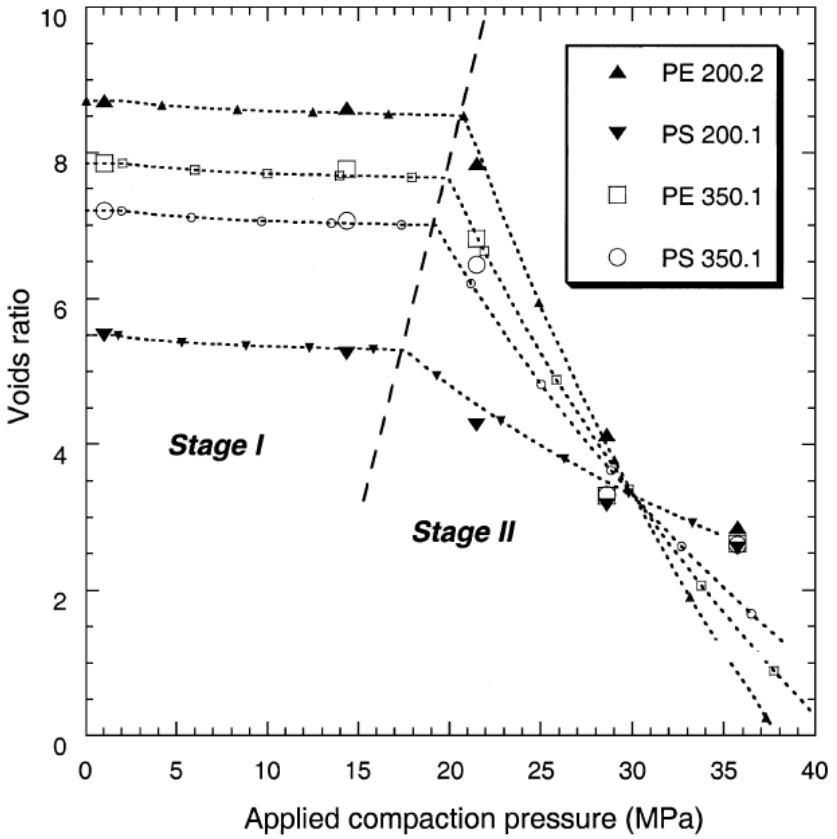

Fig. 7. Predicted evolution of the void ratio with the applied compaction pressure during stages I and II (curves with small symbols). Comparison to experimental measurements (large symbols). The interrupted line represents the limit between stages I and II.

Stage II model

$$e = e(P_{i0}) - \lambda \log_{10}\left(\frac{P_c}{P_{i0}}\right)$$

$$\lambda = \frac{e^0 - 3.5}{1.48 - \log_{10}(P_{i0})}$$

$$P_{i0} = 12 + e^0$$

Microscopic constitutive models

- This approach considers powder compaction through the modeling of the contact regions between the particles
- Early models consider the compact as a random packing of spheres in terms of the radial distribution function G(r)
- Here, densification was studied by application of a uniform strain field.
- Such models do not consider rearrangement.

Densification of random packings

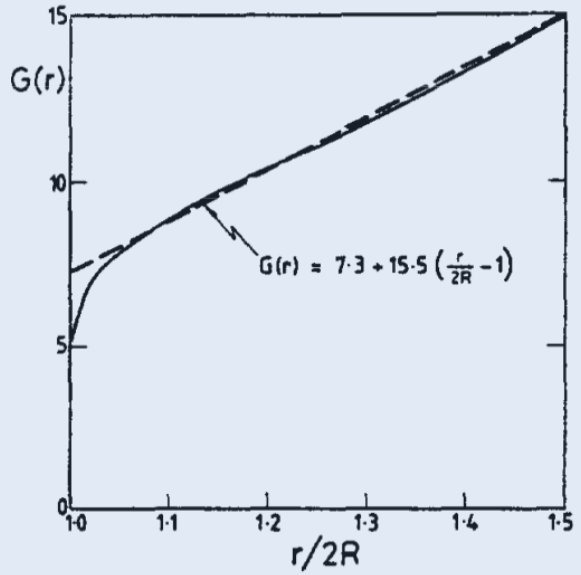

RDF of a random dense packing

Cumulative radial distribution function

$$G(r) = 0 \qquad \text{for} \quad r < 2R$$

$$G(r) = Z_0 + C\left(\frac{r}{2R} - 1\right) \qquad r \geq 2R$$

G. D. Scott, Nature 194, 956 (1962).
G. Mason, Nature 217, 733 (1968).

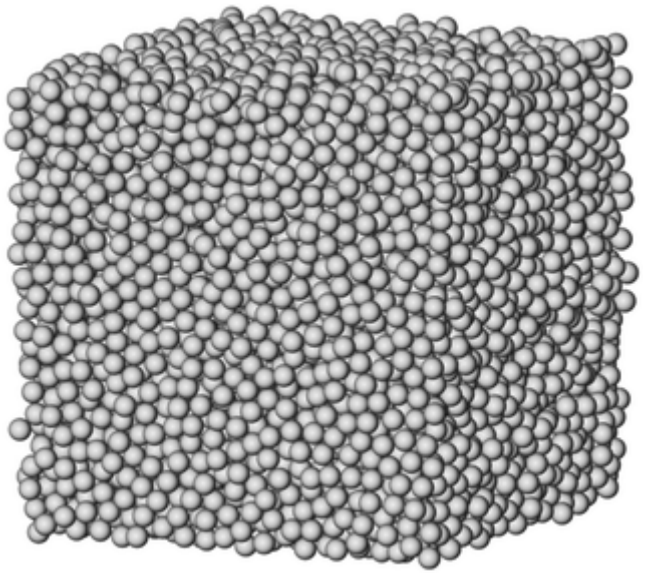

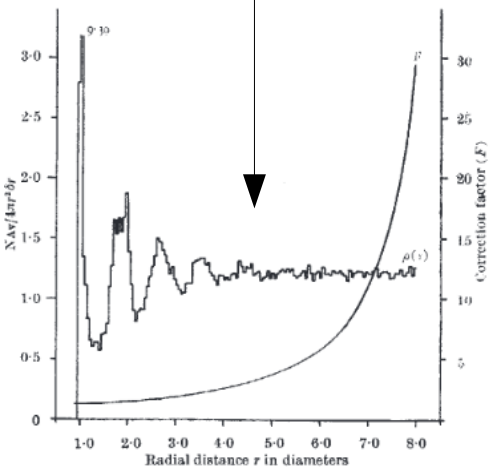

Baranau et al, Soft Matter, 2013, 9, 3361-3372

Densification of random packings

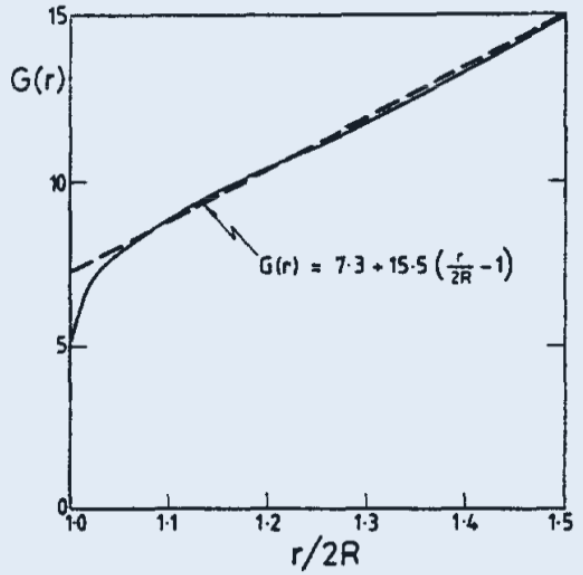

RDF of a random dense packing

Cumulative radial distribution function

$$G(r) = 0 \qquad \text{for} \quad r < 2R$$

$$G(r) = Z_0 + C\left(\frac{r}{2R} - 1\right) \qquad r \geq 2R$$

G. D. Scott, Nature 194, 956 (1962).
G. Mason, Nature 217, 733 (1968).

What happens when a isotropic volume reduction occurs?

Acta metall. Vol. 30, pp. 1883 to 1890, 1982
Printed in Great Britain.

0001-6160/82/101883-08$03.00/0

THE INFLUENCE OF AN INCREASING PARTICLE COORDINATION ON THE DENSIFICATION OF SPHERICAL POWDERS

E. ARZT
Engineering Department, Cambridge University, Cambridge, England

Densification of random packings

Densification of a random dense packing

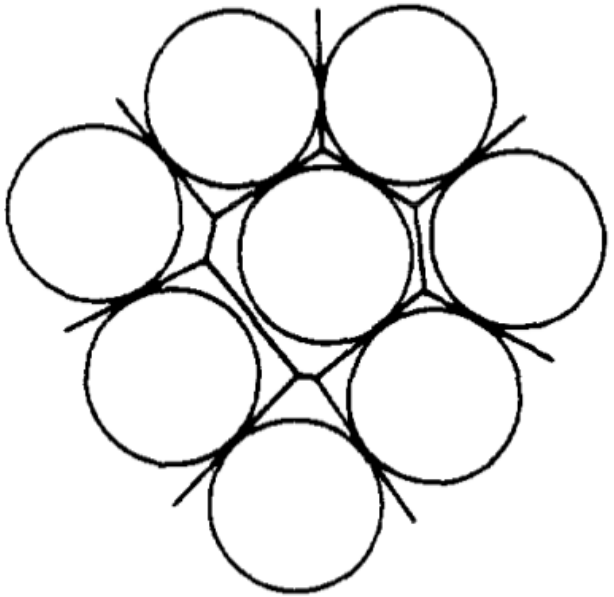

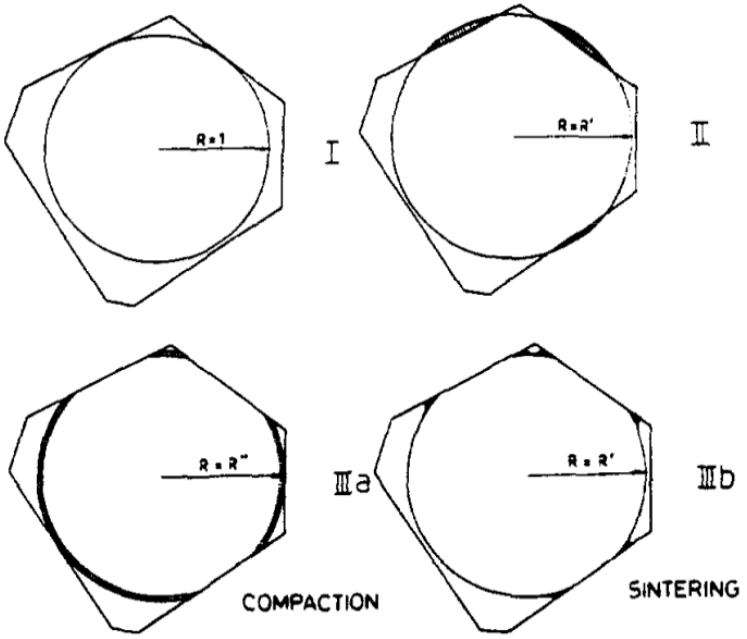

- Starting from an average particle, with an average Voronoi cell (I), densification is modelled as concentric growth of the particle, beyond the stationary walls of its cell (new particle radius R') (II).
- The excess volume outside the polyhedron (shaded) is redistributed either (a) evenly across the free surface of the sphere; this produces a truncated sphere of radius R" ('compaction' case. IIIa), or (b) near the contact region, forming necks ('sintering' case. IIIb).
- The average area of contact between the particle and the cell walls are calculated in each case. The coordination numbers are given by the RDF of the packing: G(2R") and G(2R'), respectively.

Densification of random packings

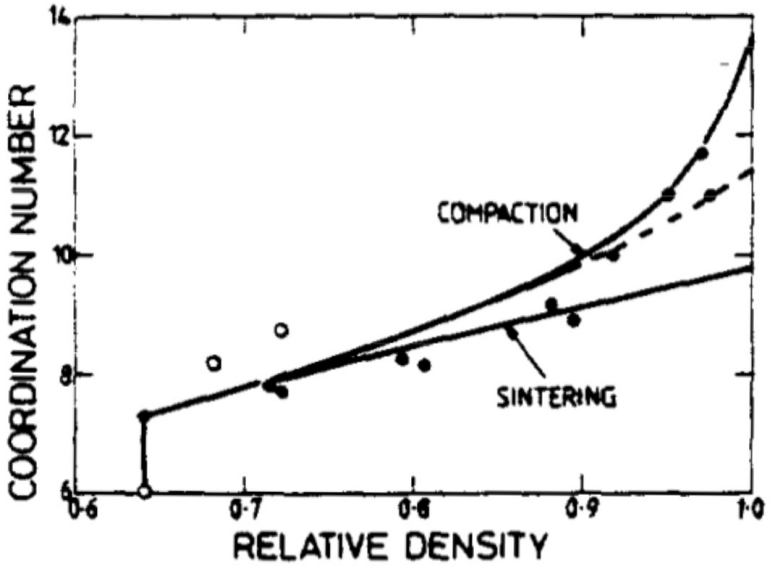

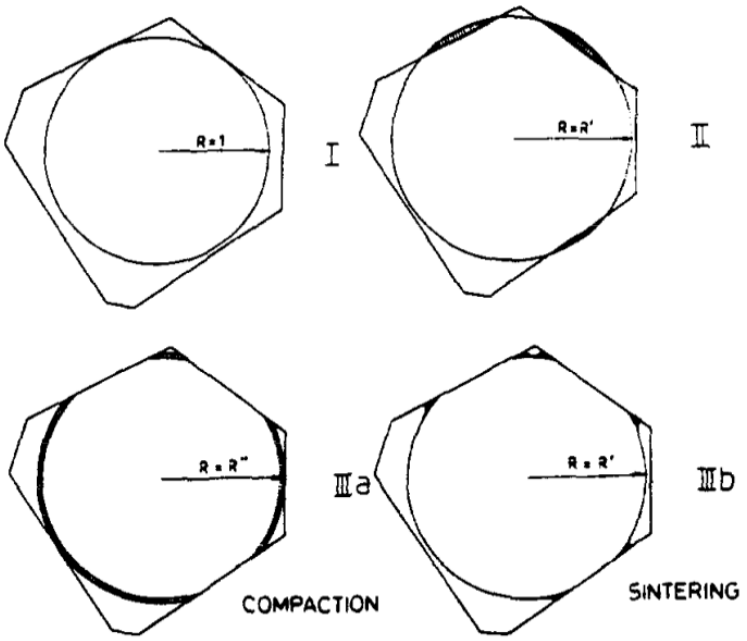

- Starting from an average particle, with an average Voronoi cell (I), densification is modelled as concentric growth of the particle, beyond the stationary walls of its cell (new particle radius R') (II).
- The excess volume outside the polyhedron (shaded) is redistributed either (a) evenly across the free surface of the sphere; this produces a truncated sphere of radius R" ('compaction' case. IIIa), or (b) near the contact region, forming necks ('sintering' case. IIIb).
- The average area of contact between the particle and the cell walls are calculated in each case. The coordination numbers are given by the RDF of the packing: G(2R") and G(2R'), respectively.

Microscopic constitutive models

To consider rearrangement, the relative motion between particles must be taken into account

PERGAMON

Journal of the Mechanics and Physics of Solids
51 (2003) 667–693

JOURNAL OF THE MECHANICS AND PHYSICS OF SOLIDS

www.elsevier.com/locate/jmps

Study of particle rearrangement during powder compaction by the Discrete Element Method

C.L. Martin[a,*], D. Bouvard[a], S. Shima[b]

[a] *Laboratoire GPM2, Institut National Polytechnique de Grenoble, UMR CNRS 5010, ENSPG, BP46, 38402 Saint Martin d'Héres cedex, France*
[b] *Department of Mechanical Engineering, Kyoto University, Kyotol606-8501, Japan*

Received 10 January 2002; received in revised form 5 September 2002; accepted 9 September 2002

Discrete element methods

- This approach models the microstructure of particles interacting via contact forces.
- The contact forces have both an elastic and plastic origin → constitutive equations for the contact.
- Each particle is modelled as an elasto-plastic material with elastic constants *E* and *ν* and the following hardening relation in the plastic regime

$$\longrightarrow \quad \sigma = \sigma_0 \varepsilon^{\frac{1}{m}}$$

Discrete element methods

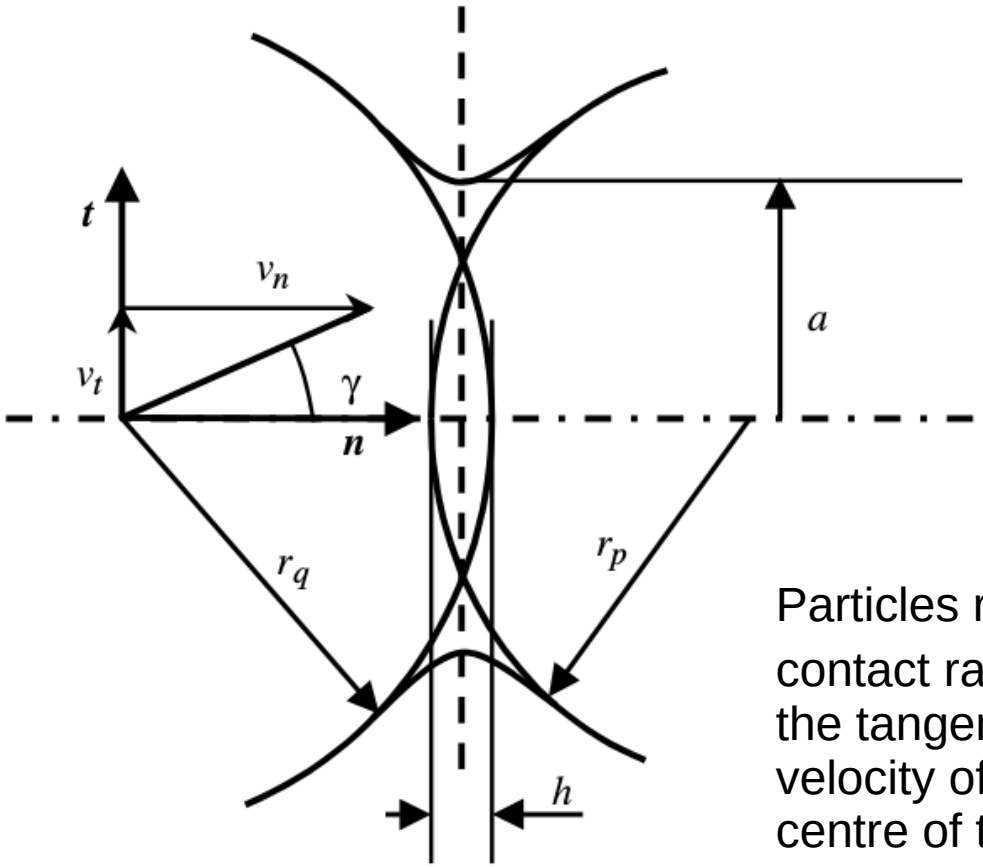

$$r^* = \frac{r_q r_p}{r_q + r_p}$$

Particles radius are r_p and r_q, the overlap is *h* and the contact radius is *a*. The angle of obliquity *y* is given by the tangential and normal components of the relative velocity of the centre of one particle with respect to the centre of the other.

Discrete element methods

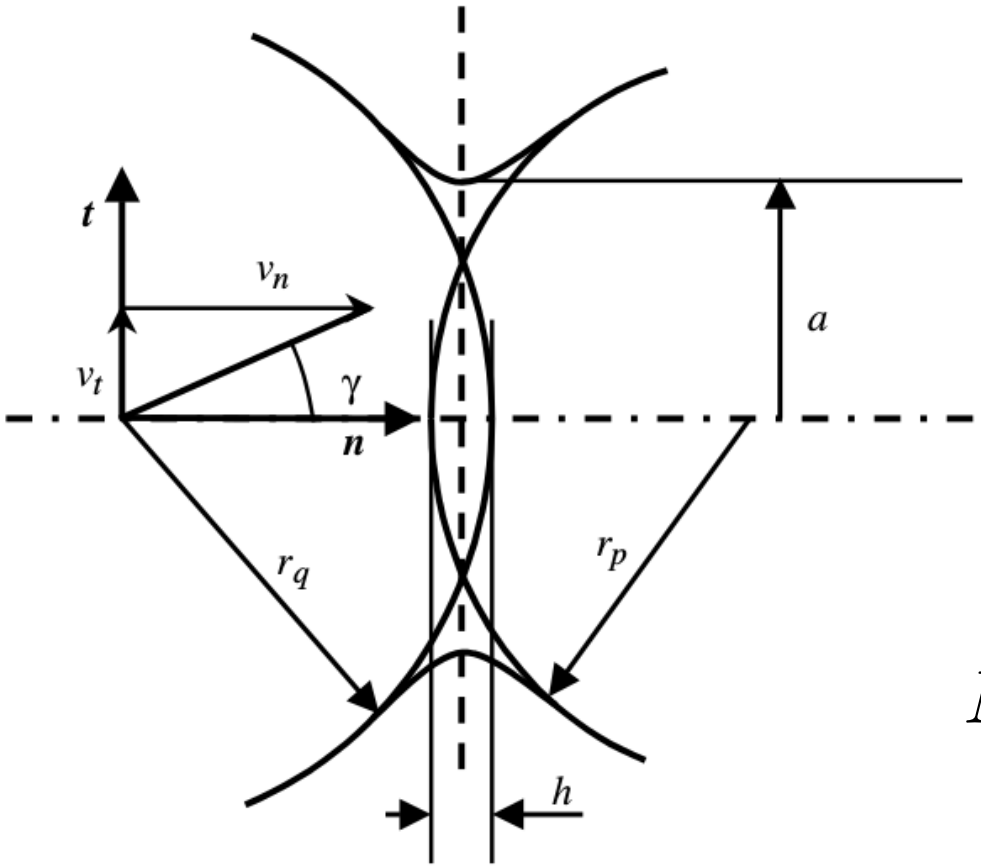

$$\mathbf{N} = -\mathrm{Min}(N_\mathrm{e}, N_\mathrm{p})\mathbf{n}$$

Elastic contact force

Plastic contact force

$$N_\mathrm{e} = \frac{2}{3}\frac{E}{1-\nu^2}\sqrt{r^*}h^{\frac{3}{2}}$$

$$N_\mathrm{p} = \pi\sigma_0 2^{1-\frac{3}{2m}} 3^{1-\frac{1}{m}} \left(C(m)\right)^{2+\frac{2}{m}} \left(r^*\right)^{1-\frac{1}{2m}} h^{1+\frac{1}{2m}}$$

Discrete element methods

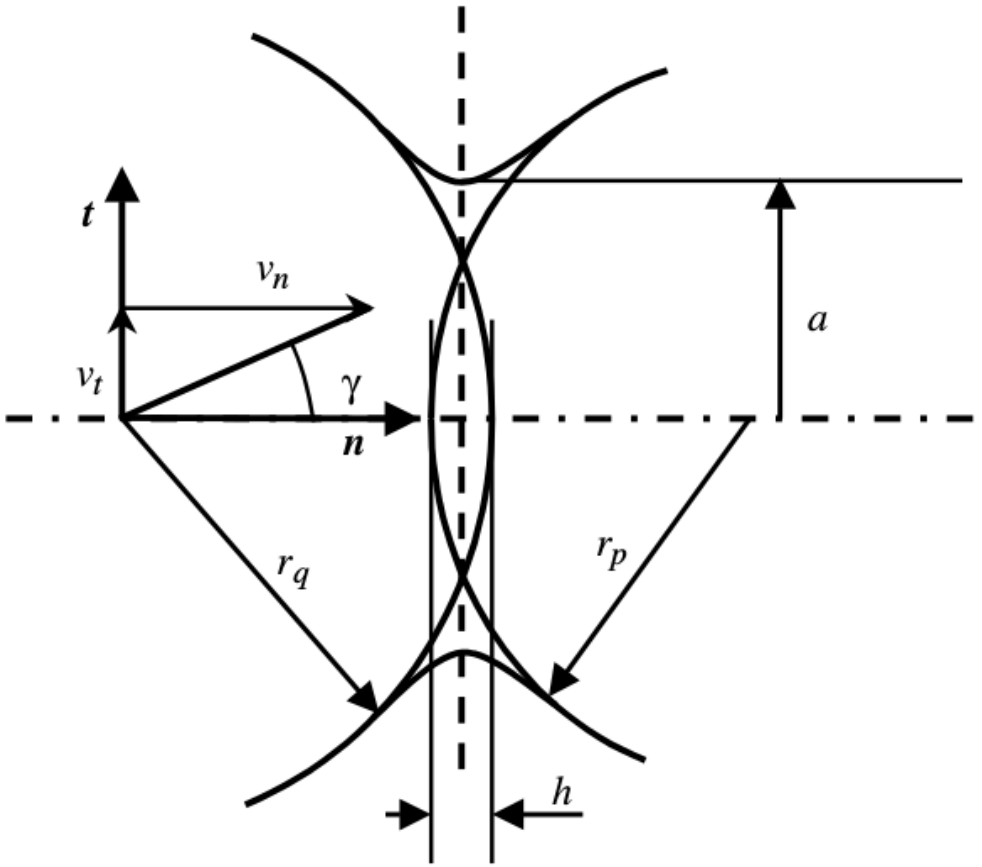

The tangential force is considered to be either in a sticking state, with negligible relative tangential displacement, or in a state of gross sliding. When the contact is not sliding, a sufficiently large tangential stiffness is assigned to the contact in order to ensure sticking. When the contact is sliding, a simple Coulomb law of friction is used:

$$\mathbf{T} = \mu|\mathbf{N}|\mathbf{t}$$

Discrete element methods

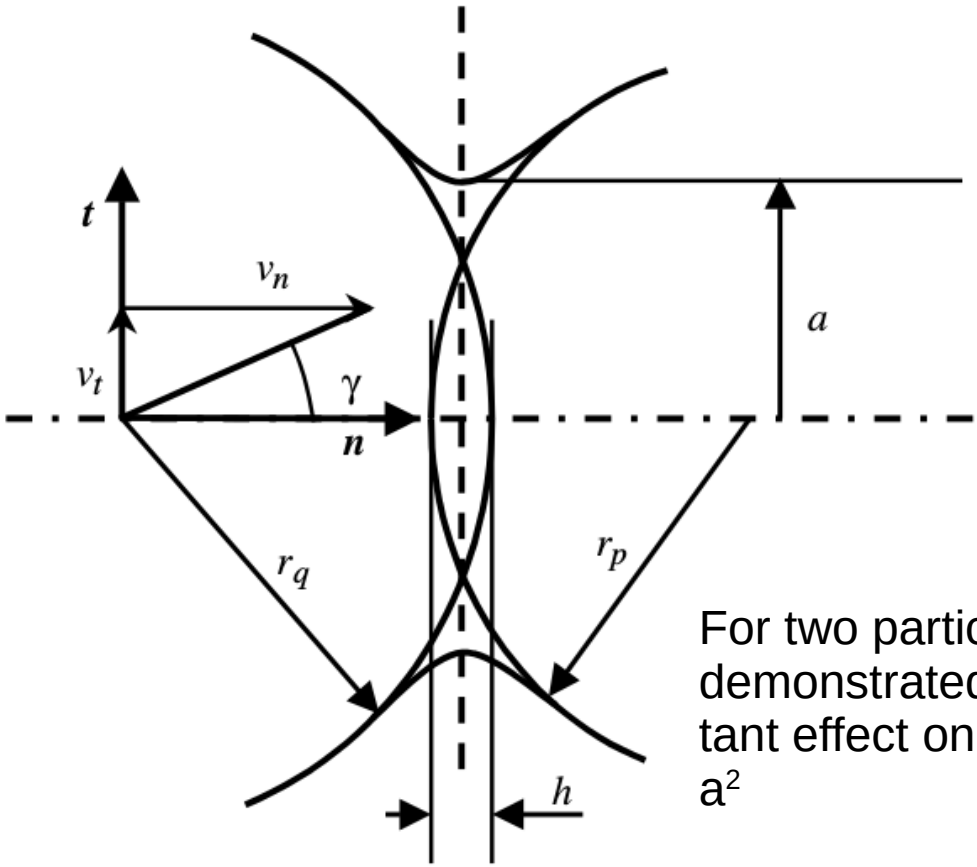

When plastic deformation occurs, the excess material at the contact between the two overlapping particles is transported away from the contact zone. Depending on the constitutive behaviour of the powder, the material may be deposited far away from the contact zone or stay in the vicinity of the contact.

For two particles indenting normally, it has been demonstrated that the hardening exponent m has an important effect on the redistribution profile and on the contact area a^2

$$\pi a^2 = 2\pi (c(m))^2 r^* h$$

Discrete element methods

- A framework now exists to model the dynamics of the particles.
- The positions of the particles are evolved using Newton's equations of motion and the contact forces between the particles.
- This is called the discrete element method.
- Newton's equations of motion are solved by using a discrete integrator for a small time step Δt

Discrete element methods

J.C. Steuben et al. / Comput. Methods Appl. Mech. Engrg. 305 (2016) 537–561

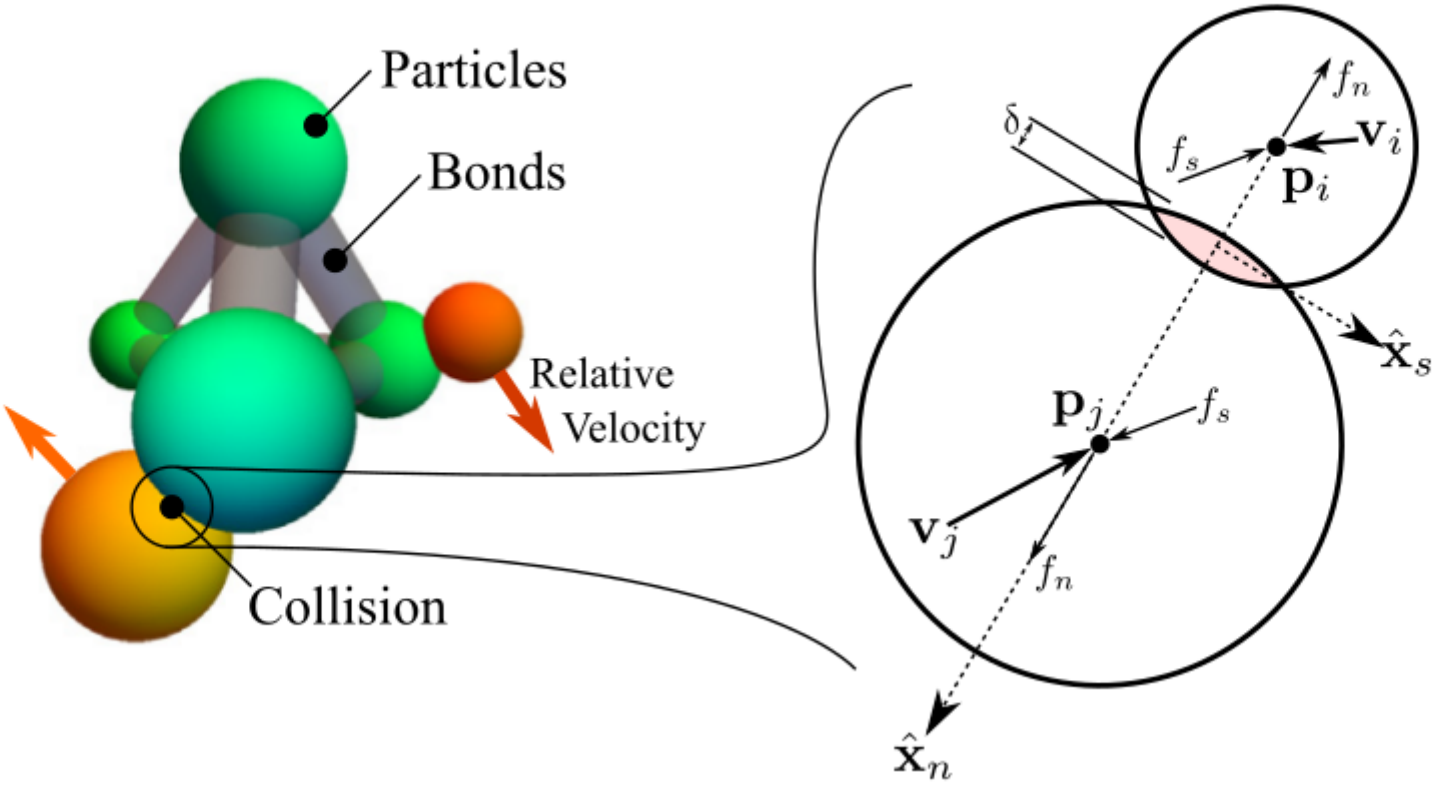

Discrete element methods

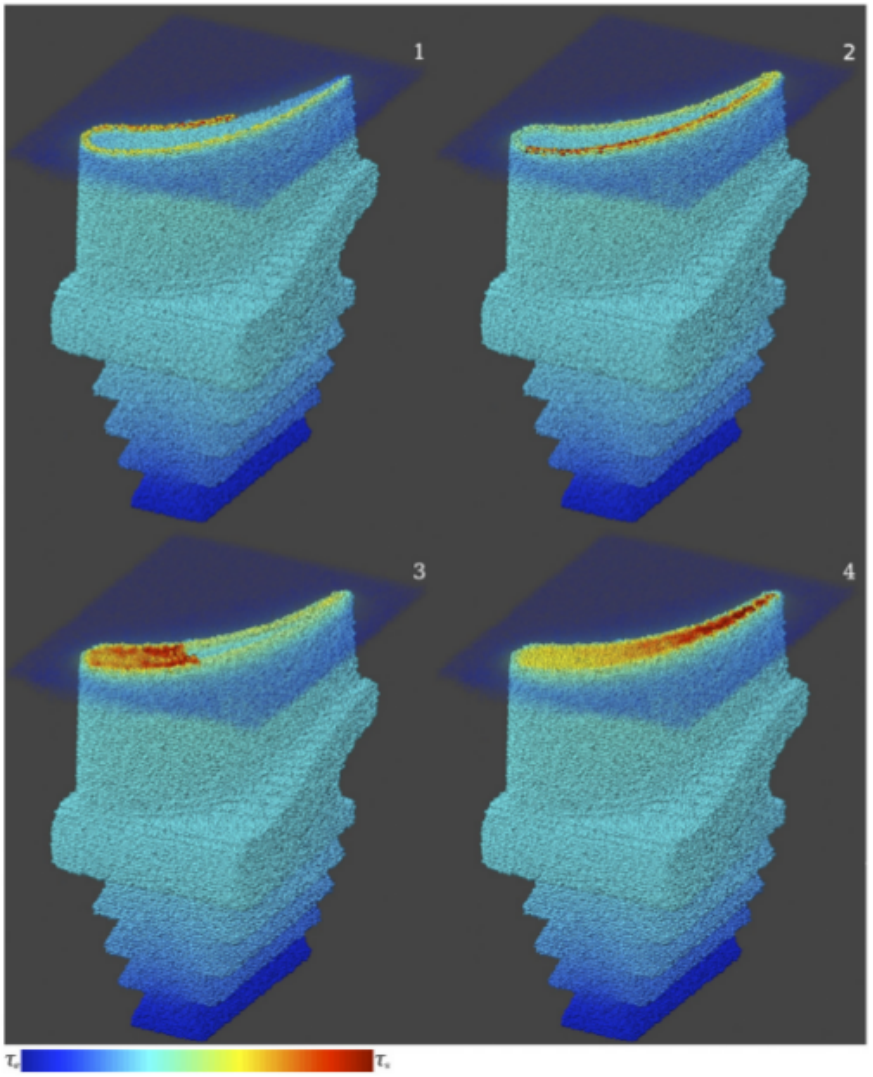

Quite complicated and large components can be simulated in this way.

J.C. Steuben et al. / Comput. Methods Appl. Mech. Engrg. 305 (2016) 537–561

Discrete element methods

- The particles are within a cell and periodic boundary conditions are used
- Deformation is modeled by imposing a fixed strain rate: $\dot{\epsilon}_{ij}$
- At each time step, the cell shape is strained according to the imposed strain: $\epsilon_{ij} = \dot{\epsilon}_{ij}\Delta t$
- The coordinates of the atoms are similarly strained, $\Delta x_i = \dot{\epsilon}_{ij} x_j \Delta t$ and the stress is measured as

$$\sigma_{ij} = \frac{1}{V}\left(\sum_c (r_\mathrm{p} + r_\mathrm{q} - h) N n_i n_j + \sum_c (r_\mathrm{p} + r_\mathrm{q} - h) T n_i t_j\right)$$

Summation is carried out on all contacts

Discrete element methods

Bronze, copper and aluminium powder properties

Material	ρ (Kg/m^3)	E (Gpa)	V	σ_0 (MPa)	m	D_0 (experimental)	$2R$ (μm) (numerical)	$2R$ (μm) (experimental)
Bronze	8750	120	0.34	300	∞	0.64	290	290 ± 20
Copper	8920	130	0.34	500	2.8	0.64	115	115 ± 10
Al	2700	70	0.35	146	4.2	0.61–0.63	6	4.5–7

- To generate an acceptable random dense packing of particles,4000 particles are randomly generated in a cubical cell with no initial contact between the particles (relative density ~0.32) and the packing is in a gas-like condition.
- From this stage, the preparation of the sample consists in imposing an isostatic densifcation with the friction set to zero. The zero friction coefficient allows packings to attain a high relative density at the end of the sample preparation.
- Contact damping is introduced during the preparation stage in order to ease the convergence toward the equilibrium solution by dissipating kinetic energy.

Discrete element methods

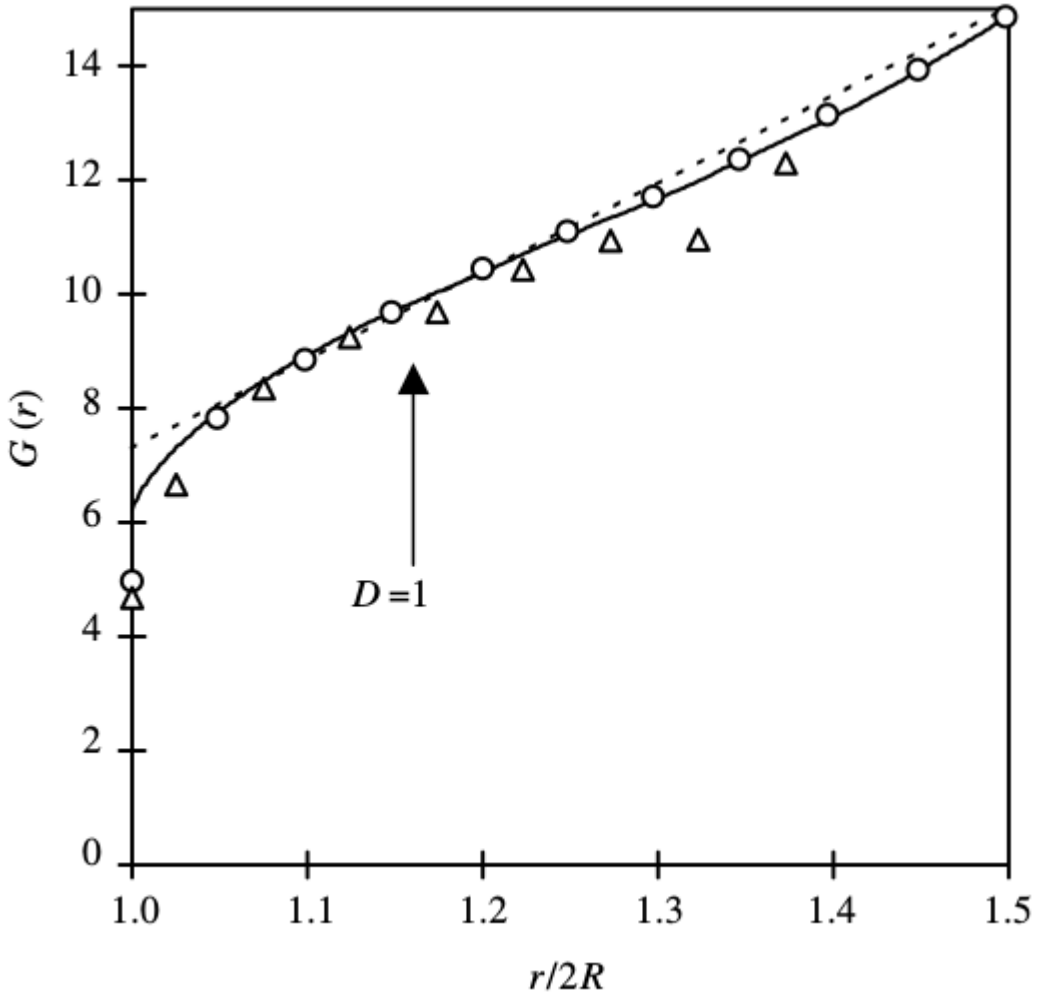

$$G(r) = 0 \qquad \text{for} \quad r < 2R$$

$$G(r) = Z_0 + C\left(\frac{r}{2R} - 1\right) \qquad r \geq 2R$$

Simulation data taken for the configuration when the first contact event is detected

Martin et al, Journal of the Mechanics and Physics of Solids 51 (2003) 667 – 693

Discrete element methods

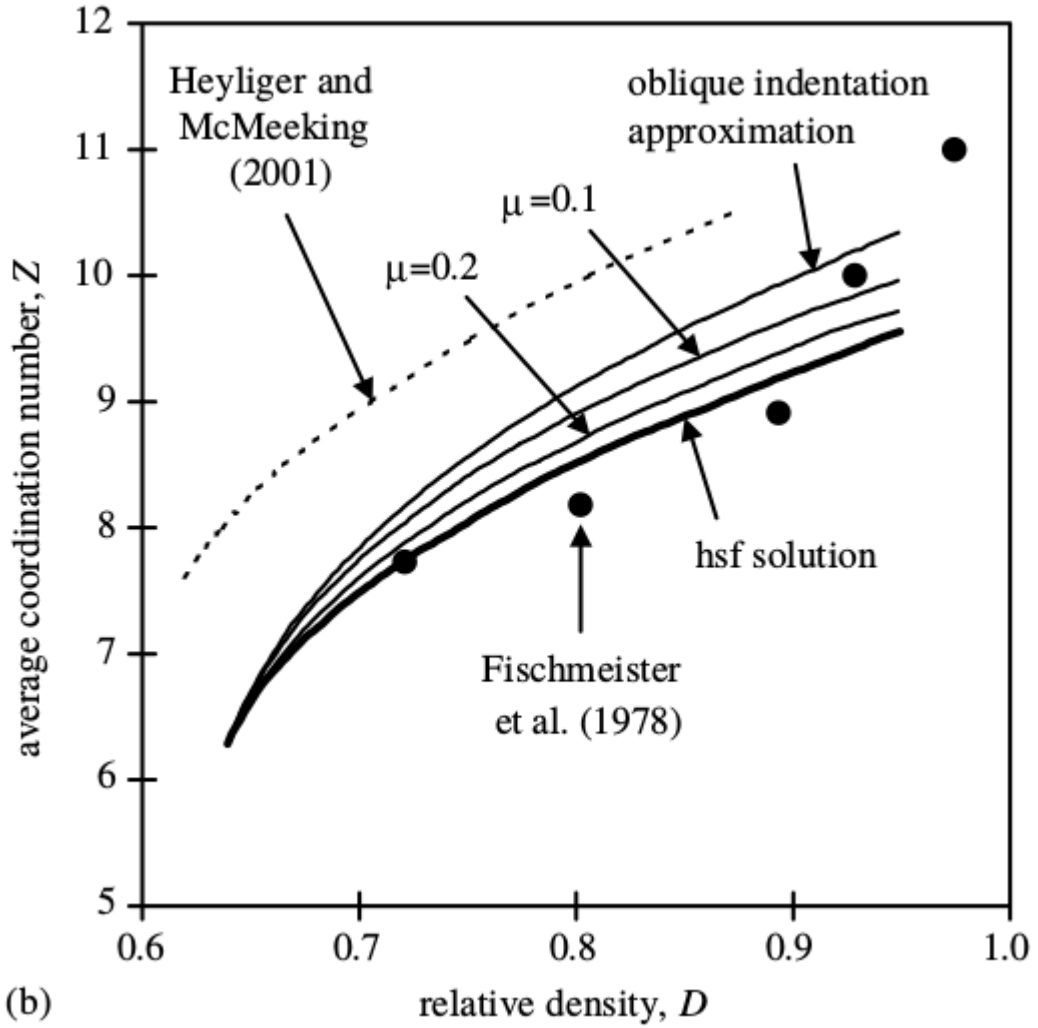

$$\Delta x_i = \Delta x_i^h + \Delta x_i^c$$

Displacement due to homogeneous strain field (hsf)

Separate motion of particles

Decreasing friction, promotes sliding and therefore rearrangement → increases coordination

Martin et al, Journal of the Mechanics and Physics of Solids 51 (2003) 667 – 693

Discrete element methods

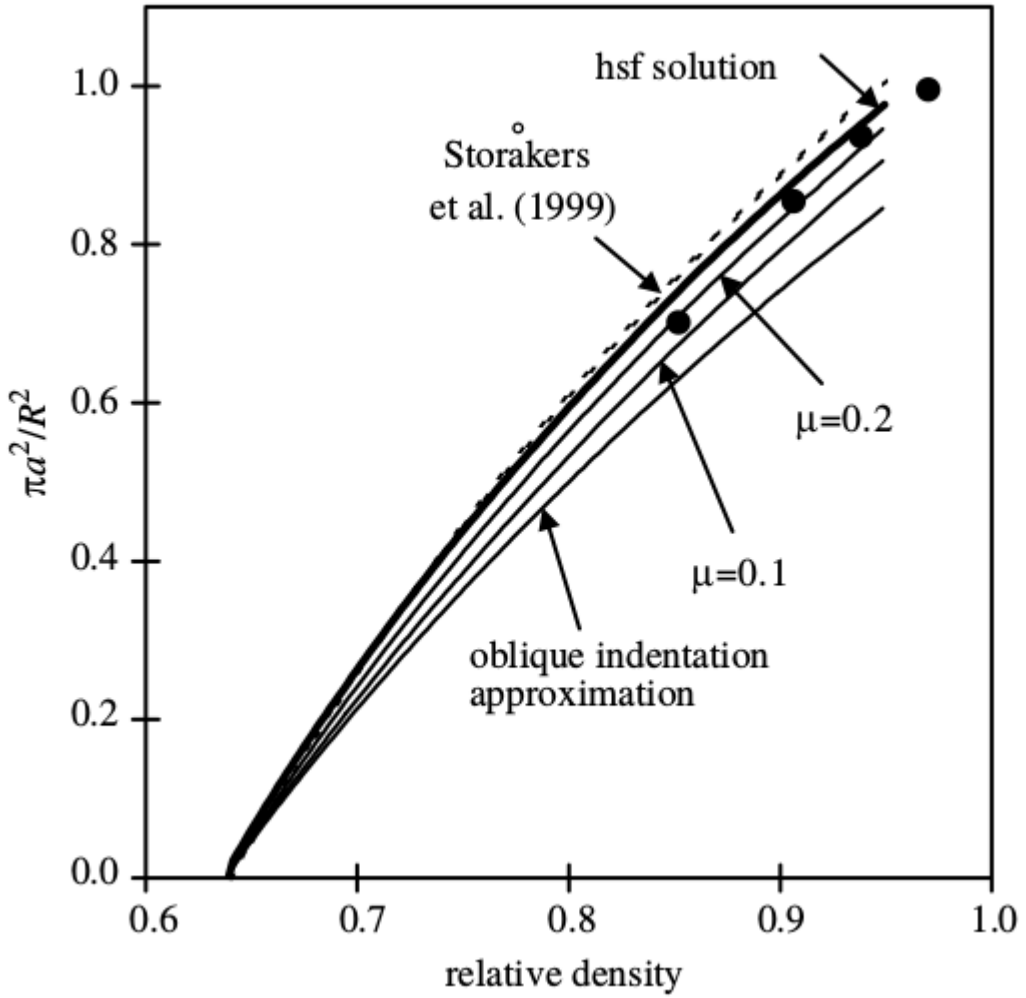

Decreased contact area correlates with increased coordination number.

Martin et al, Journal of the Mechanics and Physics of Solids 51 (2003) 667 – 693

Discrete element methods

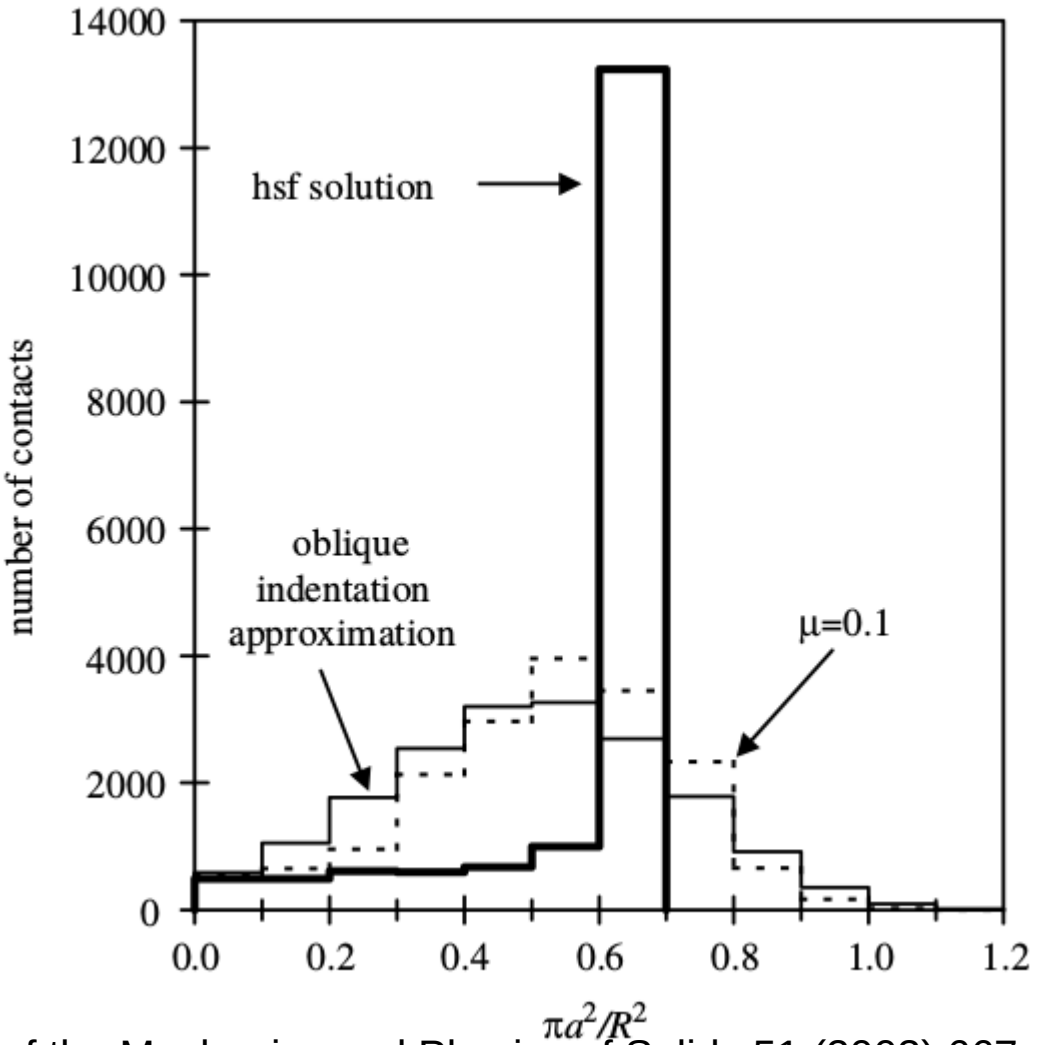

Dynamic rearrangement produces a broader distribution of contact areas (increases the number of smaller contact areas)

Martin et al, Journal of the Mechanics and Physics of Solids 51 (2003) 667 – 693

Microscopic constitutive models

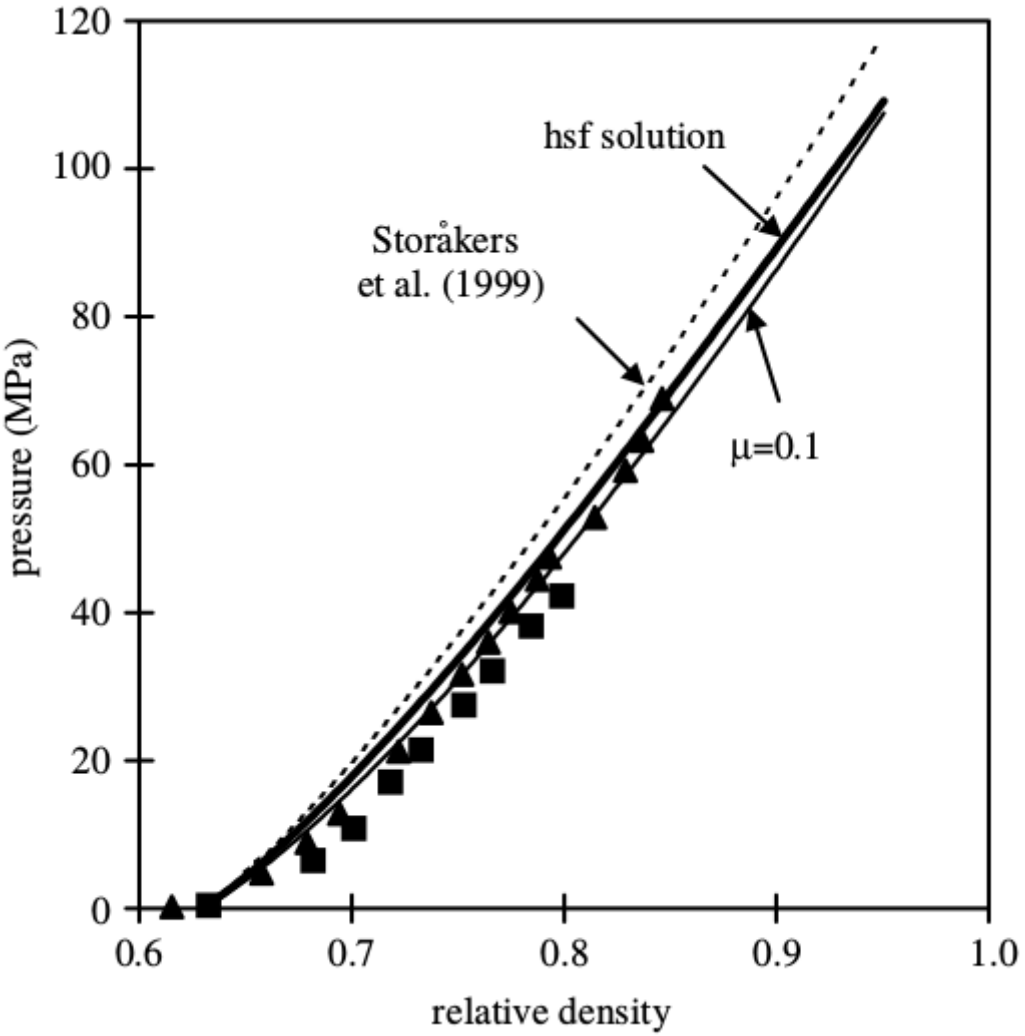

No strong difference in terms of pressure versus relative density → rearrangement induces a higher average coordination number together with a lower average contact area → the macroscopic pressure is proportional to the product of these two quantities.

Martin et al, Journal of the Mechanics and Physics of Solids 51 (2003) 667 – 693

Lecture Summary

- Phenomenology
- Elasto-plastic Constitutive Modelling Primer
  - Stress invariants
  - Porous elasticity
  - Yield surfaces and “associated” models
- Macroscopic constitutive models
  - Cam Clay model
  - The Drucker-Prager-Cap (DPC) model
- Microscopic constitutive models
  - Densification of random packings
  - Discrete element methods

Typical questions

1) Show the density versus compaction pressure during metal powder compaction (key stages).
2) How changes the particle coordination and contact area with increasing density?
3) How a typical density distribution in a compacted cylinder with h/d of 1, pressed from one or from both side.
4) What are the parameters (properties) used in an elastoplastic constitutive model to describe the powder compaction process.
5) Show the powder compression behavior for the Cam-clay model.
6) Explain the hardening behavior of a Cam-clay material.
7) Explain the concept used in the micromechanical compaction models.
8) Compaction: what is the difference between metal powder and ceramic powder.